Contraction-induced damage in skeletal muscles of young and old mice: investigating reactive oxygen species and myeloid cells as contributing factors

by

Darcée D. Sloboda

A dissertation submitted in partial fulfillment
of the requirements for the degree of
Doctor of Philosophy
(Biomedical Engineering)
in the University of Michigan
2014

Doctoral Committee:

Professor Susan V. Brooks, Chair
Associate Professor Lisa M. Larkin
Associate Professor Carey N. Lumeng
Professor Jan P. Stegemann

Acknowledgements

I would like to thank my outstanding advisor, Dr. Susan Brooks, for her guidance, support, generosity, and enthusiasm over the last several years. Thank you for giving me the freedom to pursue my own research interests, for challenging me, and for having confidence in me. I will always remember my time at the University of Michigan fondly.

Thank you to my committee members, Dr. Lisa Larkin, Dr. Carey Lumeng, and Dr. Jan Stegemann for careful evaluation of my research and for helpful discussions.

Thank you to past and present members of the lab. It has been a pleasure to work with you over the past several years. Thank you Dr. Dennis Claflin, for your patient and thorough teaching of lumbrical dissections and additional experimental methods, for editing of manuscripts, and for your general support and help. Carol Davis, thank you for help with experimental techniques and general lab support. Jane Heibel, thank you for excellent administrative support. Thank you Dr. Lauren Wood and Katelyn Russell for making the lab a fun place to work.

Thank you to my family for their loving support over the years and for making several trips out to Ann Arbor to visit me during graduate school.

Finally, thank you to my husband Andrew. I could not have finished this work without your support, encouragement and humor. I love you.

Table of Contents

List of Figures

List of Tables

Abstract

Muscles of aged individuals display high susceptibility to injury and impaired regeneration. Developing strategies to restrict damage or enhance repair for older individuals requires a mechanistic understanding of both the damage and repair processes following injury and the impact of aging on those processes. The overall objective of this dissertation was to address fundamental gaps in our knowledge of cellular and molecular events associated with a common form of muscle injury and to identify age-related changes in key events. We conducted experiments using established models of lengthening contraction-induced injury in young and old mice. We first pursued the question of whether reactive oxygen species (ROS) generated during damaging lengthening contractions contribute to the initiation of the injury. We found that lengthening contractions did not generate more ROS than non-damaging isometric contractions, arguing against ROS as an initiating factor in the injury process. Because neutrophils exacerbate muscle damage while macrophages contribute to repair, we next investigated molecular mechanisms of neutrophil migration into injured muscle and the associations between myeloid cell levels and muscle degeneration and regeneration in old animals. Treatment with blocking antibodies for P- and E-selectin reduced neutrophil levels in injured muscles by half, supporting the importance of these molecules for neutrophil accumulation after lengthening contractions. Despite 50% fewer neutrophils, no reduction in damage was observed, indicating no direct relationship between

neutrophil levels and injury. Moreover, 30-50% more neutrophils in muscles of old compared with adult mice was not associated with more severe injury. Despite more neutrophils, impaired regeneration in muscles of old mice was not associated with an inability to clear these cells nor impaired recruitment of macrophages with age. Indeed, for a given level of muscle injury in old mice, we found 20-50% more macrophages, including anti-inflammatory macrophages. Muscles of old mice also showed aberrant expression of macrophage-associated inflammatory mediators including tumor necrosis factor-alpha and interleukin-10, which have the potential to undermine muscle regeneration. In summary, our studies do not support antioxidant or anti-P/E-selectin therapies to mitigate damage in older individuals. Instead, targeting specific myeloid cell functions may represent a superior therapeutic approach.

Chapter 1

Introduction

Motivation

Age-related declines in skeletal muscle

Aging is associated with progressive declines in skeletal muscle mass and function (1). Studies comparing men and women between the ages of 40 and 80 years have shown a 30-50% decrease in muscle mass and at least an equal but usually even greater decrease in strength in older individuals (2). Muscle power (force x velocity) also decreases with age. Studies comparing healthy subjects in the 20-40 year age range to healthy subjects in the 70-80 year age range have demonstrated 20-40% declines in muscle power in older individuals (3). The age-related loss of muscle mass is attributed, at least in part, to a loss of muscle fibers as well as a decrease in size (i.e. cross-sectional area) of the remaining fibers (3, 4). There is particularly a loss of type II (fast twitch) fibers, which contribute to the loss of muscle power (3). The decrease in strength is attributed to the decrease in muscle mass (4), as force generation is proportional to cross-sectional muscle area (5). However, decreases in strength are still observed after normalizing strength to the cross-sectional muscle area, suggesting the remaining muscle from older individuals is intrinsically weaker (3). This decline in muscle quality

may be due in part to age-related changes in muscle composition, as muscles from older individuals contain more fat and connective tissue (3, 4).

The age-related declines in muscle mass, strength, power and quality can have serious consequences for older individuals. Impaired muscle strength and muscle fat infiltration are predictors of impaired mobility, defined as difficulty walking or climbing stairs (6), and impaired muscle strength, especially in the lower extremities, is a risk factor for falls and associated fractures (7). The loss of muscle mass increases the risk of developing physical disability, defined as difficulty performing the activities of daily living (8). Thus, age-related muscle declines can significantly impact quality of life and limit independence in older individuals, as well as contribute to the need for residential care and associated health care costs.

Causes of age-related declines in skeletal muscle

Age-related declines in muscle mass, function, and quality are likely due to many contributing factors, and many have been proposed, including muscle fiber denervation and the loss or remodeling of motor units, changes in protein metabolism, changes in the endocrine milieu, increased systemic inflammation, and increased oxidative stress, to name a few (2, 3, 9-12).

Also proposed as a contributing factor is the response of aged muscle to certain activities that can cause muscle damage (10, 11, 13). Muscles of aged individuals are more susceptible to damage following certain types of exercise or contractions (14-17). Muscles from aged individuals also have a diminished ability for repair, as shown by slowed recovery of strength (18) and increased fat accumulation (19). Cycles of

frequent damage followed by incomplete repair may be an important contributing factor to the progressive losses of muscle mass and function that occur with aging.

Therefore, restricting damage or enhancing repair after muscle injury is a worthwhile goal for the benefit of older individuals. Developing strategies to restrict damage or enhance repair requires a mechanistic understanding of both the damage and repair processes following injury as well as an understanding of the mechanisms underlying the age-related increase in susceptibility to damage and impaired repair.

Background

Causes of skeletal muscle injury

Skeletal muscle injuries are extremely common. Muscle constitutes a large proportion of the body and many muscles have superficial locations, rendering them susceptible to injuries caused by physical insults (e.g. lacerations, contusions, puncture wounds, crush injuries), extreme temperatures (e.g. freeze injuries, burns) or invasive surgery. Muscles can also be injured by toxins (e.g. snake venoms), periods of unloading followed by reloading, and periods of ischemia followed by reperfusion. Finally, muscles can also be injured by their own contractions. Injuries caused by contractions are probably the most common injuries experienced by skeletal muscle.

Muscle is especially susceptible to injury during lengthening (or eccentric) contractions (20). Lengthening contractions occur when muscles are stretched while activated and injuries caused by lengthening contractions are referred to as contraction-induced injuries. Lengthening contractions occur during normal, everyday movements,

such as lowering oneself into a chair, walking down a flight of stairs, or lowering a heavy package onto a table. Certain activities, such as downhill running, involve repetitive lengthening contractions. Repetitive lengthening contractions, especially when muscles are unaccustomed to such movements, often produce injury and associated symptoms of soreness, swelling, decreased range of motion and loss of strength (21). Alternatively, even a single lengthening contraction can produce injury, perhaps during an accidental fall, especially if the stretch is severe and the muscle is maximally activated (2).

Repair process following skeletal muscle injury

Contraction-induced muscle injury and repair are similar in humans and animals (i.e. rodents and rabbits) and an extensive series of studies from these species has contributed to our understanding of the injury and repair process. Most of the events described in the following paragraphs are from studies in which the injury was initiated by lengthening contractions or eccentric exercise. However, it should be noted that regardless of the nature of the initial insult, injured muscles generally go though similar sequential but overlapping stages of degeneration, inflammation and necrosis followed by regeneration and remodeling.

Lengthening contractions produce immediate disruptions in skeletal muscle (22). Within minutes of lengthening contractions, ultrastructural damage to contractile proteins and sarcomeres is evident within muscle fibers (23-25), as well as disruption of components of the cytoskeleton involved in force transmission (26, 27). There is evidence of damage to the muscle cell membrane (27) and impaired excitation-

contraction coupling, perhaps from damage to T-tubules and the sarcoplasmic reticulum (28). The immediate damage is accompanied by an impaired ability to generate force (i.e. a force deficit) (25, 29).

The degenerative stage of muscle injury occurs within hours after lengthening contractions and lasts for several days. Calcium moves down its concentration gradient into the muscle cell cytoplasm, possibly through damage to the cell or sarcoplasmic reticulum membranes (22). Increased intracellular calcium causes hypercontractions of portions of muscle fibers, which are visible as large, swollen fibers in transverse muscle sections and leave adjacent portions of the same fibers barely visible or missing (24, 30). Increased intracellular calcium can also activate the calpains, proteolytic enzymes that initiate the breakdown of myofibrils and cytoskeletal elements (31). Degenerating and necrotic fibers are visible in transverse muscle sections (29), and a loss of muscle fibers is observed along with an increased or maintained force deficit (13, 29, 32).

Repair and regeneration begin within the first week and the regenerative stage can last for a few weeks. Successful muscle regeneration relies on muscle stem cells known as satellite cells, named for their location at the periphery of mature muscle fibers. In response to injury, satellite cells exit their normal quiescent state, proliferate, and migrate to the site of injury. These cells then differentiate and fuse together to form new myofibers or fuse to existing fibers to repair damage (33, 34). Repaired and regenerating muscle fibers are identified by their centrally located nuclei. Early in the regeneration process, new myofibers are visible as small basophilic centronucleated myofibers, which increase in size over time (35). Finally, a remodeling stage occurs, characterized by extracellular matrix production and remodeling, and angiogenesis (36).

Accompanying the degenerative and regenerative phases is the accumulation of myeloid cells (i.e. neutrophils and macrophages) (37). Neutrophils are the first to increase in number in injured muscle, arriving from the circulation within hours of the initial insult. Neutrophil levels peak within 1-2 days following the initial insult and then their numbers decline to control levels within 7 days after the injury (38). Following the arrival of neutrophils, macrophages begin to accumulate in injured muscle. Pro- and anti-inflammatory macrophages are observed. Early arriving, pro-inflammatory macrophages invade muscle fibers and are associated with the removal of damaged and necrotic tissue (39-41). Pro-inflammatory macrophage numbers decline within a few days as the number of anti-inflammatory macrophages increases. Anti-inflammatory macrophages can remain in the muscle for many days and their presence generally coincides with the regenerative stage of muscle repair (39-41).

Ultimately, in young and healthy muscles, the injured muscles return to a state not detectably different from muscles that were never injured.

Dissertation objectives and overview of chapters

Dissertation objectives

Although much is known about the sequence of events following muscle injury, the underlying cellular and molecular mechanisms remain incompletely understood. Furthermore, the mechanisms underlying the age-related increase in susceptibility to damage and delayed or incomplete repair are not well understood. Understanding these mechanisms may reveal key therapeutic targets for restricting damage or enhancing

repair for individuals whose muscles do not fully recover after injury due to advanced age.

Therefore, the overall objectives of this research were 1) to address fundamental gaps in our knowledge of cellular and molecular events associated with a common form of muscle injury and 2) to identify age-related changes in key events.

Overview of dissertation chapters

Early initiators of degenerative and regenerative processes following contraction-induced injury have not been clearly defined. ROS generated during lengthening contractions may contribute to degenerative or regenerative processes, as ROS can cause direct damage to macromolecules (42) and ROS signaling can affect many processes that contribute to degeneration or regeneration following injury (43, 44). Furthermore, age-related changes in damage and repair are accompanied by aberrant ROS homeostasis (45, 46) and at least one study suggests that ROS production around the time of injury enhances initial damage in old animals (47). Chapter 2 describes published work (48) that examines whether ROS generated at the time of injury are an early initiator of downstream processes of degeneration and regeneration.

Despite accumulating evidence that the number of myeloid cells present in injured muscle is a critical factor in the success of muscle repair (32, 49-53), the effect of aging on the magnitude and the timing of the myeloid cell response to injury has received little attention. Chapter 3 explores age-related changes in the magnitude of the myeloid cell response to injury and examines whether such changes correlate with impaired regeneration in aged animals.

Given the critical role of myeloid cells in determining the success or failure of muscle repair, manipulating myeloid cell infiltration after contraction-induced injury may be an effective strategy for either preventing damage or enhancing repair in aged populations. Neutrophils can exacerbate damage to muscle fibers following injury while macrophages generally contribute to repair (32, 50-53). Thus, preventing or blunting the neutrophil response while keeping the macrophage response intact may provide a therapeutic benefit. However, the molecules responsible for neutrophil infiltration after contraction-induced injury are not entirely known. Potential candidates are P- and E-selectin proteins that are expressed on the luminal surface of blood vessels and interact with corresponding ligands on neutrophils. The selectins mediate initial steps in a well-characterized cascade that culminates with neutrophil migration out of the blood vessel and into the surrounding tissue, at least under some circumstances (54). Chapter 4 investigates the role of P- and E-selectin molecules in neutrophil and macrophage accumulation after muscle injury and examines whether blunting neutrophil accumulation by blocking the selectins provides a therapeutic benefit. The findings in Chapter 4 also help to interpret findings from Chapter 3.

Mouse models were used for all experiments. Rodents demonstrate many of the age-related changes observed in muscle, including reductions in muscle mass and force generation (55-57), increased susceptibility to damage following contractions (47, 58, 59), and delayed or incomplete repair (56, 60-64). Experiments were conducted using well-established *in vitro* (65, 66) and *in situ* injury models (25, 29, 32, 47, 56, 57, 63, 67).

References

1. von Haehling S, Morley JE, Anker SD. An overview of sarcopenia: facts and numbers on prevalence and clinical impact. J Cachexia Sarcopenia Muscle. 2010 Dec; 1(2):129-33.

2. Faulkner JA, Larkin LM, Claflin DR, Brooks SV. Age-related changes in the structure and function of skeletal muscles. Clin Exp Pharmacol Physiol. 2007 Nov; 34(11):1091-6.

3. Lang T, Streeper T, Cawthon P, Baldwin K, Taaffe DR, Harris TB. Sarcopenia: etiology, clinical consequences, intervention, and assessment. Osteoporos Int. 2010 Apr; 21(4):543-59.

4. Porter MM, Vandervoort AA, Lexell J. Aging of human muscle: structure, function and adaptability. Scand J Med Sci Sports. 1995 Jun; 5(3):129-42.

5. Lieber RL. Skeletal muscle structure, function, and plasticity: The physiological basis of rehabilitation. Third Edition. Philadelphia: Lippincott Williams & Wilkins; 2010.

6. Visser M, Goodpaster BH, Kritchevsky SB, Newman AB, Nevitt M, Rubin SM, Simonsick EM, Harris TB. Muscle mass, muscle strength, and muscle fat infiltration as predictors of incident mobility limitations in well-functioning older persons. J Gerontol A Biol Sci Med Sci. 2005 Mar; 60(3):324-33.

7. Moreland JD, Richardson JA, Goldsmith CH, Clase CM. Muscle weakness and falls in older adults: a systematic review and meta-analysis. J Am Geriatr Soc. 2004 Jul; 52(7):1121-9.

8. Janseen I. Influence of sarcopenia on the development of physical disability: the Cardiovascular Health Study. J Am Geriatr Soc. 2006 Jan; 54(1):56-62.

9. Marcell TJ. Sarcopenia: causes, consequences, and preventions. J Gerontol A Biol Sci Med Sci. 2003 Oct; 58(10):M911-6.

10. Peake J, Della Gatta P, Cameron-Smith D. Aging and its effects on inflammation in skeletal muscle at rest and following exercise-induced muscle injury. Am J Physiol Regul Integr Comp Physiol. 2010 Jun; 298(6):R1485-95.

11. Arthur ST, Cooley ID. The effect of physiological stimuli on sarcopenia; impact of Notch and Wnt signaling on impaired aged skeletal muscle repair. Int J Biol Sci. 2012; 8(5):731-60.

12. Sakuma K, Aoi W, Yamaguchi A. Current understanding of sarcopenia: possible candidates modulating muscle mass. Pflugers Arch. 2014 May 7.

13. Faulkner JA, Brooks SV, Zerba E. Muscle atrophy and weakness with aging: contraction-induced injury as an underlying mechanism. J Gerontol A Biol Sci Med Sci. 1995 Nov; 50:124-9.

14. Manfredi TG, Fielding RA, O'Reilly KP, Meredith CN, Lee HY, Evans WJ. Plasma creatine kinase activity and exercise-induced muscle damage in older men. Med Sci Sports Exerc. 1991 Sep; 23(9):1028-34.

15. Roth SM, Martel GF, Ivey FM, Lemmer JT, Metter EJ, Hurley BF, Rogers MA. High-volume, heavy resistance strength training and muscle damage in young and older women. J Appl Physiol. 2000 Mar; 88(3):1112-8.

16. Ploutz-Snyder LL, Giamis EL, Formikell M, Rosenbaum AE. Resistance training reduces susceptibility to eccentric exercise-induced muscle dysfunction in older women. J Gerontol A Biol Sci Med Sci. 2001 Sep; 56(9):B384-90.

17. Choi SJ, Lim JY, Nibaldi EG, Phillips EM, Frontera WR, Fielding RA, Widrick JJ. Eccentric contraction-induced injury to type I, IIa, and IIa/IIx muscle fibers of elderly adults. Age. 2012 Feb; 34(1):215-26.

18. Dedrick ME, Clarkson PM. The effects of eccentric exercise on motor performance in young and older women. Eur J Appl Physiol Occup Physiol. 1990; 60(3):183-6.

19. Müller M, Tohtz S, Dewey M, Springer I, Perka C. Age-related appearance of muscle trauma in primary total hip arthroplasty and the benefit of a minimally invasive approach for patients older than 70 years. Int Orthop. 2011 Feb; 35(2):165-71.

20. Faulkner JA, Brooks SV, Opiteck JA. Injury to skeletal muscle fibers during contractions: conditions of occurrence and prevention. Phys Ther. 1993 Dec; 73(12):911-21.

21. Sayers SP, Hubal MJ. Histological, chemical and functional manifestations of muscle damage. In: Tiidus PM, editor. Skeletal muscle damage and repair. Champaign: Human Kinetics; 2008. p. 37-48.

22. Koh TJ. Physiology and mechanisms of skeletal muscle damage. In: Tiidus PM, editor. Skeletal muscle damage and repair. Champaign: Human Kinetics; 2008. p. 3-12.

23. Fridén J, Lieber RL. Segmental muscle fiber lesions after repetitive eccentric contractions. Cell Tissue Res. 1998 Jul; 293(1):165-71.

24. Lieber RL, Woodburn TM, Fridén J. Muscle damage induced by eccentric contractions of 25% strain. J Appl Physiol. 1991 Jun; 70(6):2498-507.

25. Brooks SV, Zerba E, Faulkner JA. Injury to muscle fibres after single stretches of passive and maximally stimulated muscles in mice. J Physiol. 1995 Oct; 488(2):459-69.

26. Lieber RL, Thornell LE, Fridén J. Muscle cytoskeletal disruption occurs within the first 15 min of cyclic eccentric contraction. J Appl Physiol. 1996 Jan; 80(1):278-84.

27. Lovering RM, De Deyne PG. Contractile function, sarcolemma integrity, and the loss of dystrophin after skeletal muscle eccentric contraction-induced injury. Am J Physiol Cell Physiol. 2004 Feb; 286(2):C230-8.

28. Ingalls CP, Warren GL, Williams JH, Ward CW, Armstrong RB. E-C coupling failure in mouse EDL muscle after *in vivo* eccentric contractions. *J Appl Physiol* 85: 58-67, 1998.

29. McCully KK, Faulkner JA. Injury to skeletal muscle fibers of mice following lengthening contractions. 1985 Jul; 59(1):119-26.

30. Carpenter S, Karpati G. Segmental necrosis and its demarcation in experimental micropuncture injury of skeletal muscle fibers. J Neuropathol Exp Neurol. 1989 Mar; 48(2):154-70.

31. Belcastro AN, Shewchuk LD, Raj DA. Exercise-induced muscle injury: a calpain hypothesis. Mol Cell Biochem. 1998 Feb; 179(1-2):135-45.

32. Pizza FX, Peterson JM, Baas JH, Koh TJ. Neutrophils contribute to muscle injury and impair its resolution after lengthening contractions in mice. J Physiol. 2005 Feb; 562(3):899-913.

33. Chargé SB, Rudnicki MA. Cellular and molecular regulation of muscle regeneration. Physiol Rev. 2004 Jan; 84(1):209-38.

34. Guttridge DC. Skeletal muscle regeneration. In: Hill JA, Olson EN, editors. Muscle: fundamental biology and mechanisms of disease. New York: Academic Press; 2012. p. 921-933.

35. Shortreed K, Johnston A, Hawke TJ. Satellite cells and muscle repair. In: Tiidus PM, editor. Skeletal muscle damage and repair. Champaign: Human Kinetics; 2008. p. 77-88.

36. Carosio S, Berardinelli MG, Aucello M, Musarò A. Impact of ageing on muscle cell regeneration. Ageing Res Rev. 2011 Jan; 10(1):35-42.

37. Tidball JG, Villalta SA. Regulatory interactions between muscle and the immune system during muscle regeneration. Am J Physiol Regul Integr Comp Physiol. 2010 May; 298(5):R1173-87.

38. Pizza FX. Neutrophils and macrophages in muscle damage and repair. In: Tiidus PM, editor. Skeletal muscle damage and repair. Champaign: Human Kinetics; 2008. p. 49-58.

39. St. Pierre BA, Tidball JG. Differential response of macrophage subpopulations to soleus muscle reloading after rat hindlimb suspension. J Appl Physiol. 1994 Jul; 77(1):290-7.

40. McLennan IS. Degenerating and regenerating skeletal muscles contain several subpopulations of macrophages with distinct spatial and temporal distributions. J Anat. 1996 Feb; 188(1):17-28.

41. Deng B, Wehling-Henricks M, Villalta SA, Wang Y, Tidball JG. IL-10 triggers changes in macrophage phenotype that promote muscle growth and regeneration. J Immunol. 2012 Oct; 189(7):3669-80.

42. Bergamini CM, Gambetti S, Dondi A, Cervellati C. Oxygen, reactive oxygen species and tissue damage. Curr Pharm Des. 2004; 10(14):1611-26.

43. Barbieri E, Sestili P. Reactive oxygen species in skeletal muscle signaling. J Signal Transduct. 2012; 2012:982794.

44. Powers SK, Duarte J, Kavazis AN, Talbert EE. Reactive oxygen species are signalling molecules for skeletal muscle adaptation. Exp Physiol. 2010 Jan; 95(1):1-9.

45. Bejma J, Ji LL. Aging and acute exercise enhance free radical generation in rat skeletal muscle. J Appl Physiol. 1999 Jul; 87(1):465-70.

46. Broome CS, Kayani AC, Palomero J, Dillmann WH, Mestril R, Jackson MJ, McArdle A. Effect of lifelong overexpression of HSP70 in skeletal muscle on age-related oxidative stress and adaptation after nondamaging contractile activity. FASEB J. 2006 Jul; 20(9):1549-51.

47. Zerba E, Komorowski TE, Faulkner JA. Free radical injury to skeletal muscles of young, adult, and old mice. Am J Physiol. 1990 Mar; 258(3):C429-35.

48. Sloboda DD, Brooks SV. Reactive oxygen species generation is not different during isometric and lengthening contractions of mouse muscle. Am J Physiol Regul Integr Comp Physiol. 2013 Oct; 305(7):R832-9.

49. Teixeira CF, Zamunér SR, Zuliani JP, Fernandes CM, Cruz-Hofling MA, Fernandes I, Chaves F, Gutiérrez JM. Neutrophils do not contribute to local tissue damage, but play a key role in skeletal muscle regeneration, in mice injected with Bothrops asper snake venom. Muscle Nerve. 2003 Oct; 28(4):449-59.

50. Summan M, Warren GL, Mercer RR, Chapman R, Hulderman T, Van Rooijen N, Simeonova PP. Macrophages and skeletal muscle regeneration: a clodronate-containing liposome depletion study. Am J Physiol Regul Integr Comp Physiol. 2006 Jun; 290(6):R1488-95.

51. Arnold L, Henry A, Poron F, Baba-Amer Y, van Rooijen N, Plonquet A, Gherardi RK, Chazaud B. Inflammatory monocytes recruited after skeletal muscle injury switch into anti-inflammatory macrophages to support myogenesis. J Exp Med. 2007 May; 204(5):1057-69.

52. Tidball JG, Wehling-Henricks M. Macrophages promote muscle membrane repair and muscle fibre growth and regeneration during modified muscle loading in mice *in vivo*. J Physiol. 2007 Jan; 578(1):327-36.

53. Wang H, Melton DW, Porter L, Sarwar ZU, McManus LM, Shireman PK. Altered macrophage phenotype transition impairs skeletal muscle regeneration. Am J Pathol. 2014 Apr; 184(4):1167-84.

54. Ebnet K, Vestweber D. Molecular mechanisms that control leukocyte extravasation: the selectins and the chemokines. Histochem Cell Biol. 1999 Jul; 112(1):1-23.

55. Carlson BM, Faulkner JA. Muscle transplantation between young and old rats: age of host determines recovery. Am J Physiol. 1989 Jun; 256(6):C1262-66.

56. Brooks SV, Faulkner JA. Contraction-induced injury: recovery of skeletal muscles in young and old mice. Am J Physiol Cell Physiol. 1990 Mar; 258(3):C436-42.

57. Lockhart NC, Brooks SV. Protection from contraction-induced injury provided to skeletal muscles of young and old mice by passive stretch is not due to a decrease in initial mechanical damage. J Gerontol A Biol Sci Med Sci. 2006 Jun; 61(6):527-33.

58. Brooks SV, Faulkner JA. The magnitude of the initial injury induced by stretches of maximally activated muscle fibers of mice and rats increases in old age. J Physiol. 1996 Dec; 497(2):573-80.

59. Lynch GS, Faulkner JA, Brooks SV. Force deficits and breakage rats after single lengthening contractions of single fast fibers from unconditioned and conditioned muscles of young and old rats. Am J Physiol Cell Physiol. 2008 Jul; 295(1):C249-56.

60. Sadeh M. Effects of aging on skeletal muscle regeneration. J Neurol Sci. 1988 Oct; 87(1):67-74.

61. McBride TA, Gorin FA, Carlsen RC. Prolonged recovery and reduced adaptation in aged rat muscle following eccentric exercise. Mech Ageing Dev. 1995 Sep; 83(3):185-200.

62. Conboy IM, Conboy MJ, Wagers AJ, Girma ER, Weissman IL, Rando TA. Rejuvenation of aged progenitor cells by exposure to a young systemic environment. Nature. 2005 Feb; 433(7027):760-4.

63. Rader EP, Faulkner JA. Recovery from contraction-induced injury is impaired in weight-bearing muscles of old male mice. J Appl Physiol. 2006 Feb; 100(2):656-61.

64. Ghaly A, Marsh DR. Aging-associated oxidative stress modulates the acute inflammatory response in skeletal muscle after contusion injury. Exp Gerontol. 2010 May; 45(5):381-8.

65. Ng R, Metzger JM, Claflin DR, Faulkner JA. Poloxamer 188 reduces the contraction-induced force decline in lumbrical muscles from mdx mice. Am J Physiol Cell Physiol. 2008 Jul; 295(1):C146-50.

66. Claflin DR, Brooks SV. Direct observation of failing fibers in muscles of dystrophic mice provides mechanistic insight into muscular dystrophy. Am J Physiol Cell Physiol. 2008 Feb; 294(2):C651-8.

67. Pizza FX, Koh TJ, McGregor SJ, Brooks SV. Muscle inflammatory cells after passive stretches, isometric contractions, and lengthening contractions. J Appl Physiol. 2002 May; 92(5):1873-8.

Chapter 2

Reactive oxygen species generation is not different during isometric and lengthening contractions of mouse muscle

Abstract

Skeletal muscles can be injured by lengthening contractions, when the muscles are stretched while activated. Lengthening contractions produce structural damage that leads to the degeneration and regeneration of damaged muscle fibers by mechanisms that have not been fully elucidated. Reactive oxygen species (ROS) generated at the time of injury may initiate degenerative or regenerative processes. In the present study we hypothesized that lengthening contractions that damage the muscle would generate more ROS than isometric contractions that do not cause damage. To test our hypothesis, we subjected muscles of mice to lengthening contractions or isometric contractions and simultaneously monitored intracellular ROS generation with the fluorescent indicator 5-(and-6)-chloromethyl-2',7'-dichlorodihydrofluorescein (CM-DCFH), which is oxidized by ROS to form the fluorescent product CM-DCF. We found that CM-DCF fluorescence was not different during or shortly after lengthening contractions compared with isometric controls, regardless of the amount of stretch and damage that occurred during the lengthening contractions. The only exception was that

after severe stretches, the increase in CM-DCF fluorescence was impaired. We conclude that lengthening contractions that damage the muscle do not generate more ROS than isometric contractions that do not cause damage. The implication is that ROS generated at the time of injury are not the initiating signals for subsequent degenerative or regenerative processes.

Introduction

Skeletal muscles can be injured by lengthening contractions, when the muscles are stretched while activated. Lengthening contractions produce immediate ultrastructural damage within muscle fibers, and the damage is accompanied by a deficit in force generation. In the hours, days, and weeks following the initial injury, inflammatory cells invade the tissue and muscle fibers undergo a process of degeneration, necrosis, and regeneration (1). The cellular and molecular mechanisms by which the initial injury initiates degenerative and regenerative processes remain incompletely understood. Understanding these mechanisms may reveal key therapeutic targets for restricting degeneration or enhancing regeneration for individuals whose muscles do not fully recover after injury due to advanced age (2, 3), disease (4-6), or severe trauma (7).

Reactive oxygen species (ROS) generated at the time of initial injury may contribute to degenerative or regenerative processes. ROS can cause direct damage to macromolecules, including proteins and lipids (8) or act indirectly via a wide variety of pathways to influence gene transcription and expression (9, 10). In muscle, ROS

signaling is thought to affect many processes that could contribute to degeneration or regeneration following injury, including protein degradation, autophagy, cell death, inflammation, cell proliferation, cell differentiation, and mitochondrial biogenesis (11, 12). Despite the potential involvement of ROS or ROS signaling in degenerative or regenerative processes following the initial injury, ROS generation at the time of the initial injury has not been studied. Therefore, the main objective of our study was to examine ROS generation at the time of the initial injury, during lengthening contractions that damage the muscle.

Our expectation that lengthening contractions would generate ROS is supported by reports of increased ROS production within skeletal muscle fibers during contractions (13-17). Contraction-induced ROS generation has been attributed to non-mitochondrial sources (18,19) and specifically, NADPH oxidase has been implicated (20, 21). ROS production has also been reported during passive stretches of skeletal muscle fibers and cardiac myocytes (22-24). Although ROS production during passive stretches is not a universal finding (23, 25), it is conceivable that lengthening contractions that involve both stretch and activation generate more ROS than during activation alone. Accordingly, we hypothesized that damaging lengthening contractions would generate more ROS than isometric contractions that do not cause damage. To test the hypothesis, we subjected muscles of mice to lengthening contractions (LC) or isometric contractions (IC) and simultaneously monitored intracellular ROS generation with the fluorescent indicator 5-(and-6)-chloromethyl-2′,7′-dichlorodihydrofluorescein (CM-DCFH), which is oxidized by ROS to form the fluorescent product CM-DCF. Passive stretches (PS), i.e. stretches without activation, were also administered to examine the

degree to which increased CM-DCF fluorescence during lengthening contractions may represent an additive effect of ROS generation during stretch plus ROS generation during muscle activation.

Methods

Animals. Male C57BL/6J mice, 7-9 mo of age (retired breeders), were purchased from the Jackson Laboratory and housed in a specific-pathogen-free facility at the University of Michigan. The mice weighed 32 ± 3 g (mean ± SD, N = 59). On the day of an experiment, a mouse was anesthetized with an intraperitoneal injection of Avertin (tribromoethanol, 250 mg/kg) (chemical components from Sigma-Aldrich, St. Louis, MO). After the mouse was unresponsive to tactile stimuli, one forepaw was removed and the mouse was euthanized with an overdose of Avertin followed by induction of a bilateral pneumothorax. All animal use procedures were approved by the University of Michigan Committee on the Use and Care of Animals (UCUCA).

Lumbrical muscle preparation. All experiments were conducted *in vitro* using forepaw lumbrical (LMB) muscles. The extremely small LMB muscle offers the diffusion benefits of an isolated single fiber while providing a model of whole muscle with intact extracellular matrix and tendons (26). The forepaw was pinned in a shallow dish filled with Tyrode “dissection” solution composed of (in mM): 136.5 NaCl, 11.9 $NaHCO_3$, 5.0 KCl, 1.8 $CaCl_2$, 0.5 $MgCl_2$, 0.4 NaH_2PO_4, and 0.1 EDTA. A whole LMB muscle was dissected free from the third digit relative to the medial side of the paw and cleaned of as much connective tissue as possible to facilitate subsequent visualization of fiber

striations. Monofilament nylon suture (USP 10/0, Ashaway Line & Twine) was used to tie the LMB muscle into an experimental chamber, with the proximal tendon attached to a high-speed length controller (318B, Aurora Scientific) and the distal tendon attached to a force transducer (400A, Aurora Scientific). Ties were placed as close to muscle fibers as possible to minimize effects of tendon compliance. The chamber was perfused with Tyrode "experiment" solution (in mM): 121 NaCl, 24 $NaHCO_3$, 5.5 glucose, 5.0 KCl, 1.8 $CaCl_2$, 0.5 $MgCl_2$, 0.4 NaH_2PO_4, and 0.1 EDTA. Tyrode solutions were made with chemicals purchased from Sigma-Aldrich. The solution was bubbled with 95% O_2-5% CO_2 to maintain a pH of 7.3. The temperature of the solution was maintained at 25 °C.

The chamber was placed on the stage of an inverted microscope (Axiovert 100, Carl Zeiss Microscopy) and fiber striations were visible through the transparent bottom of the chamber. A video sarcomere length system (900B-5A, Aurora Scientific) monitored striation spacing and reported sarcomere length. For all muscles, fiber length (L_f) was calculated as previously described (27). Because LMB fibers are arranged parallel to the long axis of the muscle, the number of sarcomeres in series within a fiber can be inferred by changing the muscle length by a known amount and measuring the resulting change in sarcomere length. The number of sarcomeres in series is then multiplied by 2.5 μm to calculate fiber length. After the fiber length was calculated, the length of the muscle was adjusted until the sarcomere length was 2.5 μm (i.e. optimal length).

CM-DCF fluorescence measurements. A rectangular aperture with adjustable dimensions was placed in the image path between the muscle and the photodetector, allowing selection of the image area from which fluorescence measurements were

obtained. The aperture was adjusted to select a region of the muscle image that was 0.12 mm x 0.60 mm, equivalent to approximately 12% of the area occupied by the image. Fluorescence was elicited by light originating from a 75 W xenon lamp. A diffraction grating monochromator (Deltascan 4000, Photon Technology International) was used to select excitation wavelengths centered at 493 nm (bandwidth 2 nm). The excitation light was reflected through an angle of 90° by a dichroic mirror and passed through the microscope objective before reaching the muscle. The emitted fluorescence was collected by the objective and passed through the dichroic mirror and a band-pass filter (535 ± 20 nm) and detected using a photomultiplier detection system (814, Photon Technology International). The dichroic mirror reflected wavelengths shorter than 505 nm and passed those longer than 505 nm. Fluorescence was measured before loading any indicator to determine background fluorescence.

Loading of CM-DCFH and measuring CM-DCF fluorescence were performed at 25 °C and experiments were conducted in a darkened laboratory room to minimize photobleaching of the indicator and contaminating room light from reaching the photodetector. CM-H_2DCF-DA (C6827, Life Technologies, Carlsbad, CA) was dissolved in ethanol and combined with Tyrode dissection solution containing 0.1% (v/v) Pluronic F-127 (P-6866, Life Technologies) to facilitate suspension of CM-H_2DCF-DA. The final concentration of the CM-H_2DCF-DA solution was 15 μM. The CM-H_2DCF-DA solution was added to the chamber and 30 min were allowed for passive diffusion of CM-H_2DCF-DA into muscle fibers and conversion to the retained form, CM-DCFH, by intracellular esterases. After 30 min, the chamber was perfused with Tyrodes experiment solution for 5 min to remove residual CM-H_2DCF-DA. Perfusion with

Tyrodes experiment solution continued during the CM-DCF measurements. CM-DCF fluorescence was monitored continuously (10 samples/s) for 3 min before the onset of IC, LC, or PS to establish a baseline. CM-DCF fluorescence was then monitored during IC, LC, or PS, and for 5 min afterward. Muscles remained in the dark for 5 more min before the final isometric contraction was elicited (see *Isometric contractions*).

Preliminary experiments suggested that 15 μM of CM-H_2DCF-DA was more than sufficient for our study. When hydrogen peroxide was added to the chamber after a typical experiment, the DCF fluorescence increased by as much as 15-fold, indicating that only a small portion of the probe was oxidized during any given experiment and that our ability to detect ROS was not limited by a shortage of unoxidized probe within the muscle.

Isometric contractions. Muscle activation was accomplished by electric field stimulation via platinum plate electrodes. Stimulus pulses were 0.2 ms in duration and the stimulation current was adjusted in order to elicit maximum twitch force. The muscle was subjected to a single isometric contraction to establish “pre-protocol force”. After the muscle was loaded with CM-DCFH, the muscle was subjected to a protocol of 12 isometric tetanic contractions spaced 8 s apart. Each tetanus was 400 ms in duration, and the stimulus pulses within each tetanus were delivered at a rate of 200 s^{-1}. Force was recorded continuously throughout the contraction protocol. A single isometric tetanus was elicited 10 minutes after the 12^{th} contraction to assess the deficit in isometric force in the absence of fatigue. Force deficit was calculated by the following equation: Force deficit (%) = [(pre-protocol force – force 10 min after protocol)/(pre-protocol force)] X 100.

Lengthening contractions and passive stretches. Muscles exposed to LC were treated the same as muscles exposed to IC, except that a stretch was initiated at the beginning of the 400 ms stimulation period. Muscles were lengthened at the appropriate rate to cause the peak of the stretch to coincide with the end of the tetanic stimulation. In one series of experiments, muscles were stretched by 40% L_f at a rate of 1 L_f/s, and in a second series of experiments, muscles were stretched by 10, 30, or 50% L_f at rates of 0.25, 0.75, or 1.25 L_f/s, respectively. Muscles exposed to PS were treated the same as muscles exposed to LC, except that the muscles were not activated.

Large strains relative to fiber length were chosen to ensure that muscles would be damaged during lengthening contractions (28). Strains as large as 30-50% relative to fascicle length (an estimate of fiber length) have been reported *in vivo* for human gastrocnemius muscles during dorsiflexion (29, 30) and vastus lateralis muscles during knee flexion (31). Modeling studies incorporating subject data have also found that fascicles actively lengthened as much as 37% (splenius capitis) and 50% (semispinalis capitis) during low-velocity automobile impacts (32), and 64% near the myotendinous junction of the biceps femoris muscle (33). Similar strains have been reported for passive stretches of biceps femoris and gastrocnemius muscle (29, 30, 34). LMB muscles likely do not experience large strains *in vivo*, but can be considered models for other muscles.

Isometric contractions after lengthening contractions. For some LMB muscles, a series of IC was elicited 10 min after the 12^{th} lengthening contraction, according to the activation protocol described above for *Isometric contractions*. During the intervening 10 min, no additional CM-H_2DCF-DA was added to the chamber. CM-DCF fluorescence

was collected for 2 min before the onset of IC to re-establish baseline oxidation and CM-DCF fluorescence monitoring continued during the series of IC.

GSHEE experiments. In order to confirm that CM-DCF fluorescence was sensitive to intracellular changes in ROS, ROS generation was measured in the presence of glutathione reduced ethyl ester (GSHEE). LMB muscles were prepared and tested as previously described with the following exceptions. After the pre-protocol force was measured, dissection solution containing 2.5 mM glutathione reduced ethyl ester (GSHEE) (G1404, Sigma-Aldrich) was added to the chamber. LMB muscles were exposed to GSHEE for 1 hr before exposure to 15 μM CM-H_2DCF-DA solution for 30 min. To remove residual CM-H_2DCF-DA, fresh dissection solution was added to the chamber before isometric contractions were initiated. GSHEE was present during CM-DCFH loading and during the contractions. To conserve GSHEE, the chamber was not perfused with solution during contractions. With the absence of perfusion, we observed greater baseline CM-DCF fluorescence compared with the baseline fluorescence when solution was flowing (Table 2.1), possibly due to lower rates of leakage of the indicator from the muscles. Control muscles were treated the same as muscles exposed to GSHEE, except that GSHEE was not present.

Muscle cross-sectional area measurements. After testing, muscles were maintained at optimal length while the testing chamber was placed on the stage of a stereo microscope (MZ8, Leica Microsystems). The diameter of the muscle was measured using a scale in the eye piece of the microscope and the cross-sectional muscle area (CSA) was estimated by assuming a circular cross-section.

Data analysis. ROS oxidize CM-DCFH to form the fluorescent product CM-DCF, and the net increase in ROS over time is indicated by the increase in CM-DCF fluorescence over time (15, 20, 35). Therefore, we determined the "CM-DCF slope" (i.e. slope of the CM-DCF fluorescence-versus-time plot) during a resting period and during IC. In order to quantify the change in slope with the onset of contractions, we subtracted the slope of a line fitted to the baseline portion of the CM-DCF fluorescence record (dashed line, Figure 2.1) from the slope of a line fitted to the portion of the record corresponding to the series of contractions (dotted line, Figure 2.1). We considered only the CM-DCF fluorescence measurements collected after each contraction (i.e. after the force returned to the baseline value) to prevent motion artifact from affecting the analysis. Background fluorescence was subtracted from the CM-DCF fluorescence record before the slopes were calculated. The analysis was the same for muscles subjected to lengthening contractions and passive stretches.

Statistics. Data are presented as mean ± SD. Differences between experimental groups were analyzed by a Student's t test or a one-way ANOVA followed by the Holm-Sidak method to determine which means were significantly different. In the case of skewed distributions or unequal variance, a Mann-Whitney rank sum test or a Kruskal-Wallis one-way ANOVA on ranks was used. Correlation between two variables was determined by calculating the Pearson product-moment correlation coefficient. Differences were considered statistically significant when $P < 0.05$.

Results

To test our hypothesis that lengthening contractions that damage the muscle generate more ROS than isometric contractions, we subjected LMB muscles to LC or IC, with PS as an additional control, and examined changes in CM-DCF slope (Figures 2.1-2.3). As expected, LC caused muscle damage as indicated by a ~30% force deficit, whereas IC and PS produced no or minimal force deficits, respectively (Figure 2.3A). The CM-DCF slope increased during IC and LC relative to baseline slopes; however, the increase observed with the onset of LC was not greater than the increase observed with the onset of IC (Figure 2.3B). We did not detect a change in CM-DCF slope with the onset of PS (Figure 2.3B) and so we excluded PS from subsequent experiments.

Since we did not find that LC increased the CM-DCF slope more than IC, we completed a second series of experiments to verify the result was not due to insufficient or excessive stretch. We subjected LMB muscles to lengthening contraction protocols with the magnitude of stretch ranging from 30-50% L_f, including 0% L_f (i.e. IC) as a control, and examined changes in CM-DCF slope (Figure 2.4). As expected, the force deficit increased as the degree of stretch increased (Figure 2.4A). However, despite the large range of stretch and damage among groups, there were no differences in the change in CM-DCF slope with the onset of LC (Figure 2.4B). In case the effects of LC were not immediately apparent, we also examined the CM-DCF slope 10 min after LC, during an additional isometric contraction protocol. Prior to the isometric contraction protocol, the baseline DCF slope was not different between injured and uninjured muscles. In contrast, we found that the change in CM-DCF slope with the onset of

contractions was significantly less in muscles initially stretched by 50% L_f (Figure 2.4C), and within this group the force deficit and the change in CM-DCF slope were negatively correlated (Figure 2.4D). Overall, the second series of experiments confirmed our finding that LC did not increase CM-DCF slope more than IC.

In order to confirm that CM-DCF slope was sensitive to ROS in LMB muscles, we conducted a third series of experiments. CM-DCF slope was examined after LMB muscles were exposed to GSHEE. GSHEE is converted to the antioxidant GSH once it crosses the cell membrane and decreases contraction-induced ROS generation in single muscle fibers (15). GSHEE decreased both the baseline CM-DCF slope (Figure 2.5A) and the change in CM-DCF slope with the onset of IC, compared with controls (Figure 2.5B). GSHEE exposure did not reduce force (Figure 2.5C) indicating that GSHEE did not damage LMB muscles or impair muscle activation. These results suggest that the decrease in CM-DCF slope was due to an increase in GSH content, not impaired muscle function, and verified that CM-DCF slope is sensitive to net changes in ROS in whole LMB muscles.

Finally, our findings were not due to intrinsic differences among experimental groups. Prior to IC, LC, or PS, there were no differences in muscle size (i.e. fiber length and CSA), pre-protocol force, or baseline CM-DCF slope among experimental groups, except for a difference in baseline CM-DCF between muscles exposed to GSHEE relative to controls (Table 2.1).

Discussion

The main finding of the present study is that, contrary to our hypothesis, lengthening contractions that damage muscle do not generate more ROS than isometric contractions that do not cause damage. This finding is supported by the observation that lengthening contraction protocols with stretches of 30, 40, and 50% L_f clearly damaged mouse LMB muscles as shown by deficits in isometric force, but the increase in CM-DCF slope associated with each of the lengthening contraction protocols was not different from the increase associated with isometric contractions.

Our main finding is consistent with other studies. Kon and colleagues quantified thiobarbituric acid reactive substances (TBARS) levels in mouse tibialis anterior (TA) muscles immediately after 12 min of lengthening contractions *in situ*. TBARS were elevated after the lengthening contractions, but the increase was not different from the increase observed after shortening contractions (36). Another *in situ* study analyzed 2′,7′-dichlorofluorescein (DCF) fluorescence, melondialdehyde (MDA) levels, glutathione, and antioxidant enzyme activity in muscle homogenates immediately after single lengthening contractions of rabbit TA muscles. DCF fluorescence and MDA levels were not elevated in injured muscles compared with sham controls, and glutathione content and antioxidant enzyme activity did not appear to differ between injured muscles and controls (37). Neither of these studies examined ROS generation during the lengthening contractions, but measures of ROS were not elevated shortly after lengthening contractions beyond control levels and are therefore consistent with our main finding. Several studies report an elevation in ROS after injury, but these studies

do not conflict with ours since the elevation is observed hours to days after the initial injury and are primarily attributed to invading inflammatory cells (17, 36, 38, 39).

Although our observation that ROS levels produced during damaging and non-damaging contraction protocols were not different suggests that changes in the magnitude of ROS generation at the time of injury is not an initiating signal for subsequent inflammation, degeneration, necrosis, or regeneration, our data do not completely rule out a role for ROS in the initiation of degenerative or regenerative processes after injury. ROS indicators based on DCFH or DCFH derivatives are sensitive to a variety of ROS and oxidizing reactions (40). Therefore, the possibility remains that variations in the specific ROS generated by isometric and lengthening contractions may be different although the overall magnitude of detected ROS was not. Moreover, DCFH-based indicators are generally not sensitive to superoxide and show variable sensitivities to nitric oxide and peroxynitrite (40), allowing for the possibility that some ROS vary between isometric and lengthening contractions but were not detected by CM-DCFH in the present study. The fact that a variety of ROS measures failed to show differences after lengthening contractions versus controls argues against this possibility (36, 37). ROS are not only generated within muscle fibers (37, 44, 29, 51, 18), but are also released from muscle during contractions (14, 42, 43). ROS released from muscle fibers may contribute to degenerative or regenerative processes following injury, based on the modulation of injury caused by manipulation of extracellular antioxidants (44, 45). Because CM-DCFH is retained within the muscle fibers, released ROS were not detected in the present study, and we are unable to rule out the

possibility that *extracellular* ROS are involved in the initiation of downstream processes after injury.

An additional finding of our study was that muscles that were initially exposed to lengthening contractions with stretches of 50% L_f showed reduced ROS generation during a subsequent series of isometric contractions, compared with controls. Moreover, within this experimental group, there was a negative correlation between the force deficit induced by the stretches of 50% L_f and the change in CM-DCF slope during the isometric contractions performed after 10 min. This observation indicates that greater damage correlated with less ROS generation during ensuing contractions. Although this relationship does not necessarily imply causation, if enough damage occurs during lengthening contractions (e.g. 60% force deficit as in the LC group with stretches of 50% L_f), the muscle's ability to produce ROS appears to be impaired. Force dropped steadily *during* the LC protocol with stretches of 50% L_f, likely due to mechanical damage to force generating or force transmitting structures (46, 47) or the excitation-contraction coupling apparatus (48), but this damage did not appear to immediately disrupt the pathways involved in ROS production, as the "ROS deficit" was not apparent until 10 min later. To our knowledge a link between muscle damage and an impaired ability to produce ROS has not been established and we cannot speculate regarding the mechanism at this time. The link between muscle damage and ROS generation may represent an interesting topic of exploration in future studies, although *in vivo* strains of approximately 50% relative to fiber (fascicle) length seem to indicate an upper limit (29-33) and the result described here may only be applicable in rare instances of severe stretch.

Our hypothesis was partially based on the expectation that passive stretches would generate ROS, but we did not detect an increase in CM-DCF fluorescence during passive stretches. In agreement with our findings, passive stretches of single flexor digitorum brevis (FDB) fibers estimated to be of 10-15% strain did not increase 6-carboxy-2′,7′-dichlorofluorescein fluorescence (25) or CM-DCF fluorescence (23), although contradictory findings have been reported. DCF fluorescence increased during stretches of 20% of whole extensor digitorum longus muscles (22), 15% of strain of C2C12 myotubes (22), and 8% stretch of cardiac myocytes (24), and ethidium fluorescence was increased after 15% stretches of single FDB fibers (23). Conflicting results may be due to variations in stretch protocols, indicators, and cell or muscle type, or ROS generation during passive stretch may sometimes fall below the detection limits of commonly used methods. In any case, our results suggest that any production of ROS elicited by passively stretching muscles is minimal in comparison to the ROS produced as a byproduct of contractile activity.

Our main finding that lengthening contractions do not generate more intracellular ROS than isometric contractions has several implications. First, the magnitude of intracellular ROS generated at the time of injury is probably not an initiating signal for subsequent inflammation, degeneration, necrosis, and regeneration, although other aspects of ROS generation (e.g. composition or localization) may be important. A second implication of our finding is that the sources responsible for contraction-induced ROS generation are not sensitive to stretch. Although we did not examine the source of ROS generation in the present study, others have suggested that non-mitochondrial sources (18, 19) and specifically, NADPH oxidase (20, 21) contribute to ROS

generation during muscle contractions. While NADPH oxidase appears to be stretch-sensitive in cardiac muscle cells (24), this may not be the case in skeletal muscle. Finally, our data suggest that ROS generation during muscle contraction is highly robust. The ability to produce ROS was intact during and immediately after damaging lengthening contractions, except under circumstances of large stretch and severe damage. One could speculate that beneficial adaptations thought to result from ROS production during contractions (49, 50) can occur despite moderate muscle damage.

Acknowledgements

This work was supported by NIH grant AG-020591 to SVB.

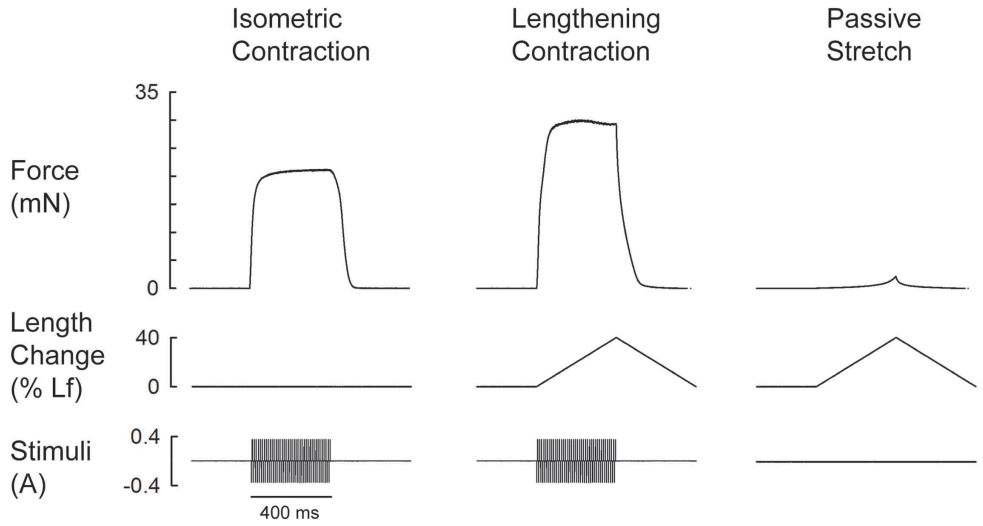

Figure 2.1: Representative force responses during a single isometric contraction, lengthening contraction and passive stretch. Imposed length change and activation stimuli are also shown.

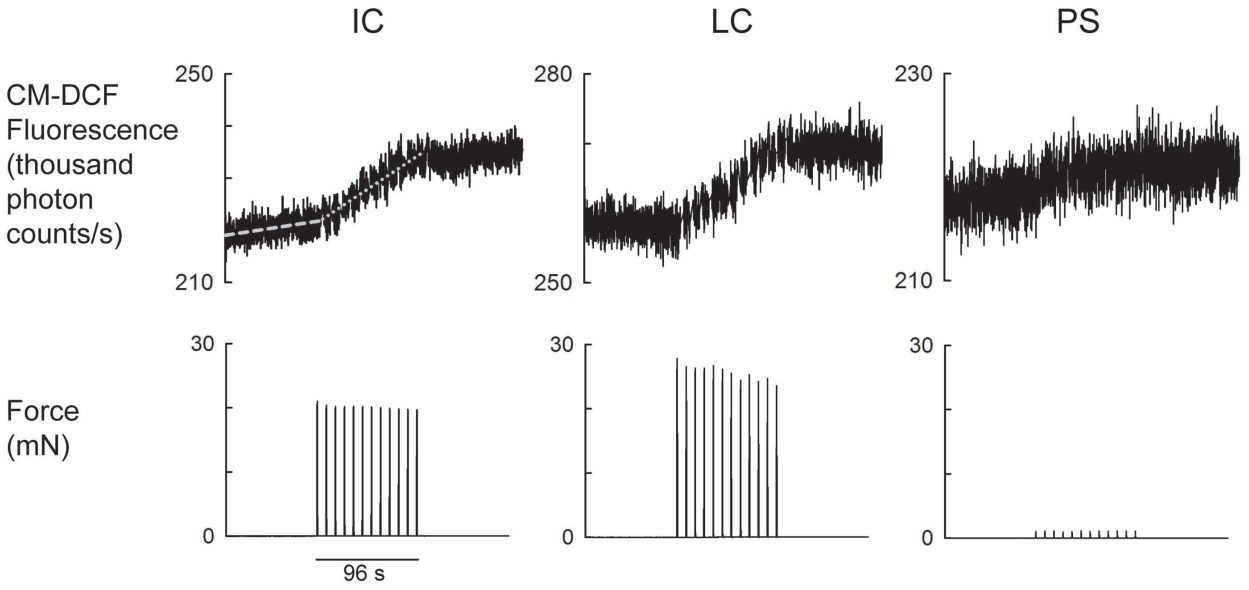

Figure 2.2: Representative force responses during series of 12 isometric contractions, lengthening contractions, and passive stretches, and simultaneous CM-DCF records. Lines were fit to the CM-DCF fluorescence signal during a resting period (dashed line) and during the contractions (dotted line) and the slopes were calculated. The same analysis was performed for lengthening contraction and passive stretch protocols.

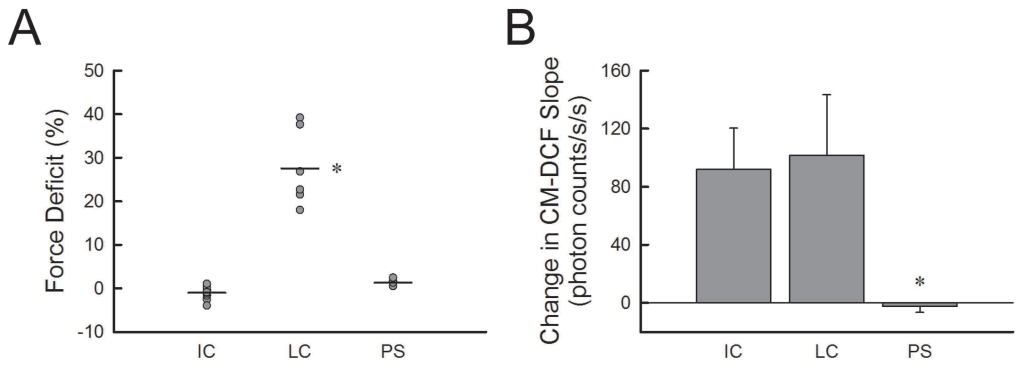

Figure 2.3: Effect of isometric contractions, lengthening contractions (40% L_f), and passive stretches (40% L_f) on (A) force deficit and (B) change in CM-DCF slope. Force deficits are expressed as a percentage of the pre-protocol force and each symbol represents data from an individual muscle. Horizontal lines indicate the mean force deficit for each group. Changes in the slope of the CM-DCF fluorescence are expressed in photon counts per second per second and each bar represents the means ± SD. ∗indicates significant difference from the other two groups. The number of LMB muscles = 14 (IC), 6 (LC), and 6 (PS).

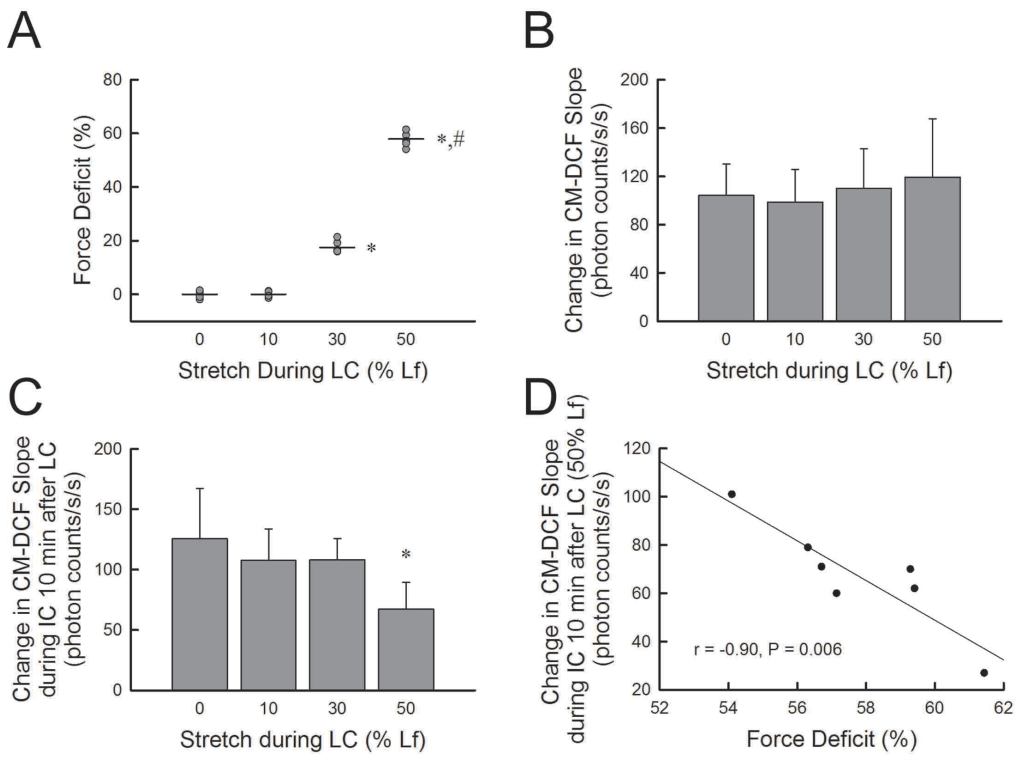

Figure 2.4: Effect of lengthening contractions on (A) force deficit and (B) change in CM-DCF slope for stretches of several magnitudes expressed as a percentage of muscle fiber length (% L_f). Force deficits are expressed as a percentage of the pre-protocol force and each symbol represents data from an individual muscle. Horizontal lines indicate the mean force deficit for each group. LC with 30% and 50% stretches produced force deficits while LC with 10% and 0% stretches did not. ∗indicates significant difference from 0% and 10% groups and #indicates significant difference from 30% group. Changes in the slope of the CM-DCF fluorescence are expressed in photon counts per second per second and each bar indicates the mean ± SD. There were no differences between groups. (C) Changes in CM-DCF slope during IC performed ten minutes after LC with stretches of several magnitudes. Each bar indicates the mean ± SD. ∗indicates significant difference from 0% group. (D) Negative correlation between the change in CM-DCF slope 10 min after LC (stretches of 50% L_f) and the force deficit. Each symbol represents data from an individual muscle. The number of LMB muscles = 8 (0%), 6 (10%), 6 (30%), and 7 (50%).

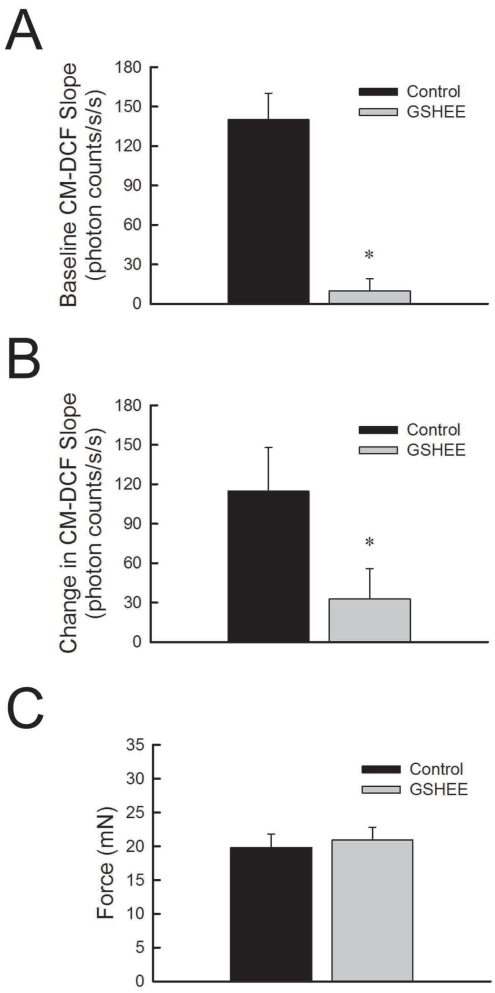

Figure 2.5: Data are shown for (A) baseline CM-DCF slope, (B) the change in CM-DCF slope with the onset of isometric contractions, and (C) force generation in millinewtons for control LMB muscles (black bars) and LMB muscles exposed to glutathione reduced ethyl ester (GSHEE) treatment (gray bars). ∗indicates significant difference from control group. The number of LMB muscles = 3 (Control) and 3 (GSHEE).

Experiment series and group	Number of LMB muscles*	Fiber length (mm)	CSA (mm²)	Pre-protocol force (mN)	Baseline CM-DCF slope (photon counts/s/s)
Series 1:					
IC	14	2.1 ± 0.4†	0.13 ± 0.02	19.7 ± 2.3	23 ± 21
LC	6	1.9 ± 0.2	0.13 ± 0.01	19.1 ± 1.4	16 ± 19
PS	6	2.1 ± 0.2	0.13 ± 0.02	19.2 ± 1.2	9 ± 13
Series 2:					
0%	8	2.0 ± 0.3	0.12 ± 0.01	18.9 ± 2.4	-3 ± 25
10%	6	2.2 ± 0.3	0.12 ± 0.01	18.5 ± 2.5	13 ± 13
30%	6	1.8 ± 0.2	0.12 ± 0.02	18.8 ± 2.4	11 ± 13
50%	7	1.8 ± 0.2	0.13 ± 0.01	19.1 ± 3.4	10 ± 28
Series 3:					
Control	3	2.1 ± 0.3	0.13 ± 0.01	17.5 ± 1.7	140 ± 20
GSHEE	3	2.0 ± 0.3	0.13 ± 0.02	18.6 ± 2.1	10 ± 09‡

Table 2.1: Experimental groups of LMB muscles are not different prior to IC, LC, or PS. Comparisons are made between experimental groups within each series of experiments. Values are means ± SD.*1 LMB muscle taken from each mouse.†1 value missing. ‡significantly different from control group

References

1. Tiidus PM, editor. Skeletal muscle damage and repair. Champaign: Human Kinetics; 2008.

2. Brooks SV, Faulkner JA. Contraction-induced injury: recovery of skeletal muscles in young and old mice. Am J Physiol Cell Physiol. 1990 Mar; 258(3):C436-42.

3. Rader EP, Faulkner JA. Recovery from contraction-induced injury is impaired in weight-bearing muscles of old male mice. J Appl Physiol. 2006 Feb; 100(2):656-61.

4. Chiu YH, Hornsey MA, Klinge L, Jørgensen LH, Laval SH, Charlton R, Barresi R, Straub V, Lochmüller H, Bushby K. Attenuated muscle regeneration is a key factor in dysferlin-deficient muscular dystrophy. Hum Mol Genet. 2009 Jun; 18(11):1976-89.

5. Rooney JE, Gurpur PB, Yablonka-Reuveni Z, Burkin DJ. Laminin-111 restores regenerative capacity in a mouse model for α7 integrin congenital myopathy. Am J Pathol. 2009 Jan; 174(1):256-64.

6. Lawlor MW, Alexander MS, Viola MG, Meng H, Joubert R, Gupta V, Motohashi N, Manfready RA, Hsu CP, Huang P, Buj-Bello A, Kunkel LM, Beggs AH, Gussoni E. Myotubularin-deficient myoblasts display increased apoptosis, delayed proliferation, and poor cell engraftment. Am J Pathol. 2012 Sep; 181(3):961-8.

7. Silder A, Heiderscheit BC, Thelen DG, Enright T, Tuite MJ. MR observations of long-term musculotendon remodeling following a hamstring strain injury. Skeletal Radiol. 2008 Dec; 37(12):1101-9.

8. Bergamini CM, Gambetti S, Dondi A, Cervellati C. Oxygen, reactive oxygen species and tissue damage. Curr Pharm Des. 2004; 10(14):1611-26.

9. Allen RG, Tresini M. Oxidative stress and gene regulation. Free Radic Biol Med. 2000 Feb; 28(3):463-99.

10. Jackson MJ, Papa S, Bolaños J, Bruckdorder R, Carlsen H, Elliott RM, Flier J, Griffiths HR, Heales S, Holst B, Lorusso M, Lund E, Øivind Moskaug J, Moser U, Di Paola M, Polidori MC, Signorile A, Stahl W, Viña-Ribes J, Astley SB. Antioxidants, reactive oxygen and nitrogen species, gene induction and mitochondrial function. Mol Aspects Med. 2002 Feb-Jun; 23(1-3):209-85.

11. Powers SK, Duarte J, Kavazis AN, Talbert EE. Reactive oxygen species are signalling molecules for skeletal muscle adaptation. Exp Physiol. 2010 Jan; 95(1):1-9.

12. Barbieri E, Sestili P. Reactive oxygen species in skeletal muscle signaling. J Signal Transduct. 2012; 2012:982794.

13. Reid MB, Haack KE, Franchek KM, Valberg PA, Kobzik L, West MS. Reactive oxygen in skeletal muscle. I. Intracellular oxidant kinetics and fatigue *in vitro*. J Appl Physiol. 1992 Nov; 73(5):1797-804.

14. Silveira LR, Pereira-Da-Silva L, Juel C, Hellsten Y. Formation of hydrogen peroxide and nitric oxide in rat skeletal muscle cells during contractions. Free Radic Biol Med. 2003 Sep; 35(5):455-64.

15. Palomero J, Pye D, Kabayo T, Spiller DG, Jackson MJ. *In situ* detection and measurement of intracellular reactive oxygen species in single isolated mature skeletal muscle fibers by real time fluorescence microscopy. Antioxid Redox Signal. 2008 Aug; 10(8):1463-74.

16. Zuo L, Nogueira L, Hogan MC. Reactive oxygen species formation during tetanic contractions in single isolated Xenopus myofibers. J Appl Physiol. 2011 Sep; 111(3):898-904.

17. Liao P, Zhou J, Ji LL, Zhang Y. Eccentric contraction induces inflammatory responses in rat skeletal muscle: role of tumor necrosis factor-α. Am J Physiol Regul Integr Comp Physiol. 2010 Mar; 298(3):R599-607.

18. Vasilaki A, Csete M, Pye D, Lee S, Palomero J, McArdle F, Van Remmen H, Richardson A, McArdle A, Faulkner JA, Jackson MJ. Genetic modification of the manganese superoxide dismutase/glutathione peroxidase 1 pathway influences intracellular ROS generation in quiescent, but not contracting, skeletal muscle cells. Free Radic Biol Med. 2006 Dec; 41(11):1719-25.

19. Michaelson LP, Shi G, Ward CW, Rodney GG. Mitochondrial redox potential during contraction in single intact muscle fibers. Muscle Nerve. 2010 Oct; 42(4):522-9.

20. Liu Y, Hernández-Ochoa EO, Randall WR, Schneider MF. NOX2-dependent ROS is required for HDAC5 nuclear efflux and contributes to HDAC4 nuclear efflux during intense repetitive activity of fast skeletal muscle fibers. Am J Physiol Cell Physiol. 2012 Aug; 303(3):C334-47.

21. Sakellariou GK, Vasilaki A, Palomero J, Kayani A, Zibrik L, McArdle A, Jackson MJ. Studies of mitochondrial and nonmitochondrial sources implicate nicotinamide adenine dinucleotide phosphate oxidase(s) in the increased skeletal muscle superoxide generation that occurs during contractile activity. Antioxid Redox Signal. 2013 Feb; 18(6):603-21.

22. Chambers MA, Moylan JS, Smith JD, Goodyear LJ, Reid MB. Stretch-stimulated glucose uptake in skeletal muscle is mediated by reactive oxygen species and p38 MAP-kinase. J Physiol. 2009 Jul; 587(13):3363-73.

23. Palomero J, Pye D, Kabayo T, Jackson MJ. Effect of passive stretch on intracellular nitric oxide and superoxide activities in single skeletal muscle fibres: Influence of ageing. Free Radic Res. 2012 Jan; 46(1):30-40.

24. Prosser BL, Ward CW, Lederer WJ. X-ROS signaling: rapid mechano-chemo transduction in heart. Science. 2011 Sep; 333(6048):1440-5.

25. Khairallah RJ, Shi G, Sbrana F, Prosser BL, Borroto C, Mazaitis MJ, Hoffman EP, Mahurkar A, Sachs F, Sun Y, Chen YW, Raiteri R, Lederer WJ, Dorsey SG, Ward CW. Microtubules underlie dysfunction in duchenne muscular dystrophy. Sci Signal. 2012 Aug; 5(236):ra56.

26. Ng R, Metzger JM, Claflin DR, Faulkner JA. Poloxamer 188 reduces the contraction-induced force decline in lumbrical muscles from *mdx* mice. Am J Physiol Cell Physiol. 2008 Jul; 295(1):C146-50.

27. Claflin DR, Brooks SV. Direct observation of failing fibers in muscles of dystrophic mice provides mechanistic insight into muscular dystrophy. Am J Physiol Cell Physiol. 2008 Feb; 294(2):C651-8.

28. Brooks SV, Faulkner JA. Severity of contraction-induced injury is affected by velocity only during stretches of large strain. J Appl Physiol. 2001 Aug; 91(2):661-6.

29. Shin DD, Hodgson JA, Edgerton VR, Sinha S. *In vivo* intramuscular fascicle-aponeuroses dynamics of the human medial gastrocnemius during plantarflexion and dorsiflexion of the foot. J Appl Physiol. 2009 Oct; 107(4):1276-84.

30. Kinugasa R, Hodgson JA, Edgerton VR, Sinha S. Asymmetric deformation of contracting human gastrocnemius muscle. J Appl Physiol. 2012 Feb; 112(3):463-70.

31. Guilhem G, Cornu C, Guével A. Muscle architecture and EMG activity changes during isotonic and isokinetic eccentric exercises. Eur J Appl Physiol. 2011 Nov; 111(11):2723-33.

32. Vasavada AN, Brault JR, Siegmund GP. Musculotendon and fascicle strains in anterior and posterior neck muscles during whiplash injury. Spine. 2007 Apr; 32(7):756-65.

33. Rehorn MR, Blemker SS. The effects of aponeurosis geometry on strain injury susceptibility explored with a 3D muscle model. J Biomech. 2010 Sep; 43(13):2574-81.

34. Chleboun GS, France AR, Crill MT, Braddock HK, Howell JN. *In vivo* measurement of fascicle length and pennation angle of the human biceps femoris muscle. Cells Tissues Organs. 2001; 169(4):401-9.

35. Shkryl VM, Martins AS, Ullrich ND, Nowycky MC, Niggli E, Shirokova N. Reciprocal amplification of ROS and Ca^{2+} signals in stressed *mdx* dystrophic skeletal muscle fibers. Pflugers Arch. 2009 Sep; 458(5):915-28.

36. Kon M, Tanabe K, Lee H, Kimura F, Akimoto T, Kono I. Eccentric muscle contractions induce greater oxidative stress than concentric contractions in skeletal muscle. Appl Physiol Nutr Metab. 2007 Apr; 32(2):273-81.

37. Best TM, Fiebig R, Corr DT, Brickson S, Ji L. Free radical activity, antioxidant enzyme, and glutathione changes with muscle stretch injury in rabbits. J Appl Physiol. 1999 Jul; 87(1):74-82.

38. McArdle A, van der Meulen JH, Catapano M, Symons MC, Faulkner JA, Jackson MJ. Free radical activity following contraction-induced injury to the extensor digitorum longus muscles of rats. Free Radic Biol Med. 1999 May; 26(9-10):1085-91.

39. Pizza FX, Peterson JM, Baas JH, Koh TJ. Neutrophils contribute to muscle injury and impair its resolution after lengthening contractions in mice. J Physiol. 2005 Feb; 562(3):899-913.

40. Zuo L, Clanton TL. Detection of reactive oxygen and nitrogen species in tissues using redox-sensitive fluorescent probes. Methods Enzymol. 2002; 352:307-25.

41. Lambertucci RH, dos Reis Silveira L, Hirabara SM, Curi R, Sweeney G, Pithon-Curi TC. Effects of moderate electrical stimulation on reactive species production by primary rat skeletal muscle cells: Cross talk between superoxide and nitric oxide production. J Cell Physiol. 2012 Jun; 227(6):2511-8.

42. Reid MB, Shoji T, Moody MR, Entman ML. Reactive oxygen in skeletal muscle. II. Extracellular release of free radicals. J Appl Physiol. 1992 Nov; 73(5):1805-9.

43. Pattwell DM, McArdle A, Morgan JE, Patridge TA, Jackson MJ. Release of reactive oxygen and nitrogen species from contracting skeletal muscle cells. Free Radic Biol Med. 2004 Oct; 37(7):1064-72.

44. Zerba E, Komorowski TE, Faulkner JA. Free radical injury to skeletal muscles of young, adult, and old mice. Am J Physiol. 1990 Mar; 258(3):C429 – 35.

45. Park JW, Qi WN, Cai Y, Zelko I, Liu JQ, Chen LE, Urbaniak JR, Folz RJ. Skeletal muscle reperfusion injury is enhanced in extracellular superoxide dismutase knockout mouse. Am J Physiol Heart Circ Physiol. 2005 Jul; 289(1):H181-7.

46. Fridén J, Sjöström M, Ekblom B. Myofibrillar damage following intense eccentric exercise in man. Int J Sports Med. 1983 Aug; 4(3):170-6.

47. Lovering RM, De Deyne PG. Contractile function, sarcolemma integrity, and the loss of dystrophin after skeletal muscle eccentric contraction-induced injury. Am J Physiol Cell Physiol. 2004 Feb; 286(2):C230-8.

48. Ingalls CP, Warren GL, Williams JH, Ward CW, Armstrong RB. E-C coupling failure in mouse EDL muscle after *in vivo* eccentric contractions. J Appl Physiol. 1998 Jul; 85(1):58-67.

49. McArdle A, Pattwell D, Vasilaki A, Griffiths RD, Jackson MJ. Contractile activity-induced oxidative stress: cellular origin and adaptive responses. Am J Physiol Cell Physiol. 2001 Mar; 280(3):C621-7.

50. Vasilaki A, McArdle F, Iwanejko LM, McArdle A. Adaptive responses of mouse skeletal muscle to contractile activity: The effect of age. Mech Ageing Dev. 2006 Nov; 127(11):830-9.

Chapter 3

Impaired regeneration in old mice is associated with elevated neutrophil and macrophage accumulation and altered expression of macrophage-related genes

Abstract

Aging is associated with delayed and possibly incomplete repair after skeletal muscle injury, but the underlying mechanisms are not entirely understood. We hypothesized that age-related deficiency in muscle repair is associated with an inappropriate myeloid cell response, specifically a persistence of neutrophils and a delay or reduction in the accumulation of macrophages, especially anti-inflammatory (M2) macrophages. To test our hypothesis, we injured muscles of young and old mice with lengthening contractions *in situ* and analyzed the muscles 2 or 5 d later. Regardless of age, injury increased neutrophil (Gr-1+), total macrophage (CD68+) and M2 macrophage (CD163+) content by 2 d. By 5 d, neutrophils declined and total macrophages increased dramatically while M2 macrophages increased to a lesser extent. We found no evidence of persisting neutrophils or reduced accumulation of M2 macrophages in old muscles. Instead, we generally found more neutrophils and macrophages (total and M2) in muscles of old mice at both time points. Messenger RNA

levels suggested age-related changes in the expression of macrophage-associated genes that have the potential to undermine or impair muscle regeneration. Therefore, the mechanism underlying age-related deficiency in muscle repair may involve altered macrophage function in old mice.

Introduction

Skeletal muscle injuries are common and have a variety of causes, including physical trauma, extreme temperatures, toxin exposure, invasive surgery, ischemia/reperfusion and unloading/reloading. Muscles can also be injured by their own contractions, especially during lengthening contractions when muscles are stretched while activated. Regardless of the cause, the initial insult is followed by degeneration and necrosis of damaged muscle fibers and subsequent regeneration and repair. Muscle repair is delayed and possibly incomplete with advanced age. After injury, muscles from old animals have fewer and smaller regenerating fibers (1, 2), more fibrosis (3-6) and more fat (6) compared with young controls. Failed restoration of normal muscle structure is accompanied by persistent and likely permanent deficits in force generation (7-10). Although the age-related deficiency in muscle repair is well established, the underlying mechanisms are incompletely understood.

Successful muscle regeneration relies on muscle stem cells known as satellite cells. In response to injury, satellite cells exit their normal quiescent state and proliferate, differentiate, and fuse together to form new myofibers or fuse to existing fibers to repair damage (11). Satellite cells from old animals are capable of repair, but

systemic and local aspects of the aged environment hinder the ability of satellite cells to successfully regenerate injured muscle (2, 12-14). Myeloid cells accumulate in injured muscle and thus contribute to the local environment of satellite cells, and a growing body of evidence suggests that myeloid cells play critical roles in muscle repair and regeneration. Neutrophils are the first to accumulate in injured muscle, arriving from the circulation within hours of the initial insult. The contribution of neutrophils to muscle repair is not well understood. Possible beneficial roles include facilitating the removal of damaged or necrotic tissue and contributing to subsequent macrophage accumulation (15). However, neutrophils may undermine the repair process by exacerbating damage to muscle fibers. Neutrophils can lyse muscle cells *in vitro* and damage membranes *in vivo* by mechanisms involving reactive oxygen species (16, 17), and preventing neutrophil infiltration after injury has been reported to reduce force deficits and histological damage to muscle fibers (18-21).

Following the arrival of neutrophils, macrophages begin to accumulate in injured muscle. Macrophage accumulation is thought to arise from the infiltration and differentiation of circulating monocytes, but the proliferation of macrophages that are already present in the muscle may also contribute (22, 23). Macrophages generally contribute to muscle repair. Preventing or delaying the accumulation of monocytes and/or macrophages induced by muscle injury results in delayed clearance of necrotic fibers, fewer or smaller regenerating fibers, increased fibrosis and more fat relative to controls (22, 24-28).

The mechanisms by which macrophages contribute to muscle repair appear to depend on macrophage phenotype. *In vitro*, macrophages can take on pro-inflammatory

(M1) or anti-inflammatory (M2) phenotypes based on their environment. After muscle injury *in vivo*, pro- and anti-inflammatory macrophages are also observed and have been referred to as M1 and M2 macrophages, although in the complex *in vivo* environment, macrophages do not perfectly conform to phenotypic categories defined *in vitro* (29, 30). After injury, M1 macrophages accumulate within 1-2 days. Because they invade muscle fibers, they are thought to contribute to repair by the removal of damaged or necrotic tissue (31-33). M1 macrophage numbers decline within a few days as the number of M2 macrophages increases. M2 macrophages can remain in the muscle for many days and their presence generally coincides with the regenerative stage of muscle repair (31-33). M2 macrophages may contribute to muscle repair by regulating satellite cell function, as M2 macrophages have been reported to stimulate proliferation and differentiation of muscle precursor cells *in vitro* (22, 33, 34).

The shift from M1 to M2 macrophages appears to be important for successful muscle regeneration. The M1 to M2 phenotype shift was impaired in mice deficient in IL-10 after muscle injury and was associated with persistent muscle membrane lesions, fewer regenerating fibers and reduced fiber growth in comparison to wild type mice (33). An impaired or delayed shift from M1 to M2 macrophages could be detrimental due to the persistence of M1 macrophages or due to the decreased number of M2 macrophages, as mice carrying a mutation that blocked downstream induction of M2- but not M1-specific genes showed severe defects in muscle fiber regeneration (35).

Despite the impairments in muscle regeneration observed in old animals as well as the accumulating evidence that myeloid cells play a critical role in muscle repair following injury, the effect of aging on the magnitude and timing of the myeloid cell

response has received little attention. The degree to which the myeloid cell response changes with age or how the changes may be associated with the age-related deficiency in muscle repair is largely unknown. Therefore, in the present study we tested the hypothesis that age-related deficiency in muscle repair is associated with an inappropriate myeloid cell response, specifically a persistence of neutrophils and either impaired total macrophage accumulation or a delayed switch from M1 to M2 macrophages. To test our hypothesis, we injured muscles of young and old mice with lengthening contractions *in situ* and analyzed the muscles 2 or 5 days later. Muscle damage and repair was determined by functional and histological measures, neutrophil and macrophage content was determined by immunohistochemistry and immunofluorescence, and myeloid cell function was studied by RT-qPCR.

Methods

Animals. Male C57BL6 young (3-5 mo) and old (25-27 mo) mice were housed in a specific-pathogen-free facility at the University of Michigan until experimentation. Between experimental procedures, mice were housed in a separate specific-pathogen-free return room. All animal use procedures were approved by the University of Michigan Committee on the Use and Care of Animals (UCUCA).

In situ evaluation of contractile properties. Procedures for *in situ* evaluation of muscle contractile properties were based on previous studies (7, 36). Each mouse was anesthetized with 3% isoflurane in oxygen delivered at a rate of 1 L/min. Anesthesia was maintained throughout *in situ* procedures with 2% isoflurane in oxygen and depth of

anesthesia was confirmed by failure of the mouse to respond to tactile stimuli. Ophthalmic ointment was placed on the mouse's eyes to prevent corneal drying and trauma and this was re-administered throughout *in situ* procedures. The mouse was placed on a platform warmed to 37 °C with a circulating water bath. The hind limb fur was removed with animal clippers followed by a minimal amount of fur removal cream. The skin was disinfected with chlorhexidine and a small incision was made at the ankle to expose the distal tendon of the EDL muscle. Another small incision was made distal to the knee to expose the peroneal nerve. A secure knot was tied around the tendon with 6.0 braided silk suture. The hind limb was immobilized by pinching the knee and the foot with small clamps secured to the platform. Using the tails of the silk suture, the intact tendon was tied to the lever arm of a servomotor (300C-LR-FP, Aurora Scientific), which controlled the length of the muscle and measured the force generated. A computer with custom-designed software controlled stimulus pulses, the servomotor, and collected and stored force data. The small area of exposed tendon was kept moist by frequent administration of sterile saline. The EDL muscle was activated using a stimulator (701C, Aurora Scientific) and platinum electrodes placed under the peroneal nerve. A stimulus pulse duration of 0.2 ms was used for all contractions. Stimulation current and muscle length were adjusted in order to elicit maximum twitch force. Tetanic contractions of 200 ms duration were elicited with trains of pulses and the frequency of the pulses was increased until the force plateaued at the maximum isometric force (P_o), typically at a frequency of 200 Hz. Finally, small adjustments in the ankle position were made to elicit maximum isometric tetanic force. The tetanic contractions were spaced 1 min apart to prevent fatigue. Optimal muscle length (L_o), defined as the muscle length at

which maximum isometric force is achieved, was measured with calipers using the knee to estimate the location of the proximal end of the EDL muscle. Optimal muscle fiber length (L_f) was determined by multiplying L_o by the previously determined L_f-to-L_o ratio of 0.45 (37).

In situ lengthening contraction protocol. Following evaluation of contractile properties, the EDL muscle was exposed to a protocol of 75 lengthening contractions spaced 4 s apart for a total duration of 5 min. Each contraction was 300 ms in duration. 100 ms after the onset of stimulation, near maximum isometric force was generated and a stretch of 20% strain relative to L_f was initiated. Muscles were lengthened at the appropriate rate (1 L_f/s) to cause the peak of the stretch to coincide with the end of the tetanic stimulation. Ten minutes after the lengthening contraction protocol, the muscle was re-lengthened to achieve maximum twitch tension and P_o was re-measured. The small incisions at the ankle and distal to the knee were closed with 7.0 sterile monofilament nylon suture and bathed with povidone-iodine solution, and mice were monitored until they recovered from anesthesia.

In vitro evaluation of contractile properties. Two or five days following administration of the lengthening contraction protocol, mice were again evaluated for P_o. Procedures for the *in vitro* evaluation of EDL contractile properties have been previously published (37). Each mouse was anesthetized with an intraperitoneal injection of Avertin (tribromoethanol, 250 mg/kg) (chemical components from Sigma-Aldrich). After the mouse was unresponsive to a tactile stimulus, the injured EDL muscle was isolated from the hindlimb of the mouse. 5-0 silk suture was tied to the proximal and distal tendons of the muscle and the muscle was placed into a chamber containing Krebs

Mammalian Ringer solution composed of (in mM): 137 NaCl, 5 KCl, 2 $CaCl_2 \cdot 2H_2O$, 1 $MgSO_4 \cdot 7H_2O$, 1 NaH_2PO_4, 24 $NaHCO_3$, 11 glucose, 0.03 tubocurarine chloride. The solution was maintained at 25 °C and bubbled with 95% O_2-5% CO_2 to maintain a pH of 7.4. The proximal tendon was attached to a stationary object and the distal tendon was attached to a force transducer (BG-50, Kulite Semiconductor Products). Muscle activation was accomplished by electric field stimulation via a high-power current stimulator (701C, Aurora Scientific) and parallel plate electrodes.

A computer and custom-designed software controlled stimulus pulses and collected and stored force data. Stimulus pulses of 0.2 ms in duration were used for all contractions. Stimulation current and the muscle length were adjusted in order to elicit maximum twitch force. A digital calipers was used to measure L_o. Muscles were held at L_o and tetanic contractions of 300 ms in duration were elicited with trains of pulses. The frequency of the pulses was increased until the force plateaued at P_o, typically at frequencies from 150-200 Hz. The tetanic contractions were spaced 1 min apart to prevent fatigue. Optimal muscle fiber length (L_f) was determined as previously mentioned. Force deficit was defined as the difference between the P_o measured immediately prior to lengthening contractions and the P_o measured two days after lengthening contractions expressed as a percentage of the pre-injury P_o. Following evaluation of the injured EDL, the contralateral EDL was removed and evaluated as described. Muscles were trimmed of their tendons, weighed, and cut in half. Half of each muscle was immersed in Tissue Freezing Medium (Electron Microscopy Sciences) and frozen in isopentane cooled by liquid nitrogen. The other half of each muscle was submerged in an RNA stabilization reagent (RNA*later*, QIAGEN). The mouse was

euthanized with an overdose of Avertin followed by induction of a bilateral pneumothorax.

Histology, immunohistochemistry and immunofluorescence. EDL muscles were cut into 10 μm thick sections on a cryostat. The sections were fixed in cold acetone and stained with Hematoxylin (Ricca Chemical Company) and Eosin Y (EMD Millipore). The number of injured fibers was counted per section and expressed as a percentage of the total number of fibers. Injured fibers included those with a swollen appearance, pale or variable staining, and obvious infiltration of inflammatory cells (36). Basophilic fibers with central nuclei were identified as regenerating fibers (38). An image analysis program (Image J) was used to count fibers and measure cross-sectional areas of entire sections and individual regenerating fibers.

Muscle sections were analyzed for neutrophil and macrophage content using immunohistochemistry. Sections were fixed in cold acetone and air-dried. Sections were exposed to BLOXALL solution to block endogenous peroxidase activity followed by 10% normal rabbit or goat serum in PBS (Phosphate Buffer Solution, Fisher Scientific) to block non-specific binding of subsequent antibodies. Neutrophils were detected with a rat anti-mouse Gr-1 antibody (RB6-8C5, 1:50 dilution, BD Pharmingen, 550291) diluted in PBS containing 10% rabbit serum and macrophages were detected with a rat anti-mouse CD68 antibody (FA-11, 1:1000, AbD Serotec, MCA1957) diluted in PBS containing 10% rabbit serum or with a rabbit anti-mouse CD163 antibody (M-96, 1:1000, Santa Cruz Biotechnology, sc-33560) diluted in PBS containing 10% goat serum. After incubation in primary antibodies, sections were exposed to biotinylated mouse adsorbed rabbit anti-rat IgG (Gr-1 and CD68) or biotinylated goat anti-rabbit IgG (CD163) in PBS

containing 10% rabbit or goat serum, respectively. Following exposure to the secondary antibodies, the sections were treated with the VECTASTAIN Elite ABC reagent containing peroxidase followed by the peroxidase substrate 3, 3'-diaminobenzidine (ImmPACT DAB). The sections were rinsed with PBS after each step except after the treatment with serum. All reagents were from Vector Laboratories unless stated otherwise. The Image J program was used to count the number of neutrophils or macrophages in one transverse section from the middle of each muscle. In the periphery, neutrophils express high levels of Gr-1 while monocytes express low or no levels of Gr-1 (39). Therefore, dark brown cells indicating high levels of Gr-1 were counted as neutrophils while the occasional light brown cell of similar size was not counted. Both light and dark brown cells were counted as macrophages in sections treated with reagents for CD68 and CD163 detection. The Image J program was used to calculate the area of each section and neutrophil or macrophage content was expressed per mm^3 of muscle. We also normalized neutrophil and macrophage content to the initial force deficit in order to provide a measure of the cellular response to a given amount of damage. Initial force deficit provides a valid and reproducible measure of the totality of the injury (40) and therefore we used the initial force deficit as a measure of initial damage.

Some muscle sections were analyzed for double labeling of either CD68 and CD163 or CD163 and CD301 with immunofluorescence. Sections were fixed in cold acetone and air-dried. Sections were exposed to 1% BSA (Jackson ImmunoResearch Laboratories) in PBS to block non-specific binding of subsequent antibodies and then exposed to a mixture of primary antibodies in PBS containing 1% BSA. To detect CD68

and CD163, the primary antibodies and concentrations were the same as for immunohistochemistry, except that anti-CD163 was diluted to 1:200 for immunofluorescence. To detect CD301, a goat anti-mouse CD301 IgG antibody was used (1:400, R&D Systems, AF4938). After exposure to primary antibodies, the sections were exposed to a mixture of appropriate secondary antibodies in PBS containing 1% BSA. Secondary antibodies were Alexa Fluor 594 goat anti-rat IgG (112-585-167), Alexa Fluor 594 bovine anti-goat IgG (805-585-180), and Alexa Fluor 488 donkey anti-rabbit IgG (711-545-152) and were purchased from Jackson ImmunoResearch Laboratories. Sections were then exposed to DAPI (D9564, Sigma-Aldrich) to detect nuclei and treated with ProLong Gold Antifade Reagent (P36930, Life Technologies). The sections were rinsed with PBS after each step except after the treatment with 1% BSA. All sections for histology, immunohistochemistry, and immunofluorescence were imaged with a Nikon E-800 microscope.

Blood analysis. Blood was collected via a scalpel nick of the lateral tail vein (50-100 μl). Whole blood was analyzed with a cell counter (Hemavet 950FS, Drew Scientific) to determine circulating white blood cell counts.

Gene expression. Muscle halves were homogenized in QIAzol lysis reagent (QIAGEN). RNA was isolated using an miRNeasy Mini Kit (QIAGEN) and treated with DNase I (QIAGEN). RNA concentration was measured with a NanoDrop 2000 Spectrophotometer (Thermo Scientific). RNA (2 μg) was reverse transcribed using a QuantiTect Reverse Transcription Kit (QIAGEN), and cDNA was diluted by 5-fold and amplified in a CFX96 real time thermal cycler (Bio-Rad) using a QuantiTect SYBR Green I PCR Kit (QIAGEN) and primers specific for inducible nitric oxide synthase

(iNOS) (41), tumor necrosis factor alpha (TNFα) (41), arginase-1 (Arg1) (33), interleukin-10 (IL-10) (33), and β2-microglobulin (42). Primers were purchased from Integrated DNA Technologies and primer concentration was adjusted to yield PCR efficiencies between 90 and 110%. The presence of single amplicons from qPCR reactions was verified using melting curve analysis. Reactions were performed in duplicate. Preliminary work revealed that mRNA from target genes was undetectable in contralateral muscles so we completed our analysis using only injured muscles. Messenger RNA levels of β2-microglobulin were not altered by age but were elevated 5 days after lengthening contractions relative to 2 days after lengthening contractions. Therefore, we normalized mRNA transcripts to β2-microglobulin and compared young and old samples within each time point. Messenger RNA levels were analyzed by the comparative C_T method (43).

Data analysis. Data are expressed as means ± 1 SEM. To compare two groups, Student's t-tests were used and in cases of non-normal distributions or unequal variance, a Mann-Whitney Rank Sum test was used. To compare multiple groups, a Two Way ANOVA (Age x Day) was used and in cases of non-normal distributions or unequal variance, the data was ranked and a Two Way ANOVA (Age x Day) was used. Significance was set *a priori* at $P < 0.05$.

Results

General characteristics of young (3-5 mo) and old (25-27 mo) groups are shown in Table 1. Muscles from old mice were weaker by all measures (Table 3.1). We did not

detect a significant difference in muscle mass between young and old mice but cross-sectional areas indicated that muscles from old mice were smaller than young (Table 3.1).

Unexpectedly, lengthening contractions caused slightly less initial damage in muscles from old mice relative to young, as assessed by the initial force deficit measured 10 minutes following the lengthening contraction protocol (Figure 3.1). The level of damage increased between 2 and 5 days after lengthening contractions for both age groups as indicated by increases in both force deficit and in the number of muscle fibers showing signs of histological damage as well as a decrease in the total number of fibers (Figure 3.2). Consistent with less initial damage in muscles from old mice, there was less damage in muscles from old mice 2 and 5 days after lengthening contractions, relative to young, according to several measures. Force deficit and the percentage of muscle fibers showing signs of histological damage were lower for muscles of old compared with young mice (Figures 3.2A-3.2B). Finally, the total number of fibers remaining in a cross-section 5 days after lengthening contractions was larger in the muscles of old compared with young mice, suggesting that fewer muscle fibers had completely degenerated in old mice by this time point (Figure 3.2C).

Regenerating fibers were detected in sections from muscles taken 5 days after lengthening contractions. Injured muscles from old mice contained fewer regenerating fibers relative to young, but the difference was not significant (Figure 3.3A). Since fewer regenerating fibers in muscle sections of old mice could be due to less initial damage in this group, we also assessed the cross-sectional area of regenerating fibers as a measure of regeneration. In spite of less initial damage in muscles from old mice,

regenerating fibers in muscle sections from old mice were smaller relative to young (Figures 3.3B-3.3D), consistent with delayed or deficient repair with age.

Neutrophil (Gr-1+ cell) content in muscles from young and old mice increased relative to control levels by 2 days after lengthening contractions (Table 3.2, Figure 3.4, $P < 0.001$ by Two Way (age x injury) ANOVA, injury effect) and then declined between 2 and 5 days after lengthening contractions (Figure 3.4). Neutrophil content was greater in old mice relative to young in control muscles (Table 3.2) and after lengthening contractions (Figure 3.4). The age-associated differences in neutrophil content between young and old mice were amplified when neutrophil content was normalized to initial damage (Figure 3.4B).

The selection of macrophage markers was guided by immunofluorescence data (Figures 3.5-3.6). Mouse CD68 (rat ED1+) is expressed on macrophages and labels early-invading macrophages that accumulate in injured skeletal muscle and invade muscle fibers (32, 33, 44, 45). We originally planned to use CD68 as a marker of M1 macrophages, but immunofluorescence showed that cells that were CD163+ were also CD68+ (Figure 3.5). Therefore we used CD68 as a marker for total macrophage content. CD163 has been used as a marker of M2 macrophages. Mouse CD163 (rat ED2+) labels a population of macrophages that accumulate in injured muscle after CD68+ cells, do not invade muscle fibers and are associated with repair (31-33). Immunofluorescence showed that CD163 co-localized with CD301 (Figure 3.6). CD301 is another marker of M2 macrophages (46, 47) and the co-localization supports the identification of CD163+ cells as M2 macrophages.

Total macrophage (CD68+ cell) content in muscles from young and old mice increased relative to control levels by 2 days after lengthening contractions (Table 3.2, Figure 3.7, $P < 0.001$ by Two Way (age x injury) ANOVA, injury effect) and increased further between 2 and 5 days after lengthening contractions (Figure 3.7). Total macrophage content was not different in control muscles of young and old mice (Table 3.2) and was not different 2 days after lengthening contractions (Figure 3.7A). Five days after lengthening contractions total macrophage content was about 25% lower in muscle from old mice relative to young (Figure 3.7A). However, when total macrophage content was normalized to the amount of initial damage, the outcome was reversed. That is, for a given level of injury, the degree of macrophage accumulation was significantly greater in old mice relative to young at both 2 and 5 days after injury (Figure 3.7B).

M2 macrophage (CD163+ cell) content in muscles from young and old mice increased relative to control levels by 2 days after lengthening contractions (Table 3.2, Figure 3.8, $P = 0.036$ by Two Way (age x injury) ANOVA, injury effect) and increased between 2 and 5 days after lengthening contractions (Figure 3.8). M2 macrophage content was greater in muscles of old compared with young mice both before (Table 3.2) and after lengthening contractions (Figure 3.8). The higher levels of M2 macrophages in muscles of old mice were observed despite less damage in old mice. Thus, the differences in M2 macrophage content between young and old mice were enhanced when M2 macrophage content was normalized to initial damage (Figure 3.8B).

Finally, we examined function of myeloid cells in injured muscles from young and old mice with a focus on macrophages, the dominant cell type. We examined

messenger RNA levels of genes expressed by M1 (iNOS, TNFα) or M2 (Arg1, IL-10) macrophages in injured muscles from young and old mice (Figure 3.9). In old injured muscles, mRNA levels of iNOS and TNFα were not different from young muscles 2 days after lengthening contractions, but were significantly elevated over young levels 5 days after lengthening contractions (Figures 3.9A-3.9D). Messenger RNA levels of Arg1 were also not different between young and old muscles 2 days after lengthening contractions (Figure 3.9E). After 5 days, mRNA levels of Arg1 were increased in old muscles relative to young, but values from old animals were highly variable and the difference was not significant (Figure 3.9F, $P = 0.083$). Two days after lengthening contractions, IL-10 mRNA levels were decreased in old muscles relative to young (Figure 3.9G) with no differences between groups 5 days after lengthening contractions (Figure 3.9H).

Finally, we questioned whether enhanced neutrophil and macrophage content in injured muscles from old mice relative to young reflected a general increase in circulating levels of neutrophils and monocytes with age. In mice that were not subjected to lengthening contractions, circulating levels of neutrophils and monocytes were significantly greater in old animals relative to young (Figure 3.10).

Discussion

Our results indicate that the myeloid cell response to injury was altered in old mice relative to young. However, contrary to our hypothesis, the altered myeloid cell response was not characterized by a persistence of neutrophils, impaired total

macrophage accumulation, or a delay in the accumulation of M2 macrophages. The supporting evidence is that in old muscles, neutrophils did not remain elevated 5 days after lengthening contractions, but similar to the young group, declined between 2 and 5 days. Neutrophil levels were greater 5 days after lengthening contractions in old muscles relative to young, but this does not reflect a persistence of neutrophils since quiescent muscles from old mice also had greater neutrophil content. Five days after injury, total macrophage content was about 25% less in muscles from old mice relative to young, but the smaller number may be explained by the proportional reduction (~20%) in initial damage in muscles of old mice relative to young rather than impaired macrophage accumulation. Furthermore, when total macrophage accumulation was normalized to the amount of initial damage, total numbers of macrophages in injured muscles from old mice were greater compared to the numbers observed in young mice. M2 macrophage content increased in injured muscles between 2 and 5 days after lengthening contractions for both young and old mice, but was greater in old muscles relative to young. Thus, neither total macrophage accumulation nor M2 macrophage accumulation was impaired in injured muscles from old mice.

Although an age-related persistence or impaired/delayed accumulation of leukocytes after muscle injury has been suggested by other studies, these studies are limited by the use of nonspecific leukocyte markers, failure to quantify cellular or protein content, or a failure to normalize data to the amount of initial damage. Prolonged expression (mRNA) of inflammatory markers, including the leukocyte marker CD18, was observed in muscles from old rats up to 3 days after myotoxin injury (48). While this finding could reflect an age-related persistence of neutrophils, macrophage levels would

also affect CD18 expression and actual neutrophil and/or macrophage cell content was not examined. Hamada et al. 2005 found that CD18 mRNA levels were increased in vastus lateralis muscles of young subjects 3 days after downhill running but increased to a lesser degree in muscles of old subjects (49). This finding suggests impaired or delayed leukocyte infiltration with age, but a trend toward less damage in old subjects as reflected by serum levels of creatine kinase was also reported (49). Thus, reduced leukocyte recruitment could explain decreased CD18 mRNA levels, but cellular content of leukocytes was once again not assessed in injured muscles in the Hamada study. Sadeh reported delayed recruitment of macrophages in muscles from old rats injured with myotoxin relative to young controls (1). However, this qualitative study estimated macrophage numbers based on nuclei observed in muscle sections stained with H&E, which would represent multiple cell types including neutrophils and satellite cells. In contrast, the present study, which uses cell specific markers, can not only quantify neutrophil and macrophage content in injured muscles but can also interpret the data with a consideration of the amount of initial damage in young and old muscles.

Instead of an age-related persistence of neutrophils or impaired or delayed macrophage accumulation after injury, the results indicated an enhanced response in the magnitude of neutrophils, total macrophages and M2 macrophages to injury in old relative to young mice. Our observations of enhanced neutrophil and macrophage accumulation in old mice in response to muscle injury is generally supported by other studies. Increased leukocyte infiltration was reported in muscles of old rats compared with young after ischemia/reperfusion injury of plantaris muscles (50). In addition, muscles from adult and old rats displayed elevated CD68 protein content relative to

young, 3 days after a contusion injury (5). Although CD68 content does not necessarily reflect the number of CD68+ cells, this finding generally agrees with ours. Koh et al. 2003 assessed neutrophil (Ly6G+ cells) and macrophage (F4/80+ cells) content after lengthening contractions (51). The authors observed similar levels of injury in young and old groups as assessed by force deficit and the number of injured fibers, but observed almost a 2-fold increase in neutrophils and a trend toward increased macrophages in muscles from old animals relative to young, in agreement with our findings. However, an age-related increase in myeloid cell content after injury is not a universal finding. Paliwal et al. 2012 found no difference in leukocyte (CD11b+ cell) content in muscles from young and old mice 3 and 5 days after a cardiotoxin injury, as assessed by flow cytometry (52). Nevertheless, the majority of studies, including the present study, suggest an age-related increase in leukocyte content after muscle injury.

Our observation of elevated levels of neutrophil and macrophage content in injured muscles from old mice relative to young may reflect a compensatory effect of impaired function of aged myeloid cells. In order to address this question, we measured mRNA levels of genes expressed by different myeloid cell populations after muscle injury. Consistent with previous reports of elevations in iNOS, TNFα, arginase-1, and IL-10 in injured muscles (33, 41, 53) and in myeloid cells isolated from injured muscles (22, 41), we detected iNOS, TNFα, arginase-1, and IL-10 mRNA in injured muscles at both 2 and 5 days after lengthening contractions. Our finding that after 5 days, mRNA levels of iNOS and TNFα were elevated in muscles from old mice relative to young suggests that rather than an age-related impairment of macrophage function, iNOS and TNFα were produced in excess by macrophages in the old mice. In support of this

conclusion, macrophages have been identified as a source of TNFα and iNOS after muscle injury (22, 41) and in the present study, iNOS and TNFα mRNA levels were elevated in muscles of old mice despite fewer macrophages in injured muscles from old compared with young mice at this time point. Although low concentrations of TNFα and some iNOS expression appear to benefit repair (41, 54), an overproduction of TNFα and iNOS can be detrimental. TNFα can inhibit myogenic differentiation *in vitro* and *in vivo*, lead to the degradation of transcription factors critical for muscle regeneration (55, 56) and induce muscle protein degradation and apoptosis (54) while iNOS-expressing macrophages can injure muscle cells *in vitro* (57) and *in vivo* (58). Therefore, excessive TNFα or iNOS production by macrophages could undermine or impair muscle regeneration in aged animals. Macrophages and specifically anti-inflammatory macrophages have been identified as the source of IL-10 after muscle injury (22, 59). After 2 days, we found less IL-10 mRNA in muscles of old mice relative to young, in spite of more CD163+ cells in old muscles as compared with young at this time point. Thus, the age-related decrease in IL-10 mRNA could suggest impaired IL-10 production in aged macrophages. Impaired IL-10 production can be detrimental to muscle repair. Mice lacking IL-10 show persistent fiber damage and greatly slowed regeneration and growth after an unloading/reloading muscle injury (33). IL-10 can contribute to repair by several mechanisms. IL-10 stimulated macrophages promote the proliferation and differentiation of myogenic precursors *in vitro* and *in vivo* (58, 59). IL-10 can also play a regulatory role, suppressing the production of pro-inflammatory cytokines IL-1, IL-6 and TNFα (60), while stimulating production of the growth factor IGF-1 (59). Therefore, insufficient IL-10 production by aged macrophages could lead to deficient repair.

Overall, our findings suggest age-related changes in the expression of macrophage-associated genes, which have the potential to undermine or impair muscle regeneration in aged animals.

An age-related increase in neutrophil and macrophage content in injured muscles may also reflect an increased pool of cells available to respond to the injury or an age-related increase in recruitment signals. The former possibility is supported by our observation of elevated levels of circulating neutrophils and monocytes in old compared with young mice. While correlation does not necessarily imply causation, the possibility exists that more neutrophils and macrophages accumulated in injured muscles of old animals relative to young because more neutrophils and monocytes were available to respond to recruitment signals by damaged muscle. Recruitment signals for neutrophils and monocytes may also be elevated with age. Resident myeloid cells can recruit other inflammatory cells to injured muscle (61). In uninjured muscles we observed more neutrophils in old mice than in young, a finding that is in agreement with others (51). Total macrophages in uninjured muscles were not different between the age groups, also in agreement with other reports (5, 51) but more CD163+ cells were observed in the present study in muscles from old mice relative to young. These findings suggest that muscle displays an age-associated change in the composition of resident myeloid cells. Age-related changes in resident cell populations could affect recruitment of myeloid cells after muscle injury, but this hypothesis remains to be tested.

An unexpected finding of the present study was that we found slightly less damage in muscles from old mice relative to young. Previous studies using the *in situ* EDL injury model using mice of the same strain, sex, and of similar age have found

force deficits that were not different between young and old mice (51, 62) while one study found greater force deficits in old mice (63). It may be that the difference we saw was due to the specific cohort tested. The old mice in the present study generated less absolute force and less specific force than young controls, but significant differences in these measures are not always observed (7, 51, 63), suggesting that our cohort showed more of an aged phenotype than cohorts from other studies. If activation was somewhat impaired in the old mice in the present study due to aging-associated degeneration of neuromuscular junctions (64), impaired blood flow (65) or other factors, less damage would be expected after lengthening contractions in the old group relative to the young. Regardless of which factors contributed to the difference in initial damage between groups, normalizing neutrophil and macrophage content to the initial force deficit provided a measure of the cellular response to a given amount of damage.

Our study is not without limitations. We assessed only two measures of regeneration, the number and size of regenerating fibers as observed by H&E staining of muscle cross-sections. Despite these limited data, age-related impairments in regeneration after muscle injury have been firmly established by a variety of studies (1-10). To examine function of myeloid cells in injured muscle, we examined mRNA levels at the tissue level. Therefore, we could not confirm the cellular source of the mRNA and altered mRNA levels do not necessarily reflect changes in protein content. Future studies could address these limitations by isolating different myeloid cell populations from injured muscles of young and old mice and examining mRNA and protein levels of purified cells.

In summary, our findings indicate that the myeloid cell response to injury was altered in old mice relative to young. However, contrary to our hypothesis, the altered myeloid cell response was not characterized by a persistence of neutrophils, impaired total macrophage accumulation, or a delay in the accumulation of M2 macrophages. The results indicated an enhanced response in the magnitude of neutrophils, total macrophages and M2 macrophages to injury in old mice relative to young, perhaps due to elevated circulating levels of neutrophils and monocytes in aged mice. In addition to the altered magnitude of the myeloid cell response to injury, aged myeloid cells may differentially express genes that have implications for muscle repair. Despite the impairments in muscle regeneration observed in old animals as well as the accumulating evidence that myeloid cells play a critical role in muscle repair following injury, the effect of aging on the magnitude and the timing of the myeloid cell response has received little attention. This study addresses gaps in our knowledge of aging-related changes in the myeloid cell response to injury, including the response of M2 macrophages, which to our knowledge, have not been examined in aged muscle after injury.

Acknowledgements

This work was supported by NIH grants AG-020591 to SVB and AG-000114 to DDS. We would like to thank the Unit for Laboratory Animal Medicine (ULAM) Pathology Core for Animal Research (PCAR) at the University of Michigan for performing the blood cell counts.

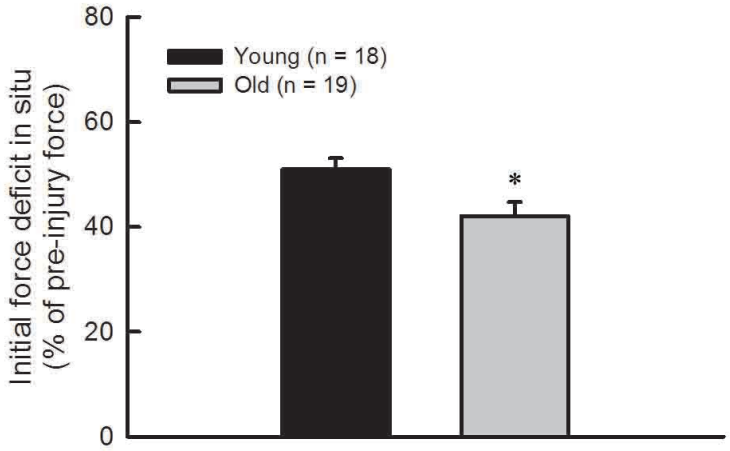

Figure 3.1: Initial force deficit after lengthening contractions was about 20% less in muscles from old mice relative to young (*P = 0.014).

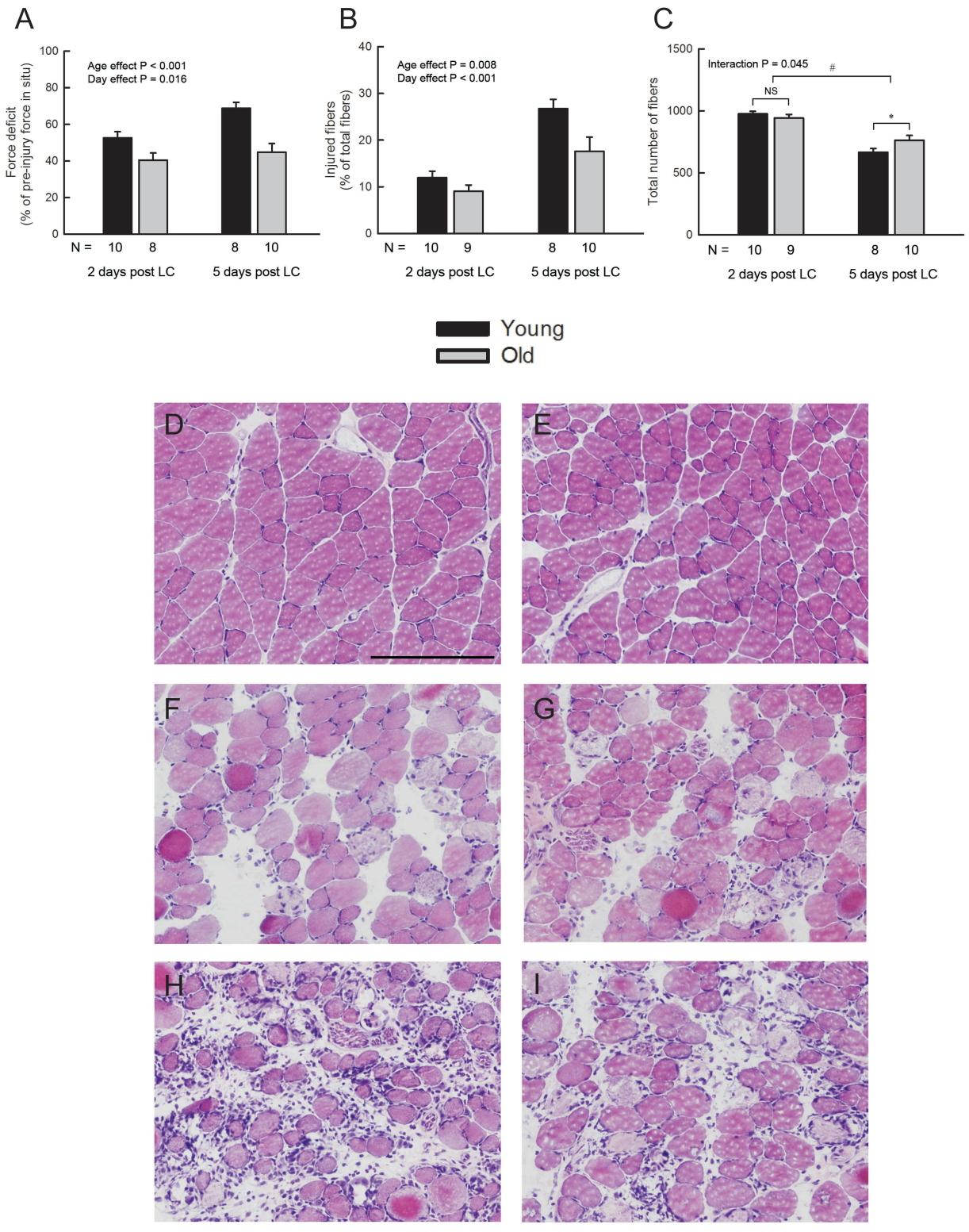
A
Force deficit
(% of pre-injury force in situ)
Age effect P < 0.001
Day effect P = 0.016
N = 10 8 8 10
2 days post LC
5 days post LC
B
Injured fibers
(% of total fibers)
Age effect P = 0.008
Day effect P < 0.001
N = 10 9 8 10
2 days post LC
5 days post LC
C
Total number of fibers
Interaction P = 0.045
#
NS
*
N = 10 9 8 10
2 days post LC
5 days post LC
Young
Old
D
E
F
G
H
I

Figure 3.2: Damage 2 and 5 days after lengthening contractions in young and old mice. Force deficits (A). Force deficits increased between 2 and 5 days (day effect, P = 0.016) and were significantly less for muscles of old mice relative to young (age effect, P < 0.001). There was no significant interaction between day and age (P = 0.151). A similar result was found when force deficit was calculated relative to the contralateral muscle {Force deficit = [(force of contralateral muscle *in vitro* – force of injured muscle *in vitro*) / (force of contralateral muscle *in vitro*)] * 100} (age effect, P = 0.004; day effect, P = 0.008; interaction, P = 0.231). Injured fibers (B). The percentage of fibers showing signs of histological damage increased between 2 and 5 days (day effect, P = 0.008) and were significantly less for muscles of old mice relative to young (age effect, P < 0.001). There was no significant interaction between day and age (P = 0.151). Total number of fibers (C). Two days after lengthening contractions, the total number of fibers was unchanged from contralateral control muscles of young and old mice (Table 2) and not significantly different between young and old groups (NS, P = 0.446). Five days after lengthening contractions, the number of total fibers decreased in young and old muscles, indicating that some fibers had completely degenerated (#P < 0.001). The number of total fibers was greater in muscles from old mice relative to young at this time point (*P = 0.039). Representative partial sections of muscles from young mice (D, F, H) and old mice (E, G, I) stained with H&E. Sections are from contralateral muscles (D, E), muscles 2 days after lengthening contractions (F, G) and muscles 5 days after lengthening contractions (H, I). Scale bar = 200 μm and applies to all images.

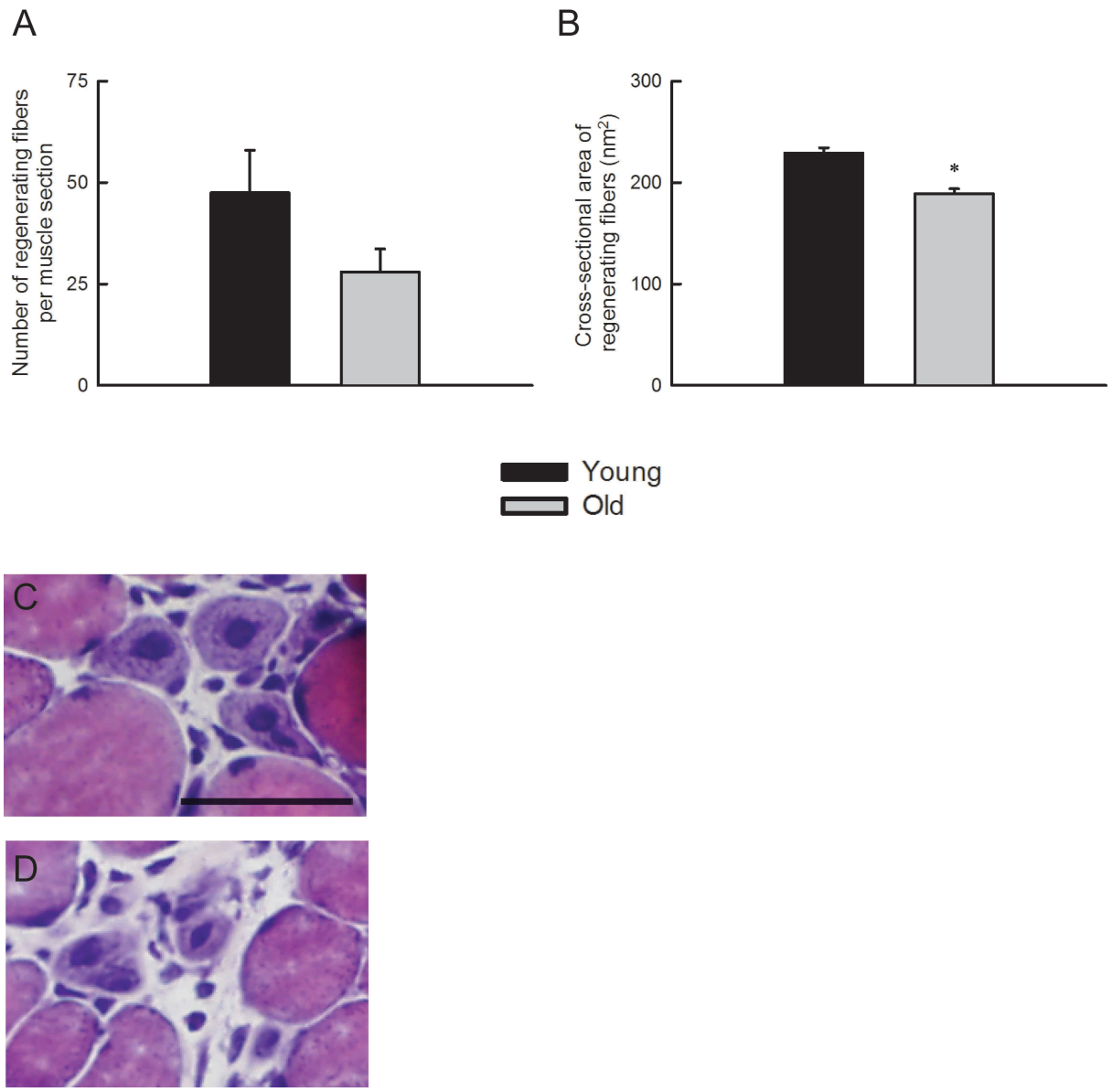

Figure 3.3: Regenerating fibers in injured muscle from young and old mice, 5 days after lengthening contractions. Number of regenerating fibers per muscle cross-section (A). While there were fewer regenerating fibers in muscle sections from old mice relative to young, the difference was not significant (P = 0.197). Average cross-sectional area of regenerating fibers (B). Cross-sectional area was significantly less in muscles from old mice (*P < 0.001). Representative partial sections of muscles from young (C) and old (D) mice showing regenerating fibers. Scale bar = 50 μm and applies to both images.

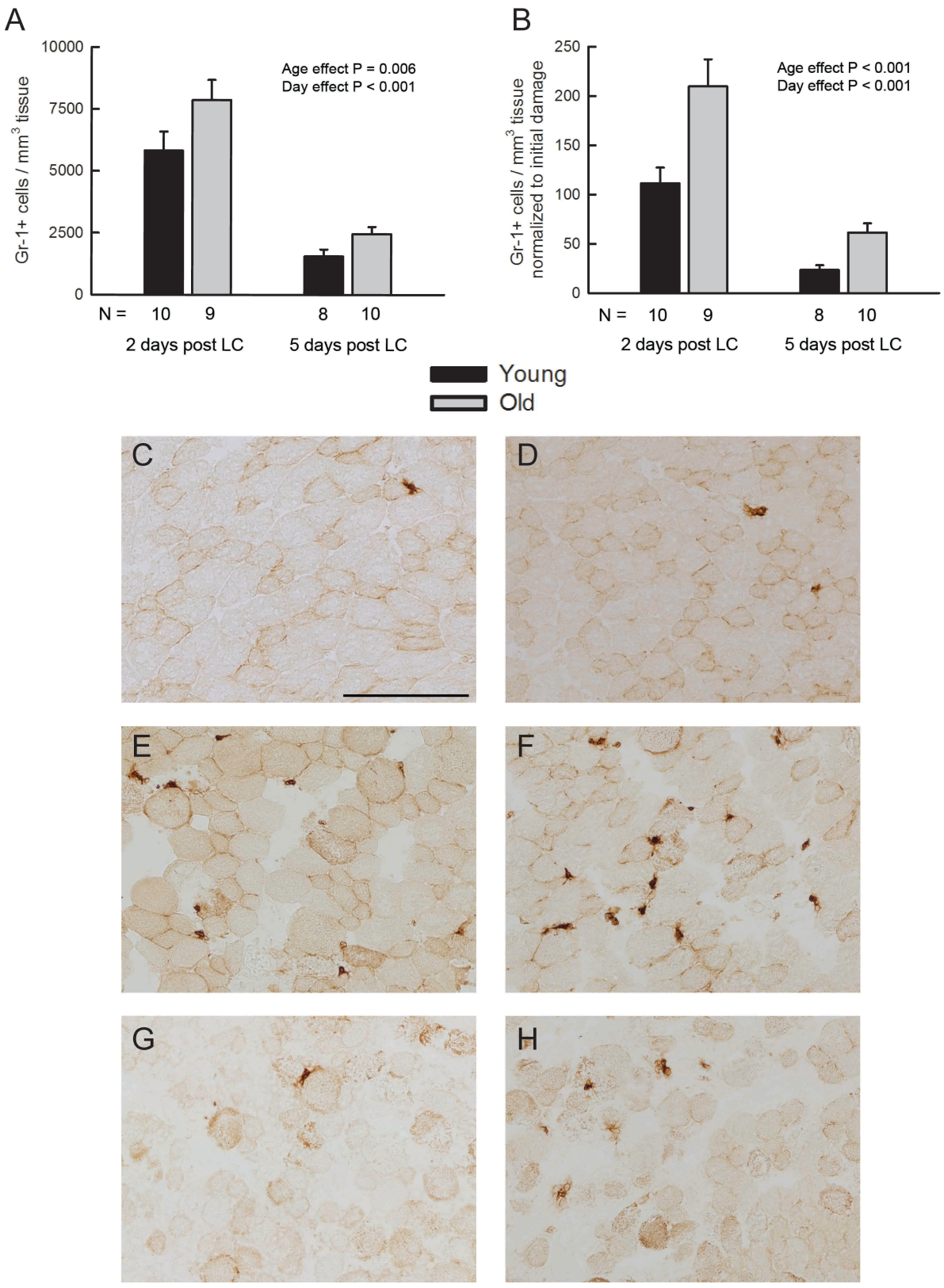
A
Gr-1+ cells / mm3 tissue
10000
7500
5000
2500
0
Age effect P = 0.006
Day effect P < 0.001
N = 10 9 8 10
2 days post LC
5 days post LC
B
Gr-1+ cells / mm3 tissue normalized to initial damage
250
200
150
100
50
0
Age effect P < 0.001
Day effect P < 0.001
N = 10 9 8 10
2 days post LC
5 days post LC
Young
Old
C
D
E
F
G
H

Figure 3.4: Neutrophil content in injured muscles from young and old mice. Neutrophil (Gr-1+ cell) content relative to size of tissue section (A). Neutrophil content declined between 2 and 5 days (day effect, $P = 0.006$) and was significantly greater in muscles from old mice relative to young (age effect, $P < 0.001$). Neutrophil content normalized to initial damage (i.e. initial force deficit) (B). Neutrophil content relative to initial damage declined between 2 and 5 days after lengthening contractions (day effect, $P < 0.001$) and was significantly greater in muscles from old mice relative to young (age effect, $P < 0.001$). Representative partial sections of muscles from young mice (C, E, G) and old mice (D, F, H) labeled for Gr-1. Sections are from contralateral muscles (C, D), muscles 2 days after lengthening contractions (E, F) and muscles 5 days after lengthening contractions (G, H). Scale bar = 200 μm and applies to all images.

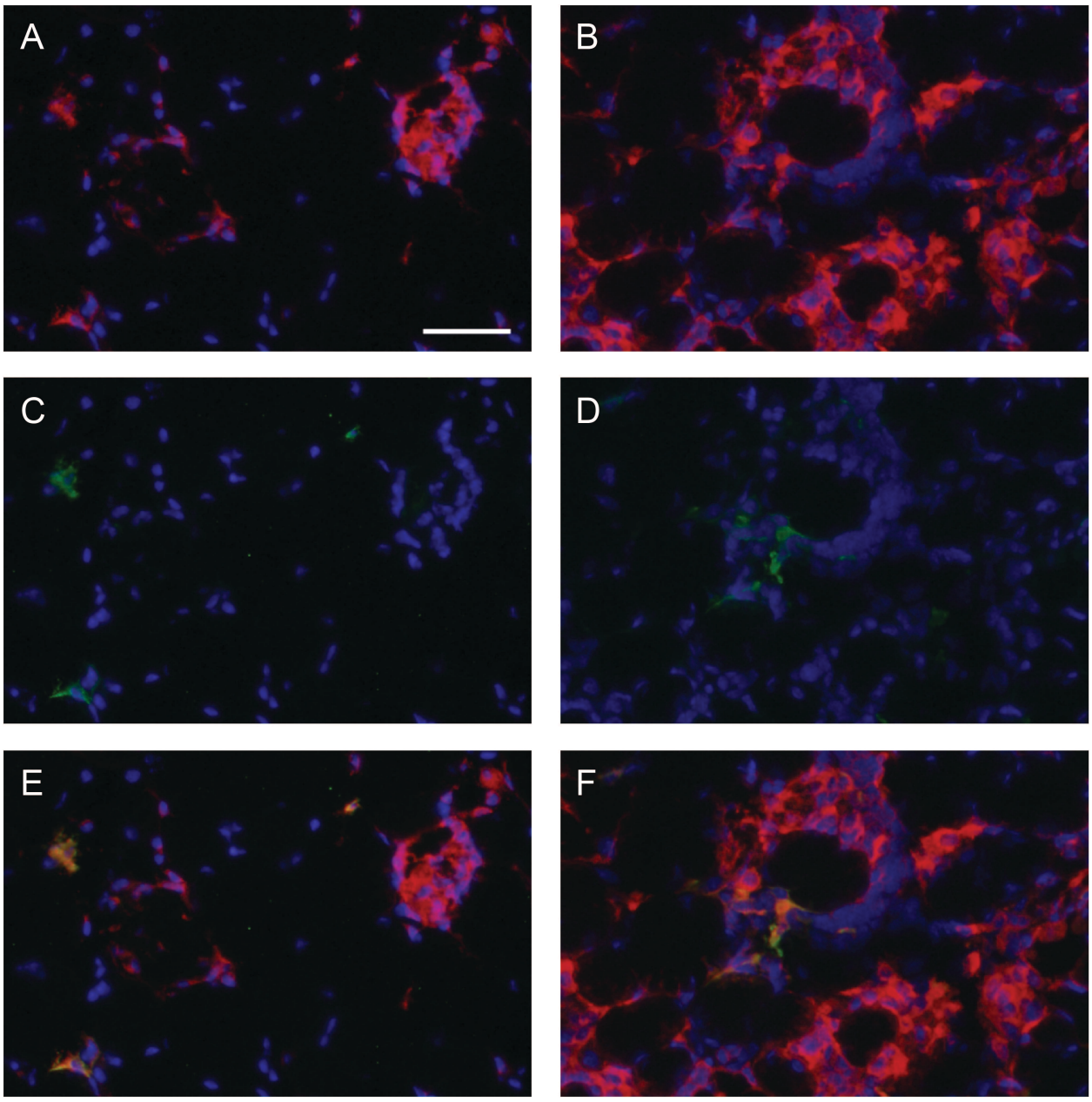

Figure 3.5: CD68+ and CD163+ cells co-localize in injured muscles. Partial muscle sections labeled for CD68 (red) and CD163 (green) 2 (A, C, E) and 5 (B, D, F) days after lengthening contractions. Cells that were CD163+ were also CD68+ (yellow), consistent with CD163 labeling a subset of total macrophages (CD68+ cells).

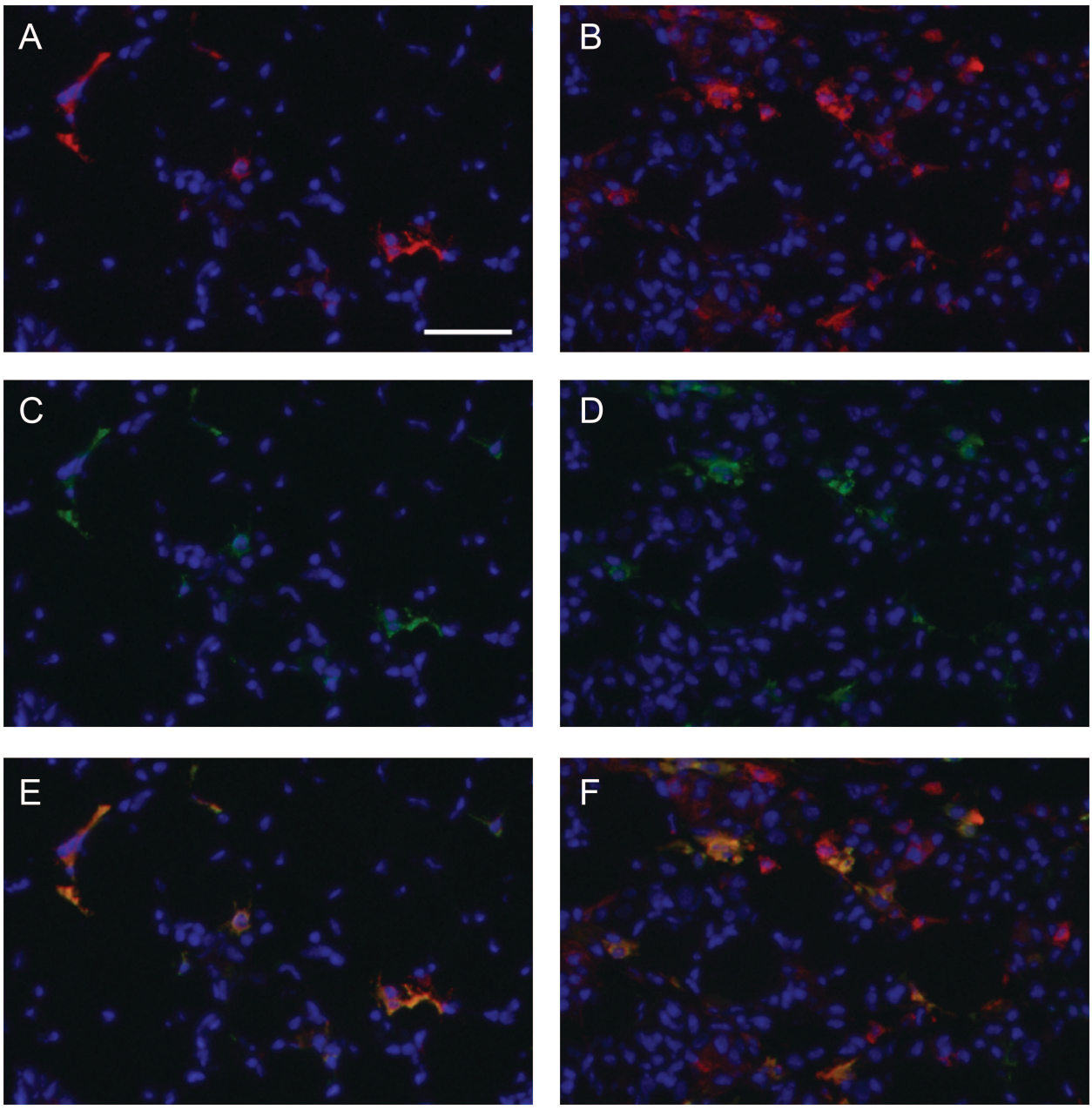

Figure 3.6: CD163+ and CD301+ cells co-localize in injured muscles. Partial muscle sections labeled for CD163 (green) and CD301 (red) 2 (A, C, E) and 5 (B, D, F) days after lengthening contractions. Cells that were CD163+ were also CD301+ (yellow), but not all CD301+ cells were CD163+.

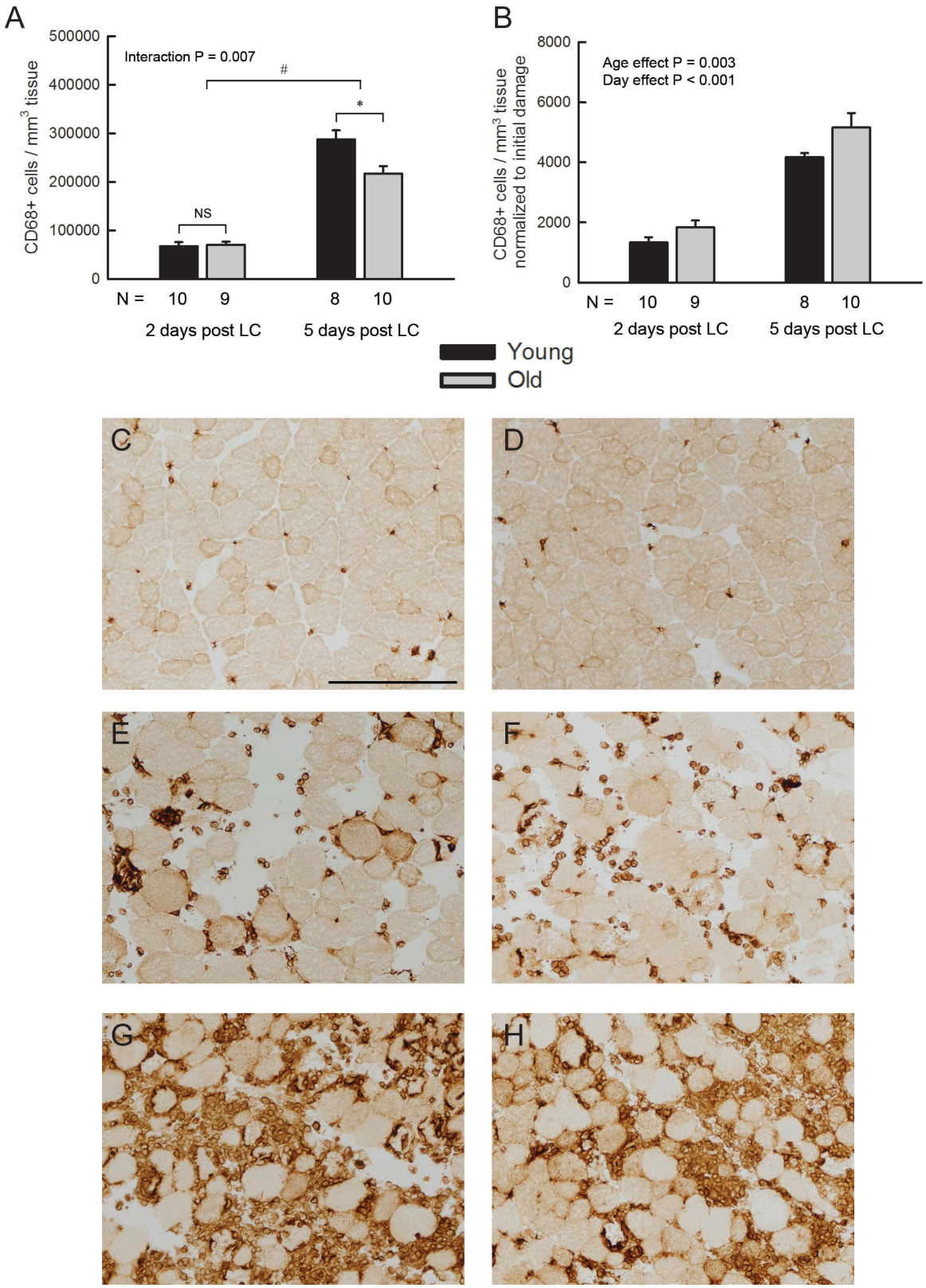
A
CD68+ cells / mm3 tissue
500000
400000
300000
200000
100000
0
Interaction P = 0.007
#
*
NS
N = 10 9 8 10
2 days post LC
5 days post LC
B
CD68+ cells / mm3 tissue normalized to initial damage
8000
6000
4000
2000
0
Age effect P = 0.003
Day effect P < 0.001
N = 10 9 8 10
2 days post LC
5 days post LC
Young
Old
C
D
E
F
G
H

Figure 3.7: Total macrophage content in injured muscles from young and old mice. Total macrophage (CD68+ cell) content relative to size of tissue section (A). Macrophage content increased between 2 and 5 days (#P < 0.001) and was significantly greater in muscles from old mice relative to young 5 days after lengthening contractions (*P < 0.001) but not after 2 days (NS, P = 0.871). Total macrophage content normalized to initial damage (i.e. initial force deficit) (B). Macrophage content relative to initial damage increased between 2 and 5 days after lengthening contractions (day effect, P < 0.001) and was significantly greater in muscles from old mice relative to young (age effect, P = 0.003). Representative partial sections of muscles from young mice (C, E, G) and old mice (D, F, H) labeled for CD68. Sections are from contralateral muscles (C, D), muscles 2 days after lengthening contractions (E, F) and muscles 5 days after lengthening contractions (G, H). Scale bar = 200 μm and applies to all images.

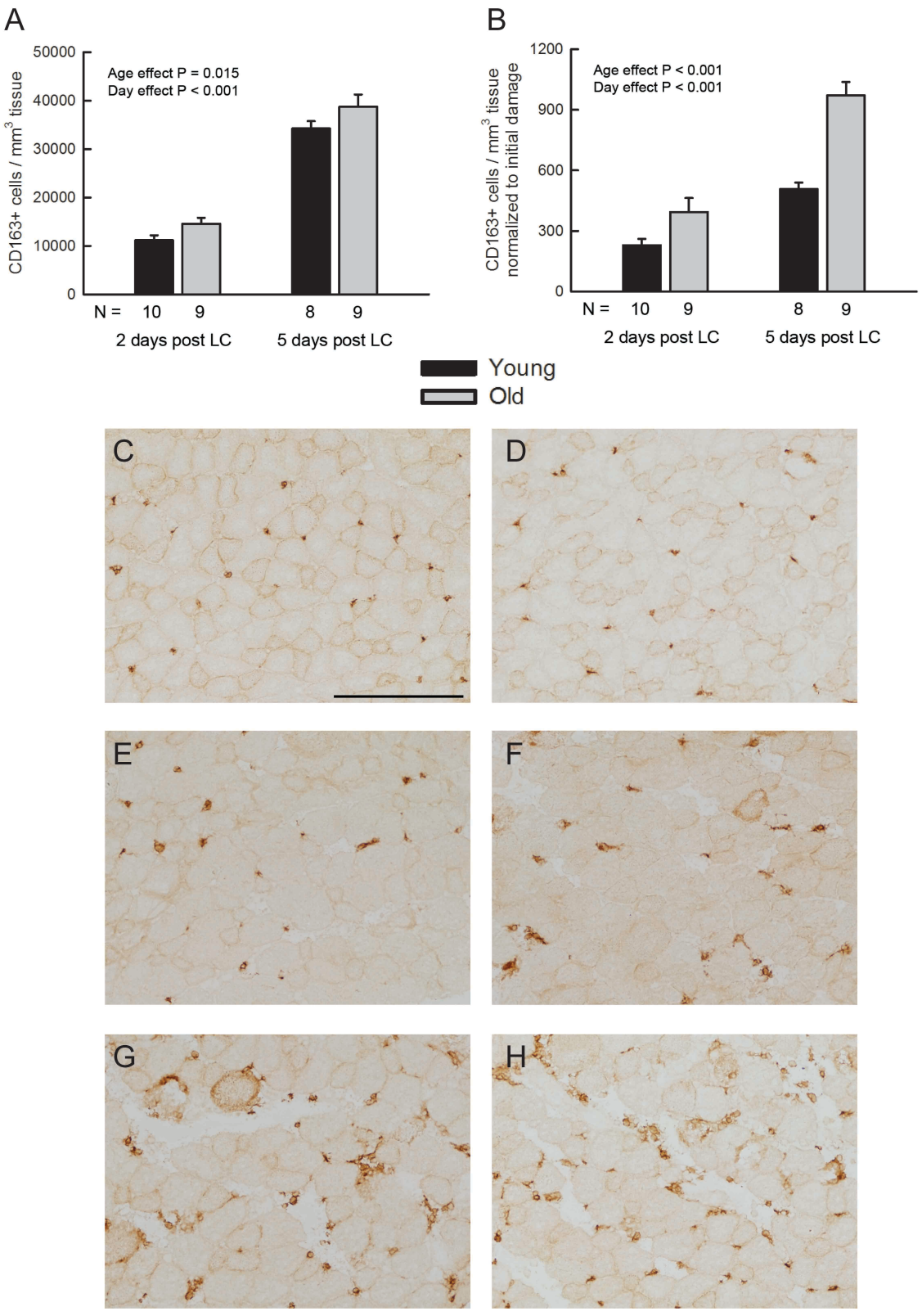
A
CD163+ cells / mm3 tissue
50000
40000
30000
20000
10000
0
Age effect P = 0.015
Day effect P < 0.001
N = 10 9 8 9
2 days post LC
5 days post LC
B
CD163+ cells / mm3 tissue normalized to initial damage
1200
900
600
300
0
Age effect P < 0.001
Day effect P < 0.001
N = 10 9 8 9
2 days post LC
5 days post LC
Young
Old
C
D
E
F
G
H

Figure 3.8: M2 macrophage content in injured muscles from young and old mice. M2 macrophage (CD163+ cell) content relative to size of tissue section (A). M2 macrophage content increased between 2 and 5 days (day effect, $P = 0.015$) and was significantly greater in muscles from old mice relative to young (age effect, $P < 0.001$). M2 macrophage content normalized to initial damage (i.e. initial force deficit) (B). M2 macrophage content relative to initial damage increased between 2 and 5 days after lengthening contractions (day effect, $P < 0.001$) and was significantly greater in muscles from old mice relative to young (age effect, $P < 0.001$). Representative partial sections of muscles from young mice (C, E, G) and old mice (D, F, H) labeled for CD163. Sections are from contralateral muscles (C, D), muscles 2 days after lengthening contractions (E, F) and muscles 5 days after lengthening contractions (G, H). Scale bar = 200 μm and applies to all images.

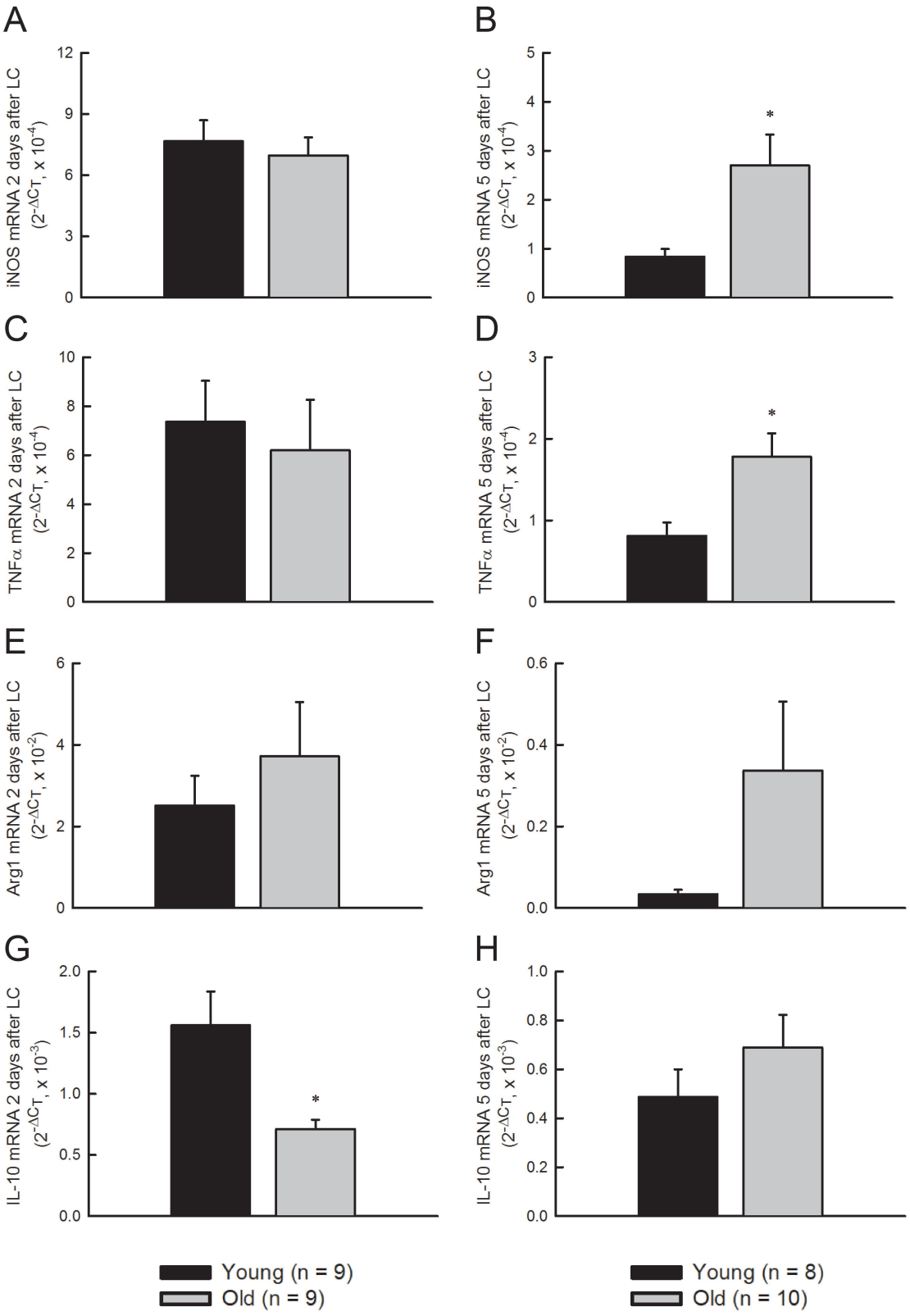
A
iNOS mRNA 2 days after LC
(2-ΔCT, x 10-4)
12
9
6
3
0
B
iNOS mRNA 5 days after LC
(2-ΔCT, x 10-4)
5
4
3
2
1
0
*
C
TNFα mRNA 2 days after LC
(2-ΔCT, x 10-4)
10
8
6
4
2
0
D
TNFα mRNA 5 days after LC
(2-ΔCT, x 10-4)
3
2
1
0
*
E
Arg1 mRNA 2 days after LC
(2-ΔCT, x 10-2)
6
4
2
0
F
Arg1 mRNA 5 days after LC
(2-ΔCT, x 10-2)
0.6
0.4
0.2
0.0
G
IL-10 mRNA 2 days after LC
(2-ΔCT, x 10-3)
2.0
1.5
1.0
0.5
0.0
*
H
IL-10 mRNA 5 days after LC
(2-ΔCT, x 10-3)
1.0
0.8
0.6
0.4
0.2
0.0
Young (n = 9)
Old (n = 9)
Young (n = 8)
Old (n = 10)

Figure 3.9: Messenger RNA levels of M1 macrophage genes (iNOS, TNFα) and M2 macrophage genes (Arg1, IL-10) in old injured muscles relative to young 2 and 5 days after lengthening contractions. Messenger RNA levels of iNOS (A, B), TNFα (C, D), Arg1 (E, F), and IL-10 (G, H) were normalized to β2-microglobulin mRNA. Messenger RNA levels of M1 macrophage genes were not different between young and old muscles 2 days after lengthening contractions but were increased in old muscles relative to young 5 days after lengthening contractions (iNOS: *P = 0.003, TNFα: *P = 0.014). Messenger RNA levels of Arg1 were not different between young and old muscles 2 or 5 days after lengthening contractions, although there was a trend toward elevated Arg1 mRNA levels in old muscle relative to young after 5 days (P = 0.083). Messenger RNA levels of IL-10 were significantly less in muscles from old mice relative to young 2 days after lengthening contractions (*P = 0.013) but not 5 days after lengthening contractions.

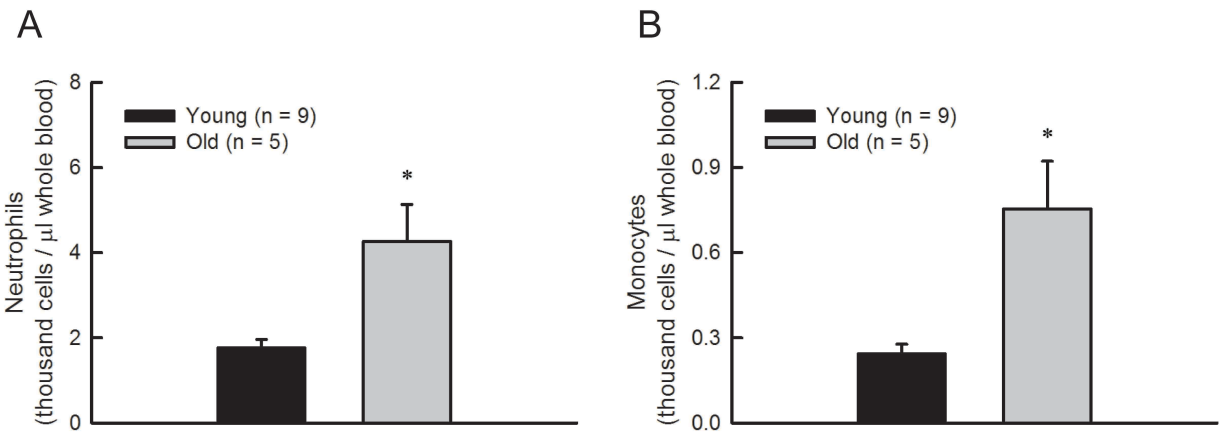

Figure 3.10: Circulating levels of neutrophils and monocytes are elevated in old mice. Summary of neutrophil data, *P = 0.008 (A). Summary of monocyte data, *P = 0.016 (B).

Group	n	Body weight (g)	Absolute force *in situ* (mN)	Absolute force *in vitro* (mN)†	Specific force *in vitro* (mN/mm²)†	Muscle mass (mg) †	CSA from H&E stained sections (mm²)†	Total number of fibers†
Young	18	32.0 ± 0.8	407 ± 8	473 ± 8	250 ± 4	12.0 ± 0.2	1.9 ± 0.1	951 ± 26
Old	19	32.7 ± 0.6	343 ± 9*	436 ± 13*	232 ± 6*	11.9 ± 0.3	1.6 ± 0.1*	936 ± 23

Table 3.1: Characteristics of young and old groups. †data taken from contralateral muscles. *significantly less than young group ($P < 0.05$). CSA = cross-sectional area. Forces are maximum forces generated during isometric tetanic contractions. Two samples are missing from young group for CSA from H&E stained sections and for total number of fibers.

Group	n	Gr-1+ cells per mm^3 tissue	CD68+ cells per mm^3 tissue	CD163+ cells per mm^3 tissue
Young	18	337 ± 53	13444 ± 465	10130 ± 348
Old	15	1470 ± 240*	14083 ± 569	12070 ± 421*

Table 3.2: Neutrophils and macrophages in uninjured and contralateral muscles from young and old mice. Neutrophil and macrophage content was not significantly different in muscles from contralateral muscles from either day and in muscles from uninjured mice. Therefore, data shown was pooled from muscles from uninjured mice and from contralateral muscles. *significantly different from young, $P \leq 0.001$.

References

1. Sadeh M. Effects of aging on skeletal muscle regeneration. J Neurol Sci. 1988 Oct; 87(1):67-74.

2. Conboy IM, Conboy MJ, Wagers AJ, Girma ER, Weissman IL, Rando TA. Rejuvenation of aged progenitor cells by exposure to a young systemic environment. Nature. 2005 Feb; 433(7027):760-4.

3. Ullman M, Ullman A, Sommerland H, Skottner A, Oldfors A. Effects of growth hormone on muscle regeneration and IGF-I concentration in old rats. Acta Physiol Scand. 1990 Dec; 140(4):521-5.

4. Brack AS, Conboy MJ, Roy S, Lee M, Kuo CJ, Keller C, Rando TA. Increased wnt signaling during aging alters muscle stem cell fate and increases fibrosis. Science. 2007 Aug; 317(5839):807-10.

5. Ghaly A, Marsh DR. Aging-associated oxidative stress modulates the acute inflammatory response in skeletal muscle after contusion injury. Exp Gerontol. 2010 May; 45(5):381-8.

6. Zhou Y, Lovell D, Bethea M, Wang Z, Christ GJ, Soker S, Criswell T. Age-dependent changes cooperatively impact skeletal muscle regeneration after compartment syndrome injury. Am J Pathol. 2014 Aug; 184(8):2225-36.

7. Brooks SV, Faulkner JA. Contraction-induced injury: recovery of skeletal muscles in young and old mice. Am J Physiol Cell Physiol. 1990 Mar; 258(3):C436-42.

8. McBride TA, Gorin FA, Carlsen RC. Prolonged recovery and reduced adaptation in aged rat muscle following eccentric exercise. Mech Ageing Dev. 1995 Sep; 83(3):185-200.

9. McArdle A, Dillmann WH, Mestril R, Faulkner JA, Jackson MJ. Overexpression of HSP70 in mouse skeletal muscle protects against muscle damage and age-related muscle dysfunction. FASEB J. 2004 Feb; 18(2):355-7.

10. Rader EP, Faulkner JA. Recovery from contraction-induced injury is impaired in weight-bearing muscles of old male mice. J Appl Physiol. 2006 Feb; 100(2):656-61.

11. Chargé SB, Rudnicki MA. Cellular and molecular regulation of muscle regeneration. Physiol Rev. 2004 Jan; 84(1):209-38.

12. Carlson BM, Faulkner JA. Muscle transplantation between young and old rats: age of host determines recovery. Am J Physiol. 1989 Jun; 256(6):C1262-66.

13. Conboy IM, Conboy MJ, Smythe GM, Rando TA. Notch-mediated restoration of regenerative potential to aged muscle. Science. 2003 Nov; 302(5650):1575-7.

14. Gopinath SD, Rando TA. Stem cell review series: aging of the skeletal muscle stem cell niche. Aging Cell. 2008 Aug; 7(4):590-8.

15. Teixeira CF, Zamunér SR, Zuliani JP, Fernandes CM, Cruz-Hofling MA, Fernandes I, Chaves F, Gutiérrez JM. Neutrophils do not contribute to local tissue damage, but play a key role in skeletal muscle regeneration, in mice injected with Bothrops asper snake venom. Muscle Nerve. 2003 Oct; 28(4):449-59.

16. Nguyen HX, Tidball JG. Null mutation of gp91phox reduces muscle membrane lysis during muscle inflammation in mice. J Physiol. 2003 Dec; 553(3):833-41.

17. Nguyen HX, Lusis AJ, Tidball JG. Null mutation of myeloperoxidase in mice prevents mechanical activation of neutrophil lysis of muscle cell membranes *in vitro* and *in vivo*. J Physiol. 2005 Jun; 565(2):403-13.

18. Walden DL, McCutchan HJ, Enquist EG, Schwappach JR, Shanley PF, Reiss OK, Terada LS, Leff JA, Repine JE. Neutrophils accumulate and contribute to skeletal muscle dysfunction after ischemia-reperfusion. Am J Physiol. 1990 Dec; 259(6):H1809-12.

19. Brickson S, Ji LL, Schell K, Olabisi R, St Pierre Schneider B, Best TM. M1/70 attenuates blood-borne neutrophil oxidants, activation, and myofiber damage following stretch injury. J Appl Physiol. 2003 Sep; 95(3):969-76.

20. Pizza FX, Peterson JM, Baas JH, Koh TJ. Neutrophils contribute to muscle injury and impair its resolution after lengthening contractions in mice. J Physiol. 2005 Feb; 562(3):899-913.

21. Lockhart NC, Brooks SV. Neutrophil accumulation following passive stretches contributes to adaptations that reduce contraction-induced skeletal muscle injury in mice. J Appl Physiol. 2008 Apr; 104(4):1109-15.

22. Arnold L, Henry A, Poron F, Baba-Amer Y, van Rooijen N, Plonquet A, Gherardi RK, Chazaud B. Inflammatory monocytes recruited after skeletal muscle injury switch into anti-inflammatory macrophages to support myogenesis. J Exp Med. 2007 May; 204(5):1057-69.

23. Côté CH, Bouchard P, van Rooijen N, Marsolais D, Duchesne E. Monocyte depletion increases local proliferation of macrophage subsets after skeletal muscle injury. BMC Musculoskelet Disord. 2013 Dec; 14:359.

24. Summan M, Warren GL, Mercer RR, Chapman R, Hulderman T, Van Rooijen N, Simeonova PP. Macrophages and skeletal muscle regeneration: a clodronate-containing liposome depletion study. Am J Physiol Regul Integr Comp Physiol. 2006 Jun; 290(6):R1488-95.

25. Tidball JG, Wehling-Henricks M. Macrophages promote muscle membrane repair and muscle fibre growth and regeneration during modified muscle loading in mice *in vivo.* J Physiol. 2007 Jan; 578(1):327-36.

26. Segawa M, Fukada S, Yamamoto Y, Yahagi H, Kanematsu M, Sato M, Ito T, Uezumi A, Hayashi S, Miyagoe-Suzuki Y, Takeda S, Tsujikawa K, Yamamoto H. Suppression of macrophage functions impairs skeletal muscle regeneration with severe fibrosis. Exp Cell Res. 2008 Oct; 314(17):3232-44.

27. Lu H, Huang D, Saederup N, Charo IF, Ransohoff RM, Zhou L. Macrophage recruited via CCR2 produce insulin-like growth factor-1 to repair acute skeletal muscle injury. FASEB J. 2011 Jan; 25(1):358-69.

28. Wang H, Melton DW, Porter L, Sarwar ZU, McManus LM, Shireman PK. Altered macrophage phenotype transition impairs skeletal muscle regeneration. Am J Pathol. 2014 Apr; 184(4):1167-84.

29. Mantovani A, Sica A, Sozzani S, Allavena P, Vecchi A, Locati M. The chemokine system in diverse forms of macrophage activation and polarization. Trends Immunol. 2004 Dec; 25(12):677-86.

30. Rigamonti E, Zordan P, Sciorati C, Rovere-Querini P, Brunelli S. Macrophage plasticity in skeletal muscle repair. Biomed Res Int. 2014; 2014:560629.

31. St. Pierre BA, Tidball JG. Differential response of macrophage subpopulations to soleus muscle reloading after rat hindlimb suspension. J Appl Physiol. 1994 Jul; 77(1):290-7.

32. McLennan IS. Degenerating and regenerating skeletal muscles contain several subpopulations of macrophages with distinct spatial and temporal distributions. J Anat. 1996 Feb; 188(1):17-28.

33. Deng B, Wehling-Henricks M, Villalta SA, Wang Y, Tidball JG. IL-10 triggers changes in macrophage phenotype that promote muscle growth and regeneration. J Immunol. 2012 Oct; 189(7):3669-80.

34. Massimino ML, Rapizzi E, Cantini M, Dalla Libera L, Mazzoleni F, Arslan P, Carraro U. ED2+ macrophages increase selectively myoblast proliferation in muscle cultures. Biochem Biophys Res Commun. 1997 Jun; 235(3):754-9.

35. Ruffell D, Mourkioti F, Gambardella A, Kirstetter P, Lopez RG, Rosenthal N, Nerlov C. A CREB-C/EBPβ cascade induces M2 macrophage-specific gene expression and promotes muscle injury repair. Proc Natl Acad Sci USA. 2009 Oct; 106(41):17475-80.

36. Koh TJ, Brooks SV. Lengthening contractions are not required to induce protection from contraction-induced muscle injury. Am J Physiol Regul Integr Comp Physiol. 2001 Jul; 281(1):R155-61.

37. Brooks SV, Faulkner JA. Contractile properties of skeletal muscles from young, adult and aged mice. J Physiol. 1988 Oct; 404:71-82.

38. Shortreed K, Johnston A, Hawke TJ. Satellite cells and muscle repair. In: Tiidus PM, editor. Skeletal muscle damage and repair. Champaign: Human Kinetics; 2008. p. 77-88.

39. Lagasse E, Weissman IL. Flow cytometric identificaton of murine neutrophils and monocytes. J Immunol Methods. 1996 Oct; 197(1-2):139-50.

40. Faulkner JA, Brooks SV, Opiteck JA. Injury to skeletal muscle fibers during contractions: conditions of occurrence and prevention. Phys Ther. 1993 Dec; 73(12):911-21.

41. Rigamonti E, Touvier T, Clementi E, Manfredi AA, Brunelli S, Rovere-Querini P. Requirement of inducible nitric oxide synthase for skeletal muscle regeneration after acute damage. J Immunol. 2013 Feb; 190(4):1767-77.

42. Gumucio JP, Flood MD, Phan AC, Brooks SV, Mendias CL. Targeted inhibition of TGF-β results in an initial improvement but long-term deficit in force production after contraction-induced skeletal muscle injury. J Appl Physiol. 2013 Aug; 115(4):539-45.

43. Schmittgen TD, Livak KJ. Analyzing real-time PCR data by the comparative C_T method. Nat Protoc. 2008; 3(6):1101-8.

44. Rabinowitz SS, Gordon S. Macrosialin, a macrophage-restricted membrane sialoprotein differentially glycosylated in response to inflammatory stimuli. J Exp Med. 1991 Oct; 174(4):827-36.

45. Holness CL, da Silva RP, Fawcett J, Gordon S, Simmons DL. Macrosialin, a mouse macrophage-restricted glycoprotein, is a member of the lamp/lgp family. J Biol Chem. 1993 May; 268(13):9661-6.

46. Lumeng CN, Bodzin JL, Saltiel AR. Obesity induces a phenotypic switch in adipose tissue macrophage polarization. J Clin Invest. 2007 Jan; 117(1):175-84.

47. Lumeng CN, DelProposto JB, Westcott DJ, Saltiel AR. Phenotypic switching of adipose tissue macrophages with obesity is generated by spatiotemporal differences in macrophage subtypes. Diabetes. 2008 Dec; 57(12):3239-46.

48. van der Poel C, Gosselin LE, Schertzer JD, Ryall JG, Swiderski K, Wondemaghen M, Lynch GS. Ageing prolongs inflammatory marker expression in regenerating rat skeletal muscles after injury. J Inflamm. 2011 Dec; 8(1): 41.

49. Hamada K, Vannier E, Sacheck JM, Witsell AL, Roubenoff R. Senescence of human skeletal muscle impairs the local inflammatory cytokine response to acute eccentric exercise. FASEB J. 2005 Feb; 19(2):264-6.

50. Hammers DW, Merritt EK, Matheny RW Jr, Adamo ML, Walters TJ, Estep JS, Farrar RP. Functional deficits and insulin-like growth factor-I gene expression following tourniquet-induced injury of skeletal muscle in young and old rats. J Appl Physiol. 2008 Oct; 105(4):1274-81.

51. Koh TJ, Peterson JM, Pizza FX, Brooks SV. Passive stretches protect skeletal muscle of adult and old mice from lengthening contraction-induced injury. J Gerontol A Biol Sci Med Sci. 2003 Jul; 58(7):592-7.

52. Paliwal P, Pishesha N, Wijaya D, Conboy IM. Age dependent increase in the levels of osteopontin inhibits skeletal muscle regeneration. Aging. 2012 Aug; 4(8):533-66.

53. Rubinstein I, Abassi Z, Coleman R, Milman F, Winaver J, Better OS. Involvement of nitric oxide system in experimental muscle crush injury. J Clin Invest. 1998 Mar; 101(6):1325-33.

54. Degens H. The role of systemic inflammation in age-related muscle weakness and wasting. Scand J Med Sci Sports. 2010 Feb; 20(1):28-38.

55. Langen RC, van der Velden JL, Schols AM, Keiders MC, Wouters EF, Janssen-Heininger YM. Tumor necrosis factor-alpha inhibits myogenic differentiation through MyoD protein stabilization. FASEB J. 2004 Feb; 18(2):227-37.

56. Langen RC, Schols AM, Keiders MC, van der Velden JL, Wouters EF, Janssen-Heininger YM. Muscle wasting and impaired muscle regeneration in a murine model of chronic pulmonary inflammation. Am J Respir Cell Mol Biol. 2006 Dec; 35(6):689-96.

57. Nguyen HX, Tidball JG. Interactions between neutrophils and macrophages promote macrophage killing of rat muscle cells *in vitro*. J Physiol. 2003 Feb; 547(1):125-32.

58. Villalta SA, Nguyen HX, Deng B, Gotoh T, Tidball JG. Shifts in macrophage phenotypes and macrophage competition for arginine metabolism affect the severity of muscle pathology in muscular dystrophy. Hum Mol Genet. 2009 Feb; 18(3):482-96.

59. Bosurgi L, Corna G, Vezzoli M, Touvier T, Cossu G, Manfredi AA, Brunelli S, Rovere-Querini P. Transplanted mesoangioblasts required macrophage IL-10 for survival in a mouse model of muscle injury.

60. Fiorentino DF, Ziotnik A, Mosmann TR, Howard M, O'Garra A. IL-10 inhibits cytokine production by activated macrophages. J Immunol. 1991 Dec; 147(11):3815-22.

61. Brigitte M, Schilte C, Plonquet A, Baba-Amer Y, Henri A, Charlier C, Tajbakhsh S, Albert M, Gherardi RK, Chrétien F. Muscle resident macrophages control the immune cell reaction in a mouse model of notexin-induced myoinjury. Arthritis Rheum. 2010 Jan; 62(1):268-79.

62. Lockhart NC, Brooks SV. Protection from contraction-induced injury provided to skeletal muscles of young and old mice by passive stretch is not due to a decrease in initial mechanical damage. J Gerontol A Biol Sci Med Sci. 2006 Jun; 61(6):527-33.

63. Zerba E, Komorowski TE, Faulkner JA. Free radical injury to skeletal muscles of young, adult, and old mice. Am J Physiol. 1990 Mar; 258(3):C429-35.

64. Sakuma K, Aoi W, Yamaguchi A. Current understanding of sarcopenia: possible candidates modulating muscle mass. Pflugers Arch. 2014 May.

65. Jackson DN, Moore AW, Segal SS. Blunting of rapid onset vasodilatation and blood flow restriction in arterioles of exercising skeletal muscle with ageing in male mice. J Physiol. 2010 Jun; 588(12):2269-82.

Chapter 4

Treatment with P/E-selectin blocking antibodies blunts neutrophil accumulation after lengthening contractions but does not reduce damage

Abstract

P- and E-selectins are expressed on the surface of endothelial cells and may contribute to neutrophil recruitment following injurious lengthening contractions of skeletal muscle. Blunting neutrophil, but not macrophage, accumulation after lengthening contractions may provide a therapeutic benefit as neutrophils exacerbate damage to muscle fibers while macrophages promote repair. In the present study we tested the hypothesis that P- and E-selectins contribute to neutrophil, but not macrophage, accumulation in muscles after contraction-induced injury and that reducing neutrophil accumulation by blocking the selectins would be sufficient to reduce damage to muscle fibers. To test our hypothesis, we treated mice with antibodies to block P- and E-selectin function and assessed leukocyte accumulation and damage in muscles two days after lengthening contractions. Treatment with P/E-selectin blocking antibodies reduced neutrophil content by about half in muscles subjected to lengthening contractions while macrophage content was reduced by about a third. In spite of the

reduction in neutrophil accumulation, we did not detect a decrease in damage two days after lengthening contractions, suggesting that the levels of neutrophils in the muscles (50% of controls) were sufficient to induce damage. From a therapeutic perspective, the implication is that blocking the selectins may not represent a beneficial approach, and additional adhesion proteins may need to be targeted to sufficiently reduce neutrophil accumulation to provide a benefit.

Introduction

Skeletal muscle injuries are common and have a variety of causes, including physical trauma, extreme temperatures, toxin exposure, invasive surgery, ischemia/reperfusion and unloading/reloading. Muscles can also be injured by their own contractions (i.e. contraction-induced injury), especially during lengthening contractions when muscles are stretched while activated. Regardless of the cause, the initial insult is followed by degeneration and necrosis of damaged muscle fibers followed by regeneration and repair. In the young and healthy, regeneration is typically rapid and complete, but advanced age, muscle disease, and severe injury is associated with delayed or incomplete repair. Therefore, reducing the degree of damage after injury is a worthwhile goal.

Accompanying the degeneration and necrosis of fibers in injured muscle is the accumulation of inflammatory cells in the tissue. Neutrophils increase in the muscle within hours to days of the initial injury. Neutrophils can lyse muscle cells *in vitro* and damage membranes *in vivo* by mechanisms involving reactive oxygen species (1, 2),

and preventing neutrophil infiltration after injury reduces force deficits and histological damage to muscle fibers (3-6), suggesting that neutrophils contribute to muscle fiber damage. Subsequent to the rise in neutrophils, pro-inflammatory macrophages begin to accumulate in injured muscle. Pro-inflammatory macrophages are also capable of lysing muscle cells *in vitro* (7). However, *in vivo* studies suggest that these cells are ultimately beneficial to the repair process, as evidenced by observations that reducing the level of invading macrophages delays the clearance of necrotic fibers, reduces the number and size of regenerating fibers, and increases fibrosis and fat relative to controls (8-11). Thus, preventing or blunting the neutrophil response while keeping the macrophage response intact may protect the muscle from unnecessary damage without interfering with repair, and provide a therapeutic benefit in cases of delayed or incomplete repair.

Methods explored to reduce neutrophil accumulation consist of systemic approaches, such as depleting cells from the circulation (6, 12) or genetically knocking out genes for proteins involved in neutrophil migration out of blood vessels (5, 13). These are appropriate experimental approaches for proof-of-concept studies but are not feasible as therapeutic interventions. One option for targeted therapeutic intervention is the administration of a compound to block the endothelial selectins, P- and E-selectin. P- and E-selectins are adhesion proteins expressed by activated vascular endothelial cells. Once expressed on the luminal surface of blood vessels, the selectins interact with corresponding ligands on neutrophils, “capturing” them from the rapidly flowing blood stream and enabling slow rolling along the vessel wall. Capture and slow rolling of neutrophils are initial steps in a well-characterized cascade that culminates with neutrophil migration out of the blood vessel and into the surrounding tissue (14).

Genetic knockout of both P- and E-selectin prevents neutrophil infiltration after an unloading/reloading injury but keeps macrophage accumulation intact (13) but, the degree to which endothelial selectins contribute to neutrophil and macrophage accumulation after other types of muscle injury is unknown. Furthermore, whether reducing neutrophil accumulation by targeting the endothelial selectins is sufficient to reduce damage to muscle fibers after contraction-induced injury has not been examined.

Therefore, in the present study we tested the hypothesis that endothelial selectins contribute to neutrophil, but not macrophage, accumulation in muscles after contraction-induced injury and that reducing neutrophil accumulation by blocking the selectins would be sufficient to reduce damage to muscle fibers after contraction-induced injury. To test our hypothesis, we subjected extensor digitorum longus (EDL) muscles of mice to lengthening contractions *in situ* and treated the animals with antibodies to block binding of neutrophils to P-selectin (RB40.34) and E-selectin (9A9). Two days after lengthening contractions, damage was assessed by functional measures and by histology, and neutrophil and macrophage accumulation was assessed by immunohistochemistry.

Methods

Animals. Male C57BL/6N mice, 3-5 mo of age were purchased from Charles River Laboratories and housed in a specific-pathogen-free facility at the University of Michigan until experimentation. Between experimental procedures, mice were housed in

a separate specific-pathogen-free return room. All animal use procedures were approved by the University of Michigan Committee on the Use and Care of Animals (UCUCA).

In situ evaluation of contractile properties. Procedures for *in situ* evaluation of muscle contractile properties were based on previous studies (15, 16). Each mouse was anesthetized with 3% isoflurane in oxygen delivered at a rate of 1 L/min. Anesthesia was maintained throughout *in situ* procedures with 2% isoflurane in oxygen and depth of anesthesia was confirmed by failure of the mouse to respond to tactile stimuli. Ophthalmic ointment was placed on the mouse's eyes to prevent corneal drying and trauma and this was re-administered throughout *in situ* procedures. The mouse was placed on a platform warmed to 37 °C with a circulating water bath. The hind limb fur was removed with animal clippers followed by a minimal amount of fur removal cream. The skin was disinfected with chlorhexidine and a small incision was made at the ankle to expose the distal tendon of the EDL muscle. Another small incision was made distal to the knee to expose the peroneal nerve. A secure knot was tied around the tendon with 6.0 braided silk suture. The hind limb was immobilized by pinching the knee and the foot with small clamps secured to the platform. Using the tails of the silk suture, the intact tendon was tied to the lever arm of a servomotor (300C-LR-FP, Aurora Scientific), which controlled the length of the muscle and measured the force generated. A computer with custom-designed software controlled stimulus pulses, the servomotor, and collected and stored force data. The small area of exposed tendon was kept moist by frequent administration of sterile saline. The EDL muscle was activated using a stimulator (701C, Aurora Scientific) and platinum electrodes placed under the peroneal

nerve. A stimulus pulse duration of 0.2 ms was used for all contractions. Stimulation current and muscle length were adjusted in order to elicit maximum twitch force. Tetanic contractions of 200 ms duration were elicited with trains of pulses and the frequency of the pulses was increased until the force plateaued at the maximum isometric force (P_o), typically at a frequency of 200 Hz. Finally, small adjustments in the ankle position were made to elicit maximum isometric tetanic force. The tetanic contractions were spaced 1 min apart to prevent fatigue. Optimal muscle length (L_o), defined as the muscle length at which maximum isometric force is achieved, was measured with calipers using the knee to estimate the location of the proximal end of the EDL muscle. Optimal muscle fiber length (L_f) was determined by multiplying L_o by the previously determined L_f-to-L_o ratio of 0.45 (17).

In situ lengthening contraction protocol. Following evaluation of contractile properties, the EDL muscle was exposed to a protocol of 75 lengthening contractions spaced 4 s apart for a total duration of 5 min. Each contraction was 300 ms in duration. 100 ms after the onset of stimulation, near maximum isometric force was generated and a stretch of 20% strain relative to L_f was initiated. Muscles were lengthened at the appropriate rate (1 L_f/s) to cause the peak of the stretch to coincide with the end of the tetanic stimulation. Ten minutes after the lengthening contraction protocol, the muscle was re-lengthened to achieve maximum twitch tension and P_o was re-measured. The small incisions at the ankle and distal to the knee were closed with 7.0 sterile monofilament nylon suture and bathed with povidone-iodine solution, and mice were monitored until they recovered from anesthesia.

Administration of blocking antibodies. Approximately 1 hour following *in situ* lengthening contractions, antibodies were administered via intraperitoneal injection(s). Mice received either tandem injections of rat anti-mouse monoclonal antibodies specific for P-selectin (200 μg, clone RB40.34, BD Pharmingen, 553741) and E-selectin (200 μg, clone 9A9, generously provided by Dr. Klaus Ley, La Jolla Institute for Allergy & Immunology) or a single injection of irrelevant isotype control antibodies (400 μg, A110-1, BD Pharmingen, 559157). Uninjected mice served as an additional control group.

The blocking function of RB40.34 and 9A9 has been demonstrated in many studies *in vitro* and *in vivo*. *In vitro*, both antibodies prevent attachment of myeloid cells to their respective selectins (18, 19). *In vivo*, RB40.34 alone or together with 9A9 prevents cytokine-induced leukocyte rolling along blood vessel walls and both antibodies reduce chemically-induced neutrophil migration into the peritoneal cavity (18-23). RB40.34 was detected on platelets in the blood 3 hours after a single intraperitoneal injection, and platelets with bound RB40.34 were detected up to 7 days after injection when a dose of 200 μg was administered (24). Therefore, this dose of RB40.34 and 9A9 was used in the present study to provide blocking coverage over the time period studied.

In vitro evaluation of contractile properties. Two days following administration of the lengthening contraction protocols, mice were again evaluated for P_o. This time point was chosen because preliminary experiments suggested the neutrophil content of injured muscles was greatest 2 days after administration of the injury protocol used in the present study. Procedures for the *in vitro* evaluation of EDL contractile properties have been previously published (17). Each mouse was anesthetized with an

intraperitoneal injection of Avertin (tribromoethanol, 250 mg/kg) (chemical components from Sigma-Aldrich). After the mouse was unresponsive to a tactile stimulus, the injured EDL muscle was isolated from the hindlimb of the mouse. 5-0 silk suture was tied to the proximal and distal tendons of the muscle and the muscle was placed into a chamber containing Krebs Mammalian Ringer solution composed of (in mM): 137 NaCl, 5 KCl, 2 $CaCl_2 \cdot 2H_2O$, 1 $MgSO_4 \cdot 7H_2O$, 1 NaH_2PO_4, 24 $NaHCO_3$, 11 glucose, 0.03 tubocurarine chloride. The solution was maintained at 25 °C and bubbled with 95% O_2-5% CO_2 to maintain a pH of 7.4. The proximal tendon was attached to a stationary object and the distal tendon was attached to a force transducer (BG-50, Kulite Semiconductor Products). Muscles activation was accomplished by electric field stimulation via a high-power current stimulator (701C, Aurora Scientific) and parallel plate electrodes.

A computer and custom-designed software controlled stimulus pulses and collected and stored force data. Stimulus pulses of 0.2 ms in duration were used for all contractions. Stimulation current and the muscle length were adjusted in order to elicit maximum twitch force. A digital calipers was used to measure L_o. Muscles were held at L_o and tetanic contractions of 300 ms in duration were elicited with trains of pulses. The frequency of the pulses was increased until the force plateaued at P_o, typically at frequencies from 150-200 Hz. The tetanic contractions were spaced 1 min apart to prevent fatigue. Optimal muscle fiber length (L_f) was determined as previously mentioned. Force deficit was defined as the difference between the P_o measured immediately prior to lengthening contractions and the P_o measured two days after lengthening contractions expressed as a percentage of the pre-injury P_o. Following evaluation of the injured EDL, the contralateral EDL was removed and evaluated as

described. Muscles were trimmed of their tendons and weighed. Muscles were then immersed in Tissue Freezing Medium (Electron Microscopy Sciences) and frozen in isopentane cooled by liquid nitrogen. The mouse was euthanized with an overdose of Avertin followed by induction of a bilateral pneumothorax.

Histology and immunohistochemistry. EDL muscles were cut into 10 μm thick sections on a cryostat. The sections were fixed in cold acetone and stained with Hematoxylin (Ricca Chemical Company) and Eosin Y (EMD Millipore). Stained sections were imaged with a Nikon E-800 light microscope. The number of injured fibers was counted per section and expressed as a percentage of the total number of fibers. Injured fibers included those with a swollen appearance, pale or variable staining, and obvious infiltration of inflammatory cells (16).

Muscle sections were analyzed for neutrophil and macrophage content using immunohistochemistry. Sections were fixed in cold acetone and air-dried. Sections were exposed to BLOXALL solution to block endogenous peroxidase activity followed by 10% normal rabbit serum in PBS (Phosphate Buffer Solution, Fisher Scientific) to block non-specific binding of subsequent antibodies. Neutrophils were detected with a rat anti-mouse Gr-1 antibody (clone RB6-8C5, 1:50 dilution, BD Pharmingen, 550291) and macrophages were detected with a rat anti-mouse CD68 antibody (clone FA-11, 1:1000, AbD Serotec, MCA1957) diluted in PBS containing 10% rabbit serum. After incubation in primary antibodies, sections were exposed to biotinylated mouse adsorbed anti-rat IgG in PBS containing 10% rabbit serum. Following exposure to the secondary antibodies, the sections were treated with the VECTASTAIN Elite ABC reagent containing peroxidase followed by the peroxidase substrate 3, 3’-diaminobenzidine

(ImmPACT DAB). The sections were rinsed with PBS after each step except after the treatment with rabbit serum. All reagents were from Vector Laboratories unless stated otherwise. In the periphery, neutrophils express high levels of Gr-1 while monocytes express low or no levels of Gr-1 (25). Therefore, dark brown cells indicating high levels of Gr-1 were counted as neutrophils while the occasional light brown cell of similar size was not counted. CD68 is expressed on macrophages and labels early-invading macrophages that accumulate in injured skeletal muscle (26-28). An image analysis program (Image J) was used to count the number of neutrophils (Gr-1+ cells) or macrophages (CD68+ cells) in one transverse section from the middle of each muscle. The same program was used to calculate the area of each section and neutrophil or macrophage content was expressed per mm^3 of muscle.

The location of neutrophils relative to blood vessels was also analyzed using immunohistochemistry. Neutrophils were labeled first according to the methods described in the preceding paragraph, except that the normal rabbit serum was replaced with Carbo-Free Blocking Solution. Carbo-Free Blocking Solution does not contain glycoproteins, which can interfere with subsequent lectin-based detection. To label blood vessels, muscle sections were first treated with solutions from an Avidin/Biotin Blocking Kit to block endogenous avidin and biotin. Sections were incubated in Carbo-Free Blocking Solution to block non-specific binding of the lectin. The sections were then treated with a biotinylated Griffonia (Bandeiraea) Simplicifolia Lectin I (GSL I, 10 µg/ml in PBS). GSL I labels all blood vessels in skeletal muscle (29). The biotinylated lectin was detected by exposing sections to a VECTASTAIN Elite ABC reagent containing peroxidase followed by a peroxidase substrate (ImmPACT SG). The

sections were rinsed with PBS containing 0.05% Tween 20 (Sigma-Aldrich) following the lectin and ABC reagent steps. All reagents were from Vector Laboratories unless stated otherwise. The number of neutrophils detected within blood vessels was counted and expressed as a percentage of total neutrophils per section. This sequential labeling technique may not detect neutrophils within capillaries but within larger vessels only.

Blood analysis. Blood was collected via a scalpel nick of the lateral tail vein (50-100 μl per day). Whole blood was analyzed with a cell counter (Hemavet 950FS, Drew Scientific) to determine circulating white blood cell counts.

Statistics. Data are expressed as means ± 1 SEM. Experimental groups were compared with a Student's t-test unless otherwise indicated, with significance set *a priori* at $P < 0.05$.

Results

There were no differences among the experimental groups for body weight, maximum force generation by the EDL muscle prior to lengthening contractions, or force deficit 10 min after the lengthening contractions (Table 4.1). Injecting the irrelevant control antibody A110-1 had no significant effect on any of the variables measured (selected variables shown in Figure 4.1). Therefore, the A110-1 injected group was pooled with the uninjected group to make one "control" group.

As hypothesized, treatment with P/E-selectin blocking antibodies reduced neutrophil content by about half in muscles subjected to lengthening contractions (Figure 4.2A). To assess whether the neutrophils that were present in spite of blocking

antibody treatment had indeed migrated out of the circulation, we examined neutrophil localization relative to blood vessels (Figures 4.2D-4.2E). Irrespective of the experimental group, only about 5% of neutrophils were clearly inside blood vessels (control: 6 ± 1% vs. anti-P/E-sel: 5 ± 2%), suggesting that most of the neutrophils we detected were extravascular. Contrary to our hypothesis, the decrease in neutrophil content was not associated with a decrease in damage as assessed by force deficit, which was approximately 50% for muscles of both treated and control mice (Figure 4.3). Muscles of both groups also showed similar numbers of injured fibers, with 10% to 15% of the fibers in a cross section showing morphological evidence of injury (Figure 4.4A). Although the number of injured fibers was not different among experimental groups, the characteristics of the injured fibers were different (Figure 4.4E), with fewer fibers showing signs of inflammatory cell infiltration and more fibers with variable or pale staining in the muscles from mice injected with blocking antibodies. Also contrary to our hypothesis was the observation that macrophage content showed a trend ($P = 0.076$) toward a reduction by approximately one-third in muscles of treated compared with control mice.

An unexpected finding was an effect of treatment with P/E-selectin blocking antibodies on the contralateral muscles that were not subject to lengthening contractions (Figure 4.6). Although force generation of contralateral control muscles was not affected by the treatment with the selectin blocking antibodies (control: 258 ± 5 mN/mm^2 vs. anti-P/E-sel: 248 ± 6 mN/mm^2) nor was there any morphological evidence of injured fibers (control: 0.13 ± 0.07% vs. anti-P/E-sel: 0.23 ± 0.10%), neutrophil content was increased by more than 4-fold (Figure 4.6A). Thirteen percent of these

neutrophils were found within blood vessels, compared with 33% in control muscle sections (control: 33 ± 8% vs. anti-P/E-sel: 13 ± 5%, t-test, P = 0.089), suggesting that the majority of the neutrophils in the contralateral muscles were also extravascular. Blood analysis revealed that the blocking antibody treatment dramatically increased circulating neutrophils (Figure 4.7A) that may have driven neutrophils into contralateral muscles in the absence of lengthening contractions, as well as contributing to the increased neutrophil levels in injured muscles. Although neutrophils were elevated in contralateral muscles of treated mice the levels did not reach those observed in injured muscles from mice treated with P/E-selectin blocking antibodies (contralateral: 1210 ± 159 Gr-1+ cells / mm^3 tissue vs. injured: 2624 ± 530 Gr-1+ cells / mm^3 tissue, t-test, P = 0.045). Treatment with P/E-selectin blocking antibodies also increased circulating monocytes (Figure 4.7B), although the difference was less dramatic than for neutrophils and did not reach significance (effect of blocking antibody treatment, P = 0.066). The trend toward elevated numbers of circulating monocytes was not associated with increased macrophage content in contralateral muscles (Figure 4.6D).

Discussion

The major implication of the present study is that endothelial selectins (P- and/or E-selectin) contribute to, but are not necessary for, neutrophil accumulation after contraction-induced injury. Support for this conclusion is provided by our observation that treating animals with blocking antibodies for P- and E-selectin reduced but did not eliminate neutrophils in sections of injured muscles. Our results also indicate that

reducing neutrophil accumulation to approximately 50% of control levels is not sufficient to reduce damage after contraction-induced injury, as evidenced by the observations that the treatment and accompanying blunted accumulation of neutrophils did not result in a reduction of the force deficit or the number of fibers showing histological evidence of damage. Our study was not decisive on the question of whether or not blocking the endothelial selectins left macrophage accumulation intact. Muscles of mice treated with blocking antibodies showed two thirds as many macrophages following lengthening contractions compared with the numbers observed in untreated mice, but the decrease did not reach reach statistical signifcance. Therefore, the remainder of the discussion will focus primarily on neutrophils.

The finding that endothelial selectins contribute to neutrophil accumulation after contraction-induced injury was not known but was expected. Many studies have demonstrated a role for the selectins in leukocyte capture and rolling along blood vessel walls in the cremaster muscle (20-23, 30). In addition, neutrophil accumulation in soleus muscle after unloading followed by reloading was reduced in mice deficient in P- and E-selectin, suggesting that the endothelial sections contribute to neutrophil accumulation in this injury model (13). Despite these previous investigations of selectin function in skeletal muscle, neutrophils can accumulate in tissues using adhesion molecules other than P- and E-selectin (see discussion in following paragraph), and the involvement of endothelial selectins in neutrophil accumulation following contractions-induced injury had not been demonstrated prior to the present study.

While our results indicate that P- and/or E-selectin contribute to neutrophil accumulation after contraction-induced injury, our observation that neutrophil content

was not completely eliminated in injured muscles after treatment with blocking antibodies suggests that selectins are not necessary for neutrophil accumulation in this model. In the absence of P- and E-selectin function, other adhesion molecules such as L-selectin or vascular cell adhesion molecule 1 (VCAM-1) may contribute to neutrophil accumulation. L-selectin expressed on free flowing leukocytes can interact with PSGL-1 on rolling or adherent leukocytes in a process known as secondary capture, and the proportion of captured cells seized by this mechanism increases after P-selectin is blocked or absent (23). Furthermore, in cremaster or gracilis pedicle muscle, leukocyte rolling and neutrophil migration out of the vasculature is impaired when L-selectin is blocked or deficient (31-33). VCAM-1 expressed on endothelial cells can interact with α_4 integrins on leukocytes, and residual leukocyte rolling after blocking P- and E-selectin or in mice lacking all three selectins was further reduced with blocking antibodies to either VCAM-1 or α_4 integrin (23, 30). Therefore, neutrophil rolling mediated by VCAM-1 and α_4 integrin followed by secondary capture mediated by L-selectin and PSGL-1 may have contributed to the neutrophil accumulation in injured muscles observed in the present study. We also cannot rule out the possibility that P- and E-selectin are, in fact, required for neutrophil accumulation but that the amount of RB40.34 and 9A9 injected in the present study (200 μg for each antibody) was insufficient to completely block P- and E-selectin function. While we have no independent measure of selectin function to allow assessment of the effectiveness of our blocking treatment, 200 μg of RB40.34 almost completely eliminated macrophage migration out of injured arteries, suggesting that the dose of at least RB40.34 was sufficient for close to complete blockage (24).

Our finding that treatment with blocking antibodies reduced neutrophil accumulation in injured muscles but did not reduce damage is compatible with existing studies. Several studies examining damage after lengthening contractions found that effectively preventing neutrophil accumulation to a great extent (80-90% reduction in neutrophils) reduced force deficit and histological damage after injury caused by lengthening contractions, with specific reductions in damage ranging from approximately 30% to 80% (4-6). However, a reduction in damage by neutrophil depletion is not a universal finding. In one study, >90% of circulating neutrophils were depleted with antisera prior to lengthening contractions of hindlimb muscles, yet no reduction in force deficit or in the quantity of injured fibers relative to controls was observed (12). Nevertheless, the majority of studies to date suggest that the damage after lengthening contractions is at least in part mediated by neutrophils. In light of these studies, the most defensible interpretation of our findings is that the residual neutrophil accumulation in the presence of blocking antibody treatment, about 50% of control levels, was sufficient to induce neutrophil-mediated damage in injured muscles.

While the blocking antibody treatment did not affect the total number of injured fibers, the characteristics of injured fibers were different (Figure 4.4E). Increased intracellular calcium after muscle injuries can cause hypercontractions of portions of muscle fibers and leave adjacent portions of the same fibers barely visible or missing (34, 35). Thus, dark, swollen fibers (Category 1) or fibers with variable staining (Category 2) could represent portions of fibers that were hypercontracted. Pale fibers (Category 2) could represent segments of fibers that were adjacent to hypercontracted regions or fibers containing degraded contractile proteins, perhaps as a result of

calcium-sensitive proteases (36). Data from a parallel experiment using untreated mice showed that 5 days after lengthening contractions, the number of Category 1 and 2 fibers declined while the number of Category 3 fibers increased (data not shown), suggesting that over the course of the degenerative stage of repair, fibers show signs of damage and degeneration and are subsequently invaded by inflammatory cells. Thus, an interpretation of Figure 4.4E is that the blocking antibody treatment did not affect the number of fibers showing signs of degeneration or necrosis, but decreased the number of degenerating or necrotic fibers that had subsequently been invaded by inflammatory cells. This finding could be explained by decreased neutrophil accumulation with antibody treatment, or it could be explained by the reduced macrophage accumulation with antibody treatment, as macrophages are frequently found within degenerating fibers 2 days after injury. Both neutrophils and macrophages are thought to participate in the removal of necrotic tissue after injury. Teixeira et al. 2003 depleted neutrophils prior to toxin-induced muscle injury and observed delayed clearance of necrotic fibers accompanied by fewer regenerating fibers and fibrosis. However, the impaired regeneration could have been due to the decrease in macrophage accumulation that was also observed (37) as other studies that have depleted only macrophages prior to muscle injury have found similar impairments in regeneration (8, 9). We did not examine whether the reduced neutrophil accumulation observed in the present study ultimately had an impact on the removal of necrotic tissue or on regeneration and repair, but this is an important consideration for future studies.

Although our study was not decisive on the question of whether or not blocking the endothelial selectins left macrophage accumulation completely intact, we can say

that macrophage accumulation was not dramatically altered with P- and E-selectin blocking antibody treatment. This conclusion is consistent with a previous report that treatment with RB40.34 did not reduce accumulation of CD11b+ cells after lengthening contractions in mouse soleus muscles (38). Although CD11b is present on neutrophils, monocytes, and macrophages, the authors report very few neutrophils in their study. Therefore, their finding suggests that monocyte/macrophage accumulation is not dependent upon P-selectin, with the caveat that they may have not seen an effect due to the small concentration of RB40.34 injected (20 μg) or the targeting of only one selectin. Another report found that macrophage accumulation after unloading and reloading of mouse soleus muscle was not affected in P/E-selectin deficient mice (13). Overall, the data from the previous studies as well as the present study suggests that macrophages accumulate in injured skeletal muscle predominantly by P/E-selectin independent mechanisms. The trend toward decreased macrophage accumulation observed in the present study could be due to the decrease in neutrophil accumulation, as macrophage recruitment is one proposed role for neutrophils after muscle injury (37).

We were surprised by the observation that treatment with P- and E-selectin blocking antibodies increased neutrophil content in the contralateral muscles that were not subject to lengthening contractions. Blood analysis showed that treatment with blocking antibodies after injury dramatically increased the level of circulating neutrophils. The latter finding is consistent with other reports also showing elevated levels of circulating neutrophils in selectin deficient mice or in mice treated with blocking antibodies for P- and E-selectin (13, 19, 39), and may reflect the displacement of marginated neutrophils from blood vessel walls. Therefore, the dramatic increase in

circulating neutrophils observed in the present study may have driven more neutrophils into the contralateral muscles and presumably into the injured muscles, as well. We did not see more macrophages in the contralateral muscles, perhaps because there was only a trend for an increase in circulating levels of monocytes. Despite the substantial increase in neutrophil content in the contralateral muscles, we saw no evidence that the presence of the neutrophils in the tissue had any damaging effects on the muscle as assessed by the maintenance of force generating capability and also by the lack of histological evidence of injury. The uncoupling between neutrophil accumulation and muscle injury implies that merely the presence of neutrophils is not sufficient to induce damage. Additional factors such as neutrophil transcriptional activity, degranulation or reactive oxygen species production, perhaps induced by the injured tissue environment, may be responsible for neutrophil-mediated exacerbation of damage to muscle fibers.

In summary, the present study provides evidence that endothelial selectins (P- and/or E-selectin) contribute to neutrophil accumulation after contraction-induced injury, while macrophage accumulation appears to occur by mostly endothelial selectin-independent mechanisms. In spite of the reduction in neutrophil accumulation, we did not detect a decrease in damage two days after lengthening contractions, suggesting that the levels of neutrophils in the muscles (50% of controls) were sufficient to induce damage. From a therapeutic perspective, the implication is that blocking the selectins may not represent a beneficial approach. Additional adhesion proteins may have to be targeted to fully prevent neutrophil accumulation. An alternative approach would be to target specific functions of neutrophils that exacerbate damage. Determining the effect of these approaches on later stages of the repair process is also an important area of

investigation. Therapies targeting adhesion molecules or specific functions of neutrophils will also have to consider the effect on the muscle at later stages of the repair process.

Acknowledgements

This work was supported by NIH grants AG-020591 to SVB and AG-000114 to DDS. We would like to thank Dr. Klaus Ley for providing the 9A9 antibody. We would also like to thank the Unit for Laboratory Animal Medicine (ULAM) Pathology Core for Animal Research (PCAR) at the University of Michigan for performing the blood cell counts.

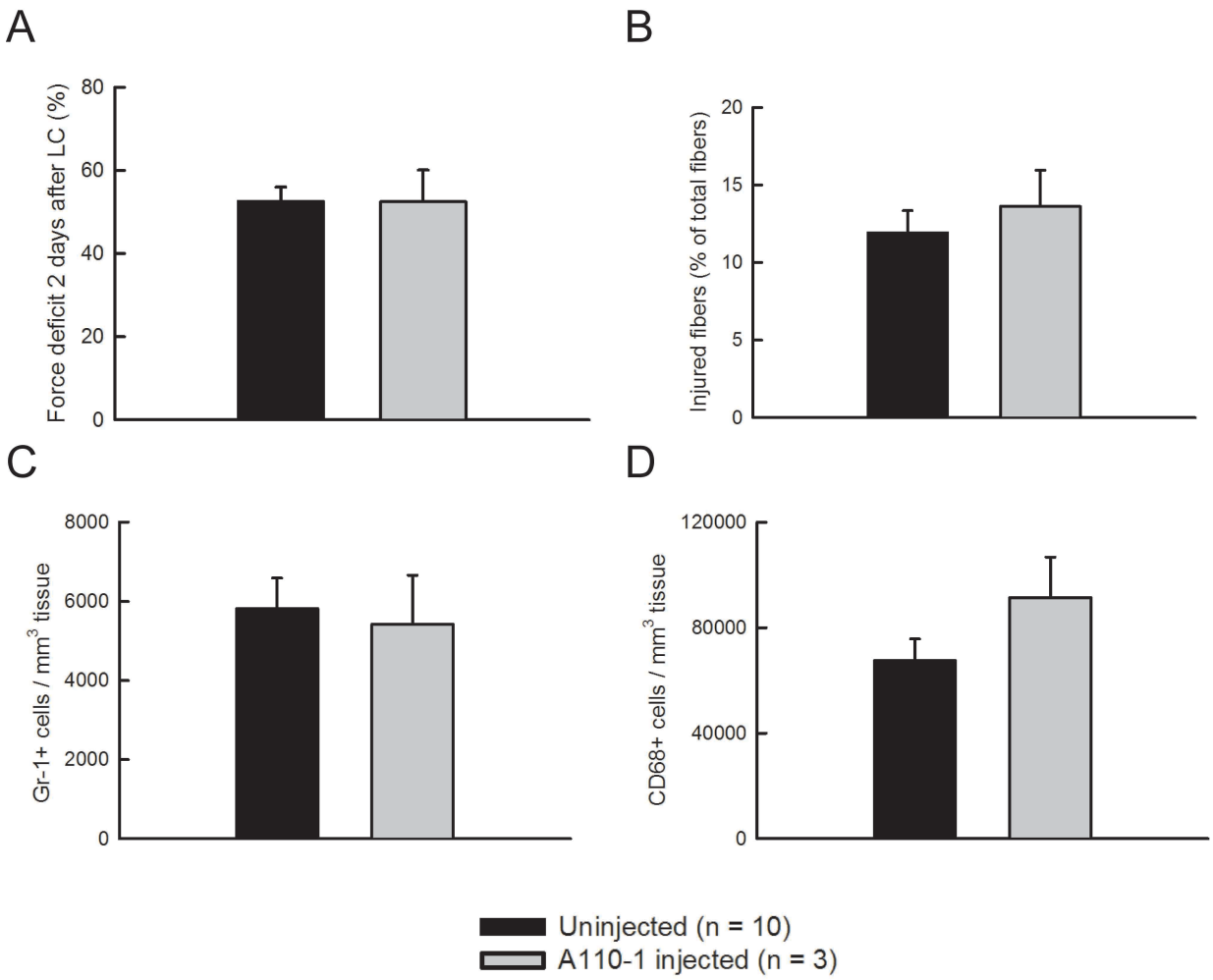

Figure 4.1: Injection of irrelevant control antibody A110-1 has no significant effect on damage or inflammatory cells in muscles 2 days after lengthening contractions. Force deficit (A). Injured fibers (B). Neutrophils (Gr-1+ cells) (C). Macrophages (CD68+ cells) (D).

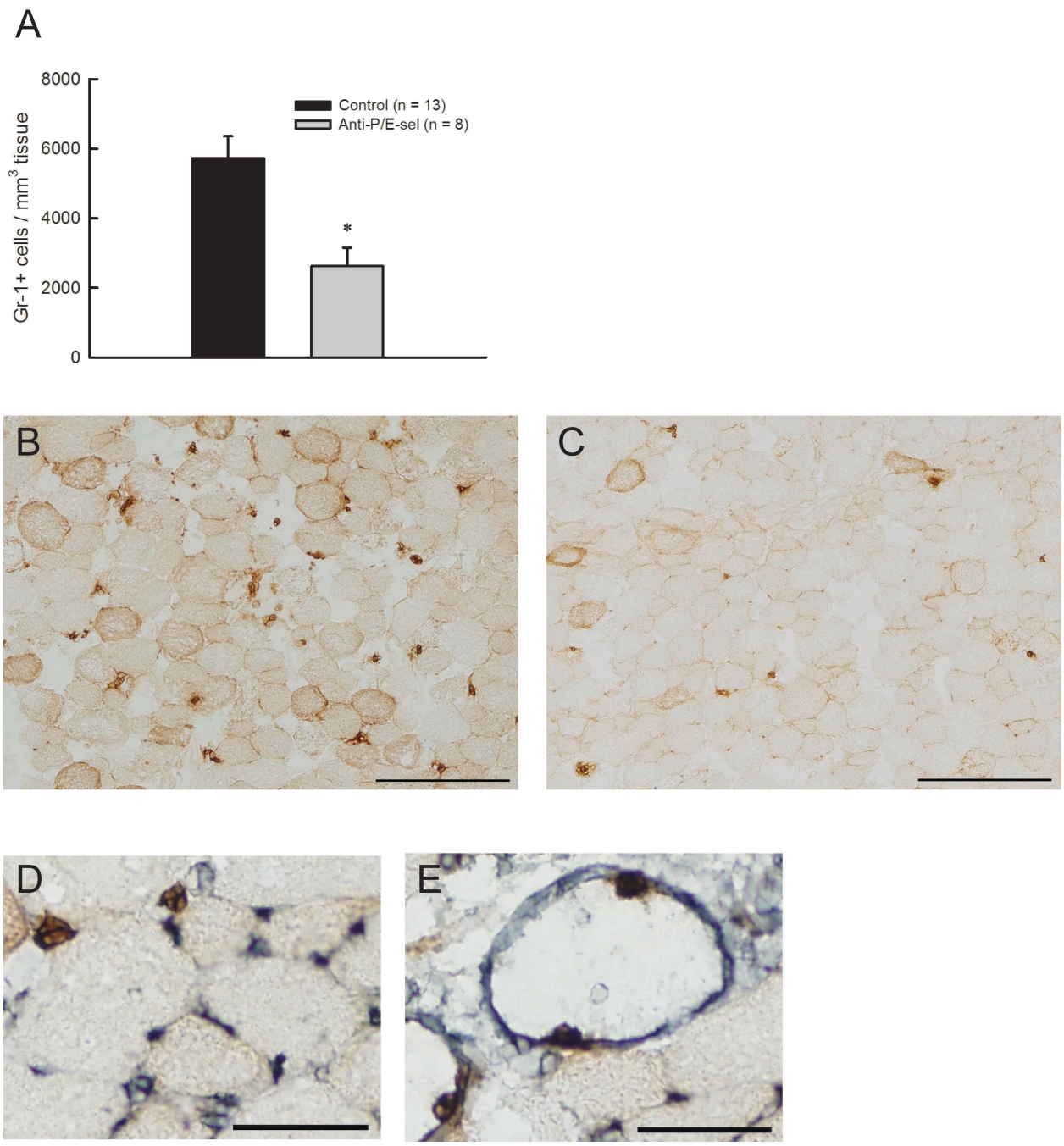

Figure 4.2: Treatment with blocking antibodies against P/E-selectin decreases neutrophil content in muscles 2 days after lengthening contractions. Neutrophils (Gr-1+ cells) ∗P = 0.005 by Mann-Whitney Rank Sum Test (A). Representative partial section of muscle from uninjected mouse (B) and mouse injected with blocking antibodies (C) with scale bars = 200 μm. Examples of neutrophil (Gr-1+ cells, brown) and blood vessel (GSL I, gray) co-labeling with scale bars = 50 μm (D, E). Neutrophils outside of vessels (D). Neutrophils on the inner surface of large vessels (E).

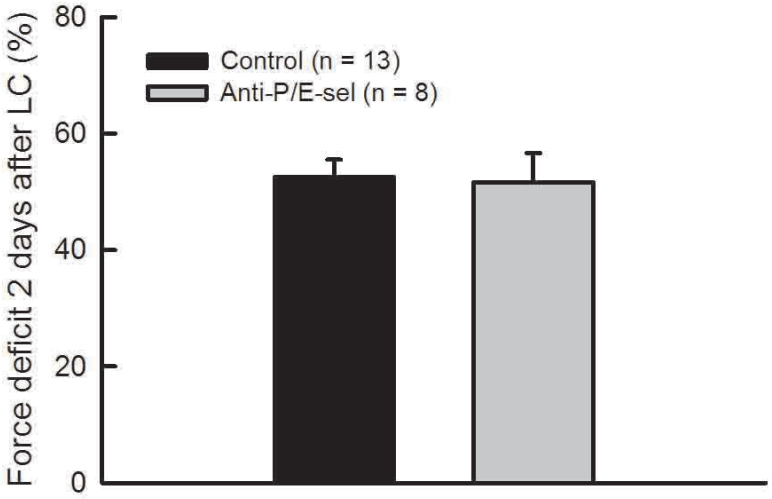

Figure 4.3: Treatment with blocking antibodies against P/E-selectin does not significantly decrease muscle damage 2 days after lengthening contractions, as assessed by force deficit.

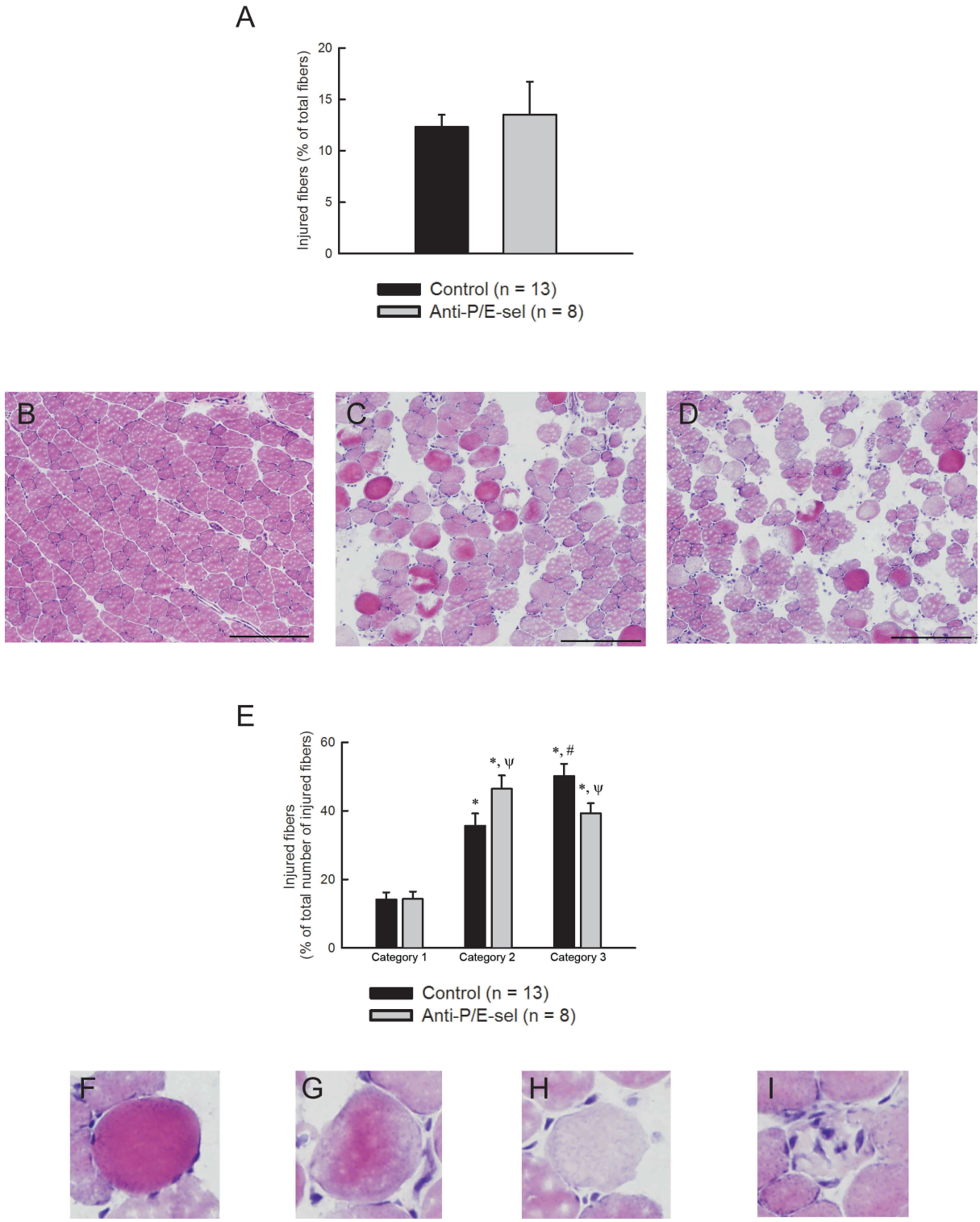
A
Injured fibers (% of total fibers)
20
15
10
5
0
Control (n = 13)
Anti-P/E-sel (n = 8)
B
C
D
E
Injured fibers
(% of total number of injured fibers)
60
40
20
0
*
*, ψ
*, #
*, ψ
Category 1
Category 2
Category 3
Control (n = 13)
Anti-P/E-sel (n = 8)
F
G
H
I

Figure 4.4: Treatment with blocking antibodies does not reduce the total number of injured fibers but reduces the percentage of injured fibers that are invaded by inflammatory cells, 2 days after lengthening contractions. Total injured fibers expressed as a percentage of the total number of fibers in a muscle section (A). Representative partial section of muscle from uninjured mouse (B), uninjected mouse (C), and mouse injected with P/E-selectin blocking antibodies (D). Injured fibers expressed as a percentage of the total number of injured fibers in a muscle section (E). Injured fibers fell into one of three categories. Category 1 consisted of round and often swollen fibers stained dark with eosin Y. Category 2 consisted of fibers with variable or pale staining with eosin Y. Category 3 consisted of fibers similar to those in category 2 but with several nuclei within the fiber, assumed to be inflammatory cells. ∗significantly different from category 1 within experimental group. #significantly different from category 2 within experimental group. ψsignificantly different from control within category. Significance was determined by a Two Way ANOVA ($P < 0.05$) (E). Magnified views of fibers from C and D (F - I). Examples of category 1 (F), category 2 (G, H) and category 3 (I) fibers. Scale bars = 200 μm.

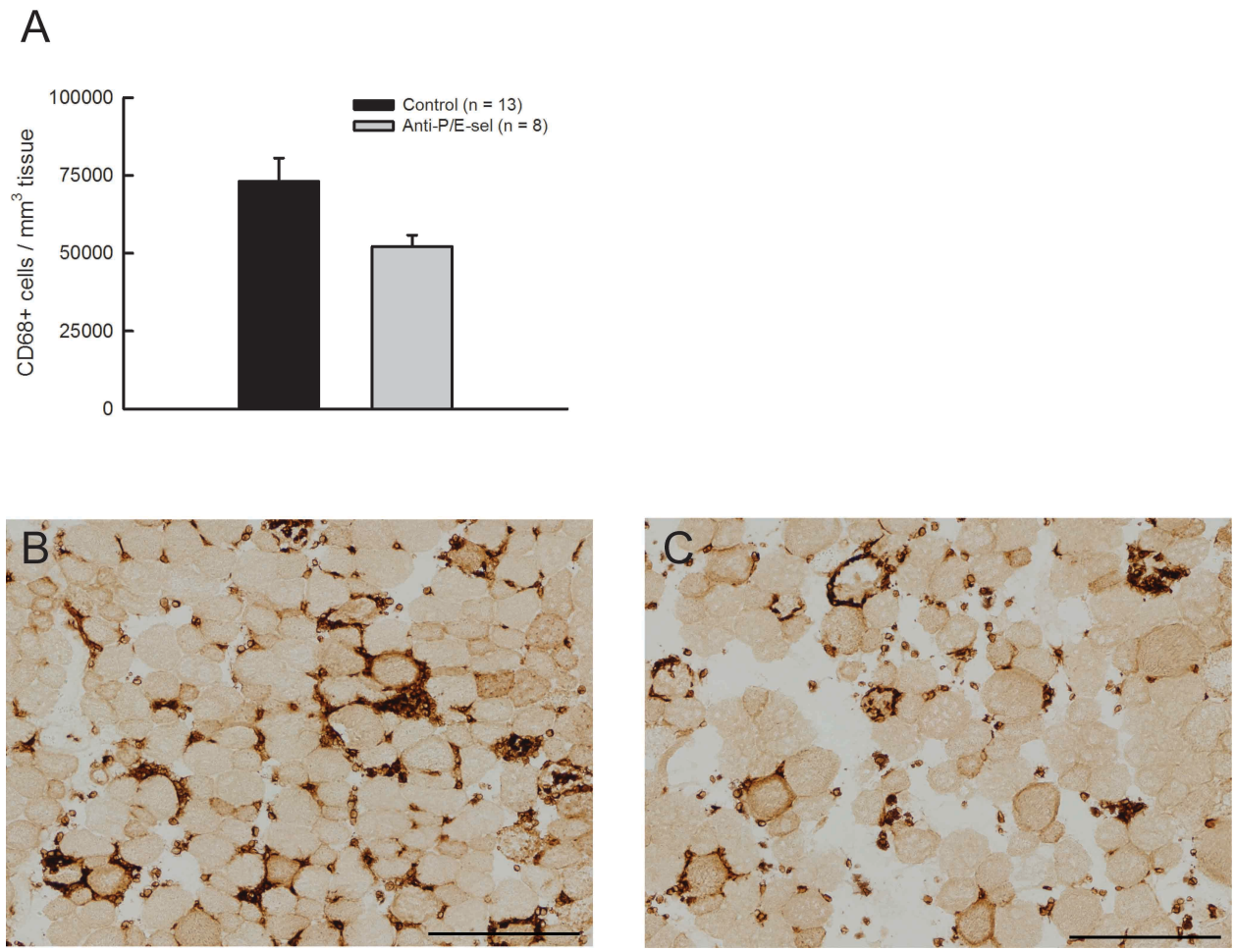

Figure 4.5: Treatment with blocking antibodies against P/E-selectin decreases macrophage content in muscles 2 days after lengthening contractions, although the decrease is not statistically significant (P = 0.076 by Mann Whitney Rank Sum Test). Macrophages (CD68+ cells) (A). Representative section of muscle from uninjected mouse (B) and mouse injected with blocking antibodies (C). Scale bars = 200 μm.

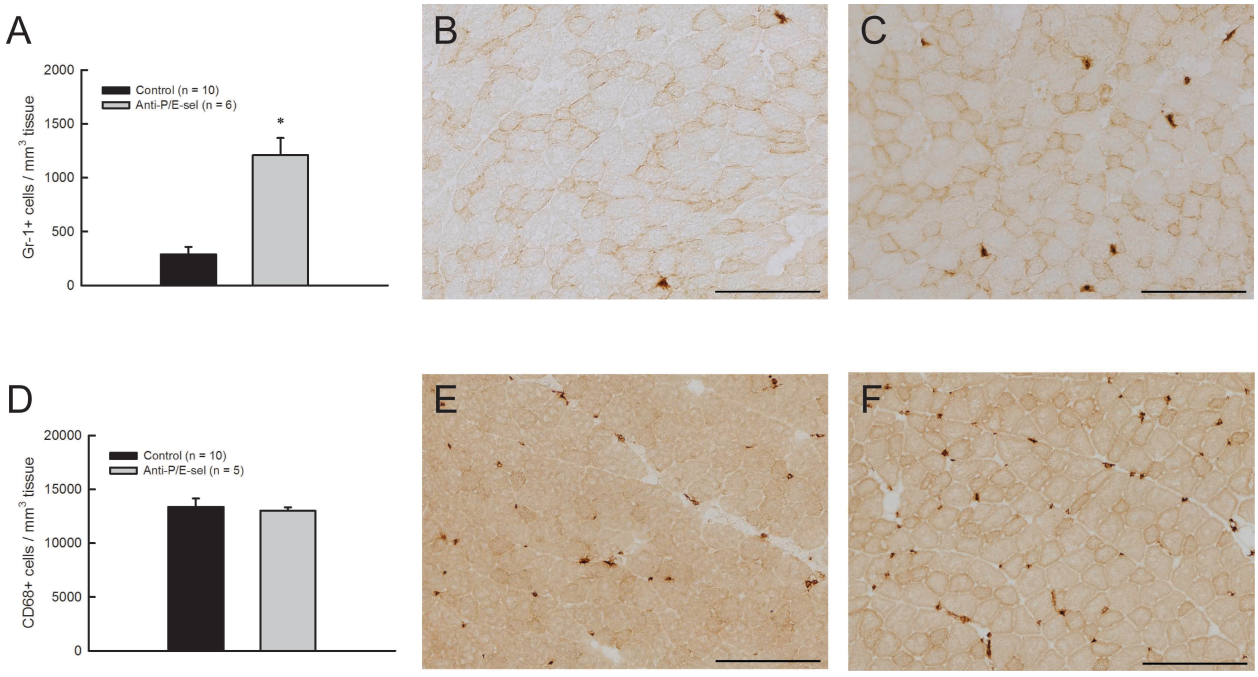

Figure 4.6: Treatment with blocking antibodies against P/E-selectin increases neutrophil but not macrophage content after 2 days, in contralateral muscles that have not been subjected to lengthening contractions. Neutrophils (Gr-1+ cells) (A). Representative partial section of muscle from uninjured mouse (B) and mouse injected with P/E-selectin blocking antibodies (C), Gr-1 labeled. Macrophages (CD68+ cells) (D). Representative partial section of muscle from uninjured mouse (E) and mouse injected with P/E-selectin blocking antibodies (F), CD68 labeled. Scale bars = 200 μm.

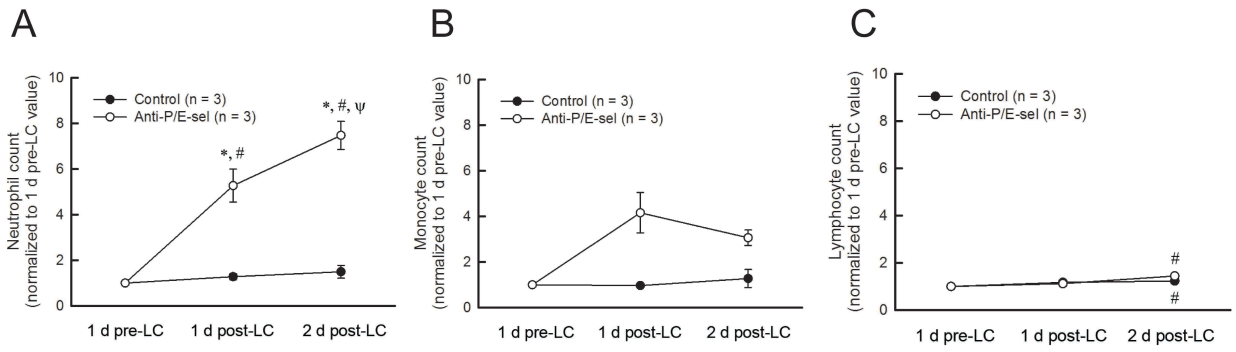

Figure 4.7: Circulating levels of major populations of white blood cells before and after lengthening contractions. Note that injection of blocking antibodies occurred within an hour of lengthening contractions. Neutrophils increased significantly with blocking antibody treatment ∗significantly different from control, #significantly different from 1 d pre-LC value ψsignificantly different from 1 d post-LC value (A). Monocytes increased with blocking antibody treatment but the increase did not reach significance (P = 0.066) (B). Lymphocytes increased 2 days after lengthening contractions in both experimental groups # significantly different from 1 d pre-LC value (C). Data was analyzed by a Two Way Repeated Measures ANOVA (significance set at $P < 0.05$).

Group	Sample size	Body weight (g)	Isometric force *in situ* (mN)	Immediate force deficit (%)
Uninjected	10	30.0 ± 0.6	414 ± 12	52 ± 3
A110-1 injected	3	31.3 ± 1.4	411 ± 2	48 ± 6
RB40.34/9A9 injected	8	29.1 ± 0.5	395 ± 7	52 ± 4

Table 4.1: Summary of data collected from experimental groups prior to antibody injections. Body weight, initial force generation of EDL muscles, and immediate force deficit after lengthening contractions were not different among experimental groups.

References

1. Nguyen HX, Tidball JG. Null mutation of gp91phox reduces muscle membrane lysis during muscle inflammation in mice. J Physiol. 2003 Dec; 553(3):833-41.

2. Nguyen HX, Lusis AJ, Tidball JG. Null mutation of myeloperoxidase in mice prevents mechanical activation of neutrophil lysis of muscle cell membranes *in vitro* and *in vivo*. J Physiol. 2005 Jun; 565(2):403-13.

3. Walden DL, McCutchan HJ, Enquist EG, Schwappach JR, Shanley PF, Reiss OK, Terada LS, Leff JA, Repine JE. Neutrophils accumulate and contribute to skeletal muscle dysfunction after ischemia-reperfusion. Am J Physiol. 1990 Dec; 259(6):H1809-12.

4. Brickson S, Ji LL, Schell K, Olabisi R, St Pierre Schneider B, Best TM. M1/70 attenuates blood-borne neutrophil oxidants, activation, and myofiber damage following stretch injury. J Appl Physiol. 2003 Sep; 95(3):969-76.

5. Pizza FX, Peterson JM, Baas JH, Koh TJ. Neutrophils contribute to muscle injury and impair its resolution after lengthening contractions in mice. J Physiol. 2005 Feb; 562(3):899-913.

6. Lockhart NC, Brooks SV. Neutrophil accumulation following passive stretches contributes to adaptations that reduce contraction-induced skeletal muscle injury in mice. J Appl Physiol. 2008 Apr; 104(4):1109-15.

7. Nguyen HX, Tidball JG. Interactions between neutrophils and macrophages promote macrophage killing of rat muscle cells *in vitro*. J Physiol. 2003 Feb; 547(1):125-32.

8. Summan M, Warren GL, Mercer RR, Chapman R, Hulderman T, Van Rooijen N, Simeonova PP. Macrophages and skeletal muscle regeneration: a clodronate-containing liposome depletion study. Am J Physiol Regul Integr Comp Physiol. 2006 Jun; 290(6):R1488-95.

9. Arnold L, Henry A, Poron F, Baba-Amer Y, van Rooijen N, Plonquet A, Gherardi RK, Chazaud B. Inflammatory monocytes recruited after skeletal muscle injury switch into anti-inflammatory macrophages to support myogenesis. J Exp Med. 2007 May; 204(5):1057-69.

10. Segawa M, Fukada S, Yamamoto Y, Yahagi H, Kanematsu M, Sato M, Ito T, Uezumi A, Hayashi S, Miyagoe-Suzuki Y, Takeda S, Tsujikawa K, Yamamoto H. Suppression of macrophage functions impairs skeletal muscle regeneration with severe fibrosis. Exp Cell Res. 2008 Oct; 314(17):3232-44.

11. Wang H, Melton DW, Porter L, Sarwar ZU, McManus LM, Shireman PK. Altered macrophage phenotype transition impairs skeletal muscle regeneration. Am J Pathol. 2014 Apr; 184(4):1167-84.

12. Lowe DA, Warren GL, Ingalls CP, Boorstein DB, Armstrong RB. Muscle function and protein metabolism after initiation of eccentric contraction-induced injury. J Appl Physiol. 1995 Oct; 79(4):1260-70.

13. Frenette J, Chbinou N, Godbout C, Marsolais D, Frenette PS. Macrophages, not neutrophils, infiltrate skeletal muscle in mice deficient in P/E selectins after mechanical reloading. Am J Physiol Regul Integr Comp Physiol. 2003 Oct; 285(4): R727-32.

14. Ebnet K, Vestweber D. Molecular mechanisms that control leukocyte extravasation: the selectins and the chemokines. Histochem Cell Biol. 1999 Jul; 112(1):1-23.

15. Brooks SV, Faulkner JA. Contraction-induced injury: recovery of skeletal muscles in young and old mice. Am J Physiol. 1990 Mar; 258(3):C436-42.

16. Koh TJ, Brooks SV. Lengthening contractions are not required to induce protection from contraction-induced muscle injury. Am J Physiol Regul Integr Comp Physiol . 2001 Jul; 281(1):R155-61.

17. Brooks SV, Faulkner JA. Contractile properties of skeletal muscles from young, adult and aged mice. J Physiol. 1988 Oct; 404:71-82.

18. Bosse R, Vestweber D. Only simultaneous blocking of the L- and P-selectin completely inhibits neutrophil migration into mouse peritoneum. Eur J Immunol. 1994 Dec; 24(12):3019-24.

19. Ramos CL, Kunkel EJ, Lawrence MB, Jung U, Vestweber D, Bosse R, McIntyre KW, Gillooly KM, Norton CR, Wolitzky BA, Ley K. Differential effect of E-selectin antibodies on neutrophil rolling and recruitment to inflammatory sites. Blood. 1997 Apr; 89(8):3009-18.

20. Kunkel EJ, Jung U, Ley K. TNF-α induces selectin-mediated leukocyte rolling in mouse cremaster muscle arterioles. Am J Physiol. 1997 Mar; 272(3):H1391-400.

21. Thorlacius H, Lindbom L, Raud J. Cytokine-induced leukocyte rolling in mouse cremaster muscle arterioles in P-selectin dependent. Am J Physiol. 1997 Apr; 272(4):H1725-9.

22. Kanwar S, Smith CW, Kubes P. An absolute requirement for P-selectin in ischemia/reperfusion-induced leukocyte recruitment in cremaster muscle. Microcirculation. 1998; 5(4):281-7.

23. Eriksson EE. No detectable endothelial- or leukocyte-derived L-selectin ligand activity on the endothelium in inflamed cremaster muscle venules. J Leukoc Biol. 2008 Jul; 84(1):93-103.

24. Phillips JW, Barringhaus KG, Sanders JM, Hesselbacher SE, Czarnik AC, Manka D, Vestweber D, Ley K, Sarembock IJ. Single injection of P-selectin or P-selectin glycoprotein ligand-1 monoclonal antibody blocks neointima formation after arterial injury in apolipoprotein E-deficient mice. Circulation. 2003 May; 107(6):2244-9.

25. Lagasse E, Weissman IL. Flow cytometric identification of murine neutrophils and monocytes. J Immunol Methods. 1996 Oct; 197(1-2):139-50.

26. Rabinowitz SS, Gordon S. Macrosialin, a macrophage-restricted membrane sialoprotein differentially glycosylated in response to inflammatory stimuli. J Exp Med. 1991 Oct; 174(4):827-36.

27. Holness CL, da Silva RP, Fawcett J, Gordon S, Simmons DL. Macrosialin, a mouse macrophage-restricted glycoprotein, is a member of the lamp/lgp family. J Biol Chem. 1993 May; 268(13):9661-6.

28. Deng B, Wehling-Henricks M, Villalta SA, Wang Y, Tidball JG. IL-10 triggers changes in macrophage phenotype that promote muscle growth and regeneration. J Immunol. 2012 Oct; 189(7):3669-80.

29. Hansen-Smith FM, Watson L, Lu DY, Goldstein I. Griffonia simplicifolia I: fluorescent tracer for microcirculatory vessels in nonperfused thin muscles and sectioned muscle. Microvasc Res. 1988 Nov; 36(3):199-215.

30. Jung U, Ley K. Mice lacking two or all three selectins demonstrate overlapping and distinct functions for each selectin. J Immunol. 1999 Jun; 162(11):6755-62.

31. Ley K, Bullard DC, Arbonés ML, Bosse R, Vestweber D, Tedder TF, Beaudet AL. Sequential contribution of L- and P-selectin to leukocyte rolling *in vivo*. J Exp Med. 1995 Feb; 181(2):669-75.

32. Lozano DD, Kahl EA, Wong HP, Stephenson LL, Zamboni WA. L-selectin and leukocyte function in skeletal muscle reperfusion injury. Arch Surg. 1999 Oct; 134(10):1079-81.

33. Hickey MJ, Forster M, Mitchell D, Kaur J, De Calgny C, Kubes P. L-selectin facilitates emigration and extravascular locomotion of leukocyte during acute inflammatory responses *in vivo*. J Immunol. 2000 Dec; 165(2):7164-70.

34. Carpenter S, Karpati G. Segmental necrosis and its demarcation in experimental micropuncture injury of skeletal muscle fibers. J Neuropathol Exp Neurol. 1989 Mar; 48(2):154-70.

35. Fridén J, Lieber RL. Segmental muscle fiber lesions after repetitive eccentric contractions. Cell Tissue Res. 1998 Jul; 293(1):165-71.

36. Belcastro AN, Shewchuk LD, Raj DA. Exercise-induced muscle injury: a calpain hypothesis. Mol Cell Biochem. 1998 Feb; 179(1-2):135-45.

37. Teixeira CF, Zamunér SR, Zuliani JP, Fernandes CM, Cruz-Hofling MA, Fernandes I, Chaves F, Gutiérrez JM. Neutrophils do not contribute to local tissue damage, but play a key role in skeletal muscle regeneration, in mice injected with Bothrops asper snake venom. Muscle Nerve. 2003 Oct; 28(4):449-59

38. Baker W, Schneider BA, Kulkarni A, Sloan G, Schaub R, Sypek J, Cannon JG. P-selectin inhibition suppresses muscle regeneration following injury. J Leukoc Biol. 2004 Aug; 76(2): 352-8.

39. Labow MA, Norton CR, Rumberger JM, Lombard-Gillooly KM, Shuster DJ, Hubbard J, Bertko R, Knaack PA, Terry RW, Harbison ML, Kontgen F, Stewart CL, McIntyre KW, Will PC, Burns DK, Wolitzky BA. Characterization of E-selectin-deficient mice: demonstration of overlapping function of the endothelial selectins. Immunity. 1994 Nov; 1(8):709-20.

Chapter 5

Conclusions and future work

Summary of objectives

Aging is associated with progressive declines in skeletal muscle mass and function that can significantly impact quality of life and limit independence in older individuals. Muscles of aged individuals are more susceptible to damage and have a diminished ability for repair. Thus, cycles of injury and incomplete recovery may occur and contribute to progressive declines in muscle function. Therefore, finding ways to restrict damage after muscle injury and/or enhance repair is a worthwhile goal for the benefit of older individuals. Developing strategies to restrict damage or enhance repair for older individuals requires a mechanistic understanding of both the damage and repair processes following injury and the impact of aging on those processes. The overall objective of this dissertation was to address fundamental gaps in our knowledge of cellular and molecular events associated with a common form of muscle injury and to identify age-related changes in key events. The specific goals were to 1) determine the role of ROS in initiating lengthening contraction-induced injury, 2) to determine the contribution of alterations in the myeloid cell response to injury and/or

regeneration in adult and old mice, and 3) to determine the role of P- and E-selectin in neutrophil accumulation following lengthening contraction-induced injury.

Summary of conclusions

The primary conclusions of this dissertation are briefly summarized below:

In vitro experiments in mouse lumbrical muscles revealed that lengthening contractions that damaged the muscle did not generate more ROS than isometric contractions that did not cause damage. This study argues against an increase in ROS in skeletal muscle fibers as an initiating factor in degenerative and regenerative processes occurring following the initial injury and does not provide support for antioxidant interventions early on in the injury process (Chapter 2).

In situ experiments using mouse EDL muscles revealed that impaired regeneration in muscles from old mice was accompanied by an altered neutrophil response to injury (Chapter 3). The altered response was not characterized by a persistence of neutrophils. Rather, neutrophils were elevated in injured muscles of old mice relative to young. Neutrophils can exacerbate damage to injured muscle fibers and therefore, an age-related elevation in neutrophils could further exacerbate damage to injured muscles beyond levels in young mice and thus undermine repair. Experiments described in Chapter 4 provided insight regarding this possibility. Treating mice with blocking antibodies for P/E-selectin after lengthening contractions decreased neutrophil accumulation by half but did not reduce damage, suggesting that only a portion of

accumulating neutrophils are sufficient to exacerbate damage (Chapter 4). Therefore, we conclude that modest changes in neutrophil content does not affect damage to muscle fibers after lengthening contractions. We speculate that the age-related increase in neutrophil content did not further exacerbate damage to injured muscles beyond levels in young mice.

In situ experiments using mouse EDL muscles also revealed that impaired regeneration in muscles from old mice was accompanied by an altered macrophage response to injury (Chapter 3). The altered response was not characterized by a delay or reduction in the accumulation of total or M2 macrophages. Instead, macrophage accumulation was generally elevated in injured muscles of old mice relative to young. Gene expression data revealed age-related changes in the expression of macrophage-associated genes that have the potential to undermine or impair muscle regeneration. Thus, we propose the mechanism underlying age-related susceptibility to damage and/or deficient repair may include altered function of aged macrophages.

In situ experiments using mouse EDL muscles revealed that endothelial selectins (P and/or E-selectin) contributed to neutrophil accumulation after lengthening contractions. However, blocking the endothelial selectins did not completely prevent neutrophil accumulation, and we did not detect a decrease in damage two days after lengthening contractions. We conclude that blocking only the selectins may not provide a therapeutic benefit, and that additional adhesion proteins may have to be targeted to fully prevent neutrophil accumulation and reduce damage after lengthening contractions (Chapter 4).

Future work

The most exciting findings described in this dissertation were the age-related differences in the myeloid cell response to muscle injury, and the indication that myeloid cells from aged mice exhibit altered function that could influence the repair process. These findings provide direction for future studies that will ultimately be aimed at manipulating pathways to reduce injury or enhance repair.

Further work should be done to clarify and further characterize the effects of aging on myeloid cell function. Because we examined mRNA at the tissue level, we could not confirm the cellular source of the mRNA and we did not assess changes in protein content. Future studies could isolate different myeloid cell populations (neutrophils and macrophages) from injured muscles of young and old mice via cell sorting methods (1) and examine mRNA and protein levels of purified cells. Enzyme activity could also be examined (e.g. arginase-1 or iNOS activity in macrophages and myeloperoxidase or elastase activity in neutrophils). In addition to the production of cytokines and molecules, other aspects of myeloid cell function could also be examined. For example, phagocytosis could be assessed by quantifying muscle protein in purified populations of myeloid cells, or by *in vitro* assays (1).

Once the effects of aging on myeloid cell function were clarified and further characterized, identified targets could be manipulated in young and/or old mice and the effects on muscle injury and/or repair could be assessed. Mice that are genetically engineered to either lack expression or conversely, overexpress certain genes in myeloid cells could be used for experiments. Alternatively, levels of certain molecules

(e.g. IL-10) could be restored at different time points by injection to injured muscles of wild-type mice. Ultimately, promising targets identified from these studies could be manipulated to reduce injury or enhance repair in old animals.

References

1. Arnold L, Henry A, Poron F, Baba-Amer Y, van Rooijen N, Plonquet A, Gherardi RK, Chazaud B. Inflammatory monocytes recruited after skeletal muscle injury switch into anti-inflammatory macrophages to support myogenesis. J Exp Med. 2007 May; 204(5):1057-69.